Université de Montréal

Surveillance non invasive de la réponse neuroimmunitaire fœtale à l'infection

Par

Lucien Daniel Durosier, M.D.

Département des Sciences biomédicales
Faculté de Médecine

Mémoire présenté à la Faculté de Médecine en vue de
l'obtention du grade de Maître ès sciences (M.Sc.) en Sciences Biomédicales
option générale

Décembre, 2014

Université de Montréal
Faculté des études supérieures et postdoctorales

Ce mémoire intitulé :

Surveillance non invasive de la réponse neuroimmunitaire fœtale à l'infection

Présenté par

Lucien Daniel Durosier, MD

a été évalué par un jury composé des personnes suivantes :

Dr. François Audibert, MD, MSc, président-rapporteur
Dr. Martin G.Frasch, MD, PhD, directeur de recherche
Dr. Guillaume Sébire, MD, PhD, membre du jury

Résumé

Introduction. In utero, l'infection des membranes maternelles et fœtales, la chorioamniotite, passe souvent inaperçue et, en particulier lorsque associée à une acidémie, due à l'occlusion du cordon ombilical (OCO), comme il se produirait au cours du travail, peut entrainer des lésions cérébrales et avoir des répercussions neurologiques péri - et postnatales à long terme chez le fœtus. Il n'existe actuellement aucun moyen de détecter précocement ces conditions pathologiques in utéro afin de prévenir ou de limiter ces atteintes.

Hypothèses. 1)l'électroencéphalogramme (EEG) fœtal obtenu du scalp fœtal pourrait servir d'outil auxiliaire à la surveillance électronique fœtale du rythme cardiaque fœtal (RCF) pour la détection précoce d'acidémie fœtale et d'agression neurologique; 2) la fréquence d'échantillonnage de l'ECG fœtal (ECGf) a un impact important sur le monitoring continu de la Variabilité du Rythme Cardiaque (VRCf) dans la prédiction de l'acidémie fœtale ; 3) les patrons de la corrélation de la VRCf aux cytokines pro-inflammatoires refléteront les états de réponses spontanées versus inflammatoires de la Voie Cholinergique Anti-inflammatoire (VCA); 4) grâce au développement d'un modèle de prédictions mathématiques, la prédiction du pH et de l'excès de base (EB) à la naissance sera possible avec seulement une heure de monitoring d'ECGf.

Méthodes. Dans une série d'études fondamentales et cliniques, en utilisant respectivement le mouton et une cohorte de femmes en travail comme modèle expérimental et clinique , nous avons modélisé 1) une situation d'hypoxie cérébrale résultant de séquences d'occlusion du cordon ombilical de sévérité croissante jusqu'à atteindre un pH critique limite de 7.00 comme méthode expérimentale analogue au travail humain pour tester les première et deuxième hypothèses 2) un inflammation fœtale modérée en administrant le LPS à une autre cohorte animale pour vérifier la troisième hypothèse et 3) un modèle mathématique de prédictions à

partir de paramètres et mesures validés cliniquement qui permettraient de déterminer les facteurs de prédiction d'une détresse fœtale pour tester la dernière hypothèse.

Résultats. Les séries d'OCO répétitives se sont soldés par une acidose marquée (pH artériel 7.35±0.01 à 7.00±0.01), une diminution des amplitudes à l'électroencéphalogramme(EEG) synchronisé avec les décélérations du RCF induites par les OCO accompagnées d'une baisse pathologique de la pression artérielle (PA) et une augmentation marquée de VRCf avec hypoxie-acidémie aggravante à 1000 Hz, mais pas à 4 Hz, fréquence d'échantillonnage utilisée en clinique. L'administration du LPS entraîne une inflammation systémique chez le fœtus avec les IL-6 atteignant un pic 3 h après et des modifications de la VRCf retraçant précisément ce profil temporel des cytokines. En clinique, avec nos cohortes originale et de validation, un modèle statistique basée sur une matrice de 103 mesures de VRCf ($R^2 = 0,90$, $P < 0,001$) permettent de prédire le pH mais pas l'EB, avec une heure d'enregistrement du RCF avant la poussée.

Conclusions. La diminution de l'amplitude à l'EEG suggère un mécanisme d'arrêt adaptatif neuroprotecteur du cerveau et suggère que l'EEG fœtal puisse être un complément utile à la surveillance du RCF pendant le travail à haut risque chez la femme. La VRCf étant capable de détecter une hypoxie-acidémie aggravante tôt chez le fœtus à 1000Hz vs 4 Hz évoque qu'un mode d'acquisition d'ECG fœtal plus sensible pourrait constituer une solution. Des profils distinctifs de mesures de la VRCf, identifiés en corrélation avec les niveaux de l'inflammation, ouvre une nouvelle voie pour caractériser le profil inflammatoire de la réponse fœtale à l'infection. En clinique, un monitoring de chevet de prédiction du pH et EB à la naissance, à partir de mesures de VRCf permettrait des interprétations visuelles plus explicites pour des prises de décision plus exactes en obstétrique au cours du travail.

Mots – clefs: Fœtus, RCF, EEG, VRC, monitoring, acidose, asphyxie, hypoxie, inflammation, LPS, fréquence d'échantillonnage, étude clinique, travail

Abstract

Introduction. *In utero*, the infection of maternal and fetal membranes, chorioamnionitis, goes frequently unnoticed and, especially when combined with acidemia due to occlusions of the umbilical cord as they occur during labour, can result in brain damage and long term neurological sequelae peri- and postnatally. Currently, there is no way to early detect these pathological conditions to prevent or limit lasting neurological deficits.

Hypotheses. (1) the fetal electroencephalogram (EEG), obtained from the scalp could serve as a useful ancillary tool to the existing fetal heart rate (FHR) monitoring for early detection of fetal acidemia and neurological injury; (2) the sampling rate of fetal ECG has a significant impact on the continuous FHR monitoring in the prediction of fetal acidemia; 3) patterns of FHR variability will reflect fetal baseline and inflammatory states; (4) FHR variability analysis should permit prediction of pH and base excess (BE) at birth.

Methods. In a series of studies using the chronically instrumented unanesthetized fetal sheep and clinical cohort, we modeled 1) worsening fetal acidemia with intermittent hypoxia resulting from umbilical cord occlusions (UCO) of increasing severity as experimental model of human labour to test the 1st and 2nd hypotheses; 2) moderate fetal inflammation by administering lipopolysaccharide (LPS) to test the 3rd hypothesis and 3) prediction of pH and BE status at birth using clinically validated FHR variability measures in a clinical cohort of laboring women to test the 4th hypothesis.

Results. Repetitive UCO resulted in marked acidosis (pH arterial 7.35±0.01 to 7.00±0.01), decreased EEG amplitudes synchronized with UCO-induced FHR decelerations and pathological arterial blood pressure decreases; in addition, we detected a significant increase in FHR variability with worsening acidemia when sampled at 1000 but not at 4 Hz, the sampling rate used clinically. LPS administration resulted in systemic fetal inflammation with IL-6 peaking at 3 h and FHR variability changes tracking this temporal cytokine profile precisely. In the clinical cohort, a statistical model based on a matrix of 103 FHR variability measures predicted pH ($R2 = 0.90$, $P < 0.001$), but not BE, from one hour of FHR recording prior to pushing stage.

Conclusions. The decrease in the EEG amplitude suggests an adaptive and neuroprotective brain shut-down; fetal EEG may complement the FHR monitoring during labour to improve early detection of incipient acidemia. FHR variability changes can detect early developing hypoxic-acidemia when sampled at 1000 Hz, but not when sampled at 4 Hz suggesting that a more sensitive mode of fetal ECG acquisition will improve early acidemia detection. Distinctive subsets of FHR variability measures permit online monitoring of fetal inflammation from ECG opening a new approach to characterizing the fetal inflammatory profile. Clinical bedside prediction of pH and BE monitoring at birth using FHR variability monitoring will allow more accurate decision making in obstetrics during labour.

Keywords: Fetus, FHR, EEG, HRV, monitoring, acidosis, asphyxia, hypoxia, inflammation, LPS, sampling rate, clinical study, labour

Liste des Abréviations

α7 nAChR	α7 nicotinic acetylcholine receptor
BF	Basse Fréquence
BHE	Barrière Hémato-encéphalique
CIMVA	Continuous individualized multiorgan variability analysis
DRO	Derivés réactifs de l'oxygène
EB	Excès de base
ECG	Electrocardiogramme
ECGf	Electrocardiogramme foetal
ECoG	Electrocorticogramme
EEG	Electroencéphalogramme
ELISA	Enzyme-linked immunosorbent assay
H/OCO	Animaux hypoxiques soumis à des occlusions du cordon ombilical
fHRV	Fetal heart rate variability
FRSQ	Fond de recherche du Québec – Santé
H/UCO	Chronically hypoxic animals subjected to umbilical cord occlusions
HF	Haute fréquence
HMGB1	High Mobility Group Box 1
HPA axis	Hypothalamic-pituitary adrenal axis
HR	Heart Rate
HRV	Heart rate variability
ICU	Intensive care unit
IL-1β	Interleukin 1β
IRSC	Institut de recherche en santé du Canada
LPS	Lipopolysaccharide
M1 agonist	Muscarinic 1 receptor agonist
MBI	*Mathematical Biosciences Institute*
NF – κB	Nuclear factor kappa light chain enhancer of activated B cells

N/OCO	Animaux normoxiques soumis à des occlusions du cordon ombilical
OCO	Occlusion du cordon ombilical
ON	Oxyde nitrique
PAS	Pression artérielle sanguine
PASM	Pression arterielle sanguine moyenne
pCO2	Pression partielle en dioxide de carbone
QTNPR	Réseau de formation en recherche périnatale du Québec
RCIU	Retard de croissance intra-utérin
RMSSD	Root mean square of successive differences of R-R intervals of ECG
SDNN	Standard deviation of NN intervals
SEF	Spectral edge frequency
SNA	Système nerveux autonome
TNF-α	Tumor necrosis factor α
TNFR	Tumor necrosis factor α receptor
VRCf	Variabilité du rythme cardiaque foetal
USI	Unité de soins intensifs

Liste des figures

Figure 1. Exemple d'une réponse ECOG / EEG à des OCO répétitifs ……..... 14
Figure 2. Réseau de la voie cholinergique anti-inflammatoire (VCA) ……..17
Figure 3. Les signaux cholinergiques provenant de la stimulation du nerf vague……18
Figure 4. Le point de réglage de la réponse du système immunitaire…….19
Figure 5. Interactions entre les systèmes nerveux, immunitaires et cardiaques…….. 19
Figure 6. Cascade inflammatoire en présence du LPS……... 20

Table des matières

Résumé iii

Abstract vi

Liste des Abréviations viii

Liste des figures x

1. INTRODUCTION 13

1.1 L'arrêt de l'activité électroencéphalographique prédit l'acidémie critique chez le fœtus ovin proche du terme 13
1.2. Les aspects méthodologiques du monitoring du rythme cardiaque fœtal : le rôle important de la fréquence d'échantillonnage 14
1.3. Corréler l'analyse multidimensionnelle de la variabilité du rythme cardiaque fœtal avec l'équilibre acido-basique à la naissance 16
1.4. La variabilité du rythme cardiaque fœtal comme indicateur potentiel de l'inflammation 17

2. PUBLICATIONS 22

2.1 Adaptive shut-down of EEG activity predicts critical acidemia in the near-term ovine fetus 23
2.2 Sampling rate of heart rate variability impacts the ability to detect acidemia in ovine fetuses near-term 56
2.3 Does heart rate variability provide a signature of fetal systemic inflammatory response in a fetal sheep model of lipopolysaccharide-induced sepsis? 63
2.4 Correlating multidimensional fetal heart rate variability analysis with acid-base balance at birth 100

3. DISCUSSION 112

3.1 L'arrêt adaptatif de l'activité EEG prédit l'acidémie critique chez le fœtus ovin proche du terme 112
3.1.1 L'EEG fœtal durant le travail peut permettre une détection précoce de l'acidémie 112
3.1.2 Les effets d'une hypoxie antérieure sur les réponses cardiovasculaires et à l'EEG suite aux occlusions du cordon ombilical 113
3.1.3 L'arrêt cérébral adaptif est un mécanisme proactive qui n'est pas influencé par une hypoxie antérieure 115
3.1.4 Significations et orientations futures 116
3.2 Le taux d'échantillonnage de la variabilité cardiaque influence la capacité de détecter l'acidémie chez les fœtus ovins proches du terme 116
3.2.1 L'impact du taux d'échantillonnage sur l'estimation correcte des propriétés de la VRCf 117
3.2.2 Signification clinique 118
3.2.3 Les forces et faiblesses de l'étude 118
3.2.4 Perspectives 118
3.3 Corréler l'analyse multidimensionnelle de la variabilité du rythme cardiaque avec l'équilibre acide-base à la naissance 119

3.3.1 Signification clinique 119
3.3.2 La VRCf comme code neural véhiculant l'information de l'axe cerveau-cœur détectant acidémie et inflammation 119
3.3.3 Les forces et faiblesses de l'étude 121
3.3.4 Conclusions et directions futures 122
3.4 Une signature de la réponse inflammatoire systémique fœtale dans le patron temporel des mesures de variabilité de la fréquence cardiaque : une étude prospective de septicémie induite par le lipopolysaccharide chez le modèle ovin 122
3.4.1 Surveillance de la voie cholinergique anti-inflammatoires avec la VRC 123
3.4.2. Le cerveau est-il sensible dans la détection de l'inflammation fœtale encodée dans la VRCf ? 125
3.4.3 Signification et perspectives 126
3.5 REMERCIEMENTS 127
3.6 PUBLICATIONS DE CETTE THESE 127
4. References 129

1. INTRODUCTION

1.1 L'arrêt de l'activité électroencéphalographique prédit l'acidémie critique chez le fœtus ovin proche du terme

Des études cliniques indiquent une augmentation du risque d'issus défavorable pour les nouveau-nés issue et des séquelles à long terme notamment paralysie cérébrale avec des valeurs de pH <7,00 du cordon ombilical. ((1-3) Cette thèse est corroborée par des études effectuées chez les fœtus ovins montrant qu'un état d'hypoxie préexistant modifie les réponses physiologiques cérébrales et cardiovasculaires, similaire à ce qui pourrait se produire lors d'une occlusion du cordon ombilical (OCO) en phase active du travail. (4-6) Cela a conduit au développement et à l'utilisation de la surveillance électronique du rythme cardiaque fœtal (RCF) comme la clef de voûte de l'évaluation de la santé du fœtus pendant le travail. (1-3) La présence de variabilité du en absence de décélérations du RCF permet de prédire de gaz sanguins et de pH normaux à la naissance. (1-3) Cependant, la visualisation du monitoring clinique du RCF lors de l'accouchement ne peut, à elle seule, déterminer la détection de l'acidémie à la naissance. Donc, la valeur prédictive positive avoisinant environ les 50 %, il y a nécessité d'améliorer les technologies existantes pour la détection des états d'hypoxie-acidémie chez le fœtus pendant le travail.(1-3)

Nous avons récemment étudiés les patrons de l'activité électrocorticale (ECoG) enregistrée à partir de la périphérie du cerveau et du RCF chez le fœtus ovin proche du terme suite aux insultes répétées d'occlusion du cordon ombilical comparable à ce qui est observé chez une femme en travail, afin de déterminer le temps et la corrélation des changements qui se produisent à l'ECoG avec une acidémie aggravante.(7) Il y a des changements cohérents à l'ECoG avec une suppression de l'amplitude et une augmentation de la fréquence pendant les phases de décélérations du RCF accompagnées d'une diminution pathologiques de la pression artérielle sanguine (PAS). Ces modifications constatées à l'ECoG suggèrent un "arrêt cérébral adaptif " et survient environ 50 minutes avant qu'un degré sévère d'acidémie ne soit atteint a (*i.e.*, pH artériel fœtal <7.00, Fig. 1). Dans la quête de mettre en application cette technologie de surveillance du bien-être fœtal en phase de travail chez l'humain, nous avons montré que l'électroencéphalogramme (EEG) fœtal, l'équivalent clinique de l'ECoG actuellement, peut être acquise en modifiant une électrode de scalp fœtal. (8); (9) En conséquence, cette application accessoire de surveillance durant le travail peut être rentable et facilement adjointe au monitoring électronique du RCF fœtal actuel

grandement utilisé en clinique et dans les hôpitaux. (3) **Nous émettons l'hypothèse qu'à la suite de la modification du scalp fœtal à des fins d'enregistrements électroencéphalographiques, cette méthode permettra la détection précoce d'une acidémie aggravante similaire à nos précédentes trouvailles à l'ECoG fœtale** (7, 10) qu'une hypoxie soit présente ou pas. En conséquence, dans cette étude après voir optimisé le signal d'acquisition de l'EEG en utilisant une électrode modifiée du scalp fœtal analogue à celles utilisées au cours du travail chez la femme, nous avons soumis des fœtus ovins proche du terme à des insultes répétées d'OCO et comparé les réponses à l'ECOG et EEG fœtal pendant une acidémie aggravante.

1.2. Les aspects méthodologiques du monitoring du rythme cardiaque fœtal : le rôle important de la fréquence d'échantillonnage

Il est urgent d'identifier les signes précoces d'une acidémie fœtale durant le travail, en raison de l'association d'une acidémie sévère avec des séquelles neurologiques à long terme et des procédures diagnostiques actuelles sous-optimales.(3, 11, 12) Les variations de l'activité vagale chez le fœtus peuvent être mesurées en monitorant la variabilité du rythme cardiaque fœtal (VRCf). (13, 14) Le RCF et la VRCf sont régulés par une interaction complexe des systèmes nerveux autonome et sympathique qui contrôlent le RCF de base ainsi que la VRCf à court et long terme avec leurs propriétés linéaires et non linéaires.(15) Ces propriétés de la VRCf sont affectées différemment par l'acidémie. (16-18)

Le RMSSD, qui se définit comme " root mean square of the successive differences of R-R intervals " à l'ECG.(19), est une mesure centrale qui reflète les modulations de la VRCf au niveau l'activité parasympathique (vagale), battement-par-battement sur l'échelle du temps et est plus précise comparée aux actuelles mesures de variations à court terme de la RCF utilisé dans le monitoring électronique du RCF (MER) (20) Cependant, cette précision dépend de la fréquence d'échantillonnage du signal ECG, signal à partir duquel dérivent les intervalles R-R ainsi que la VRCf subséquente. (19)

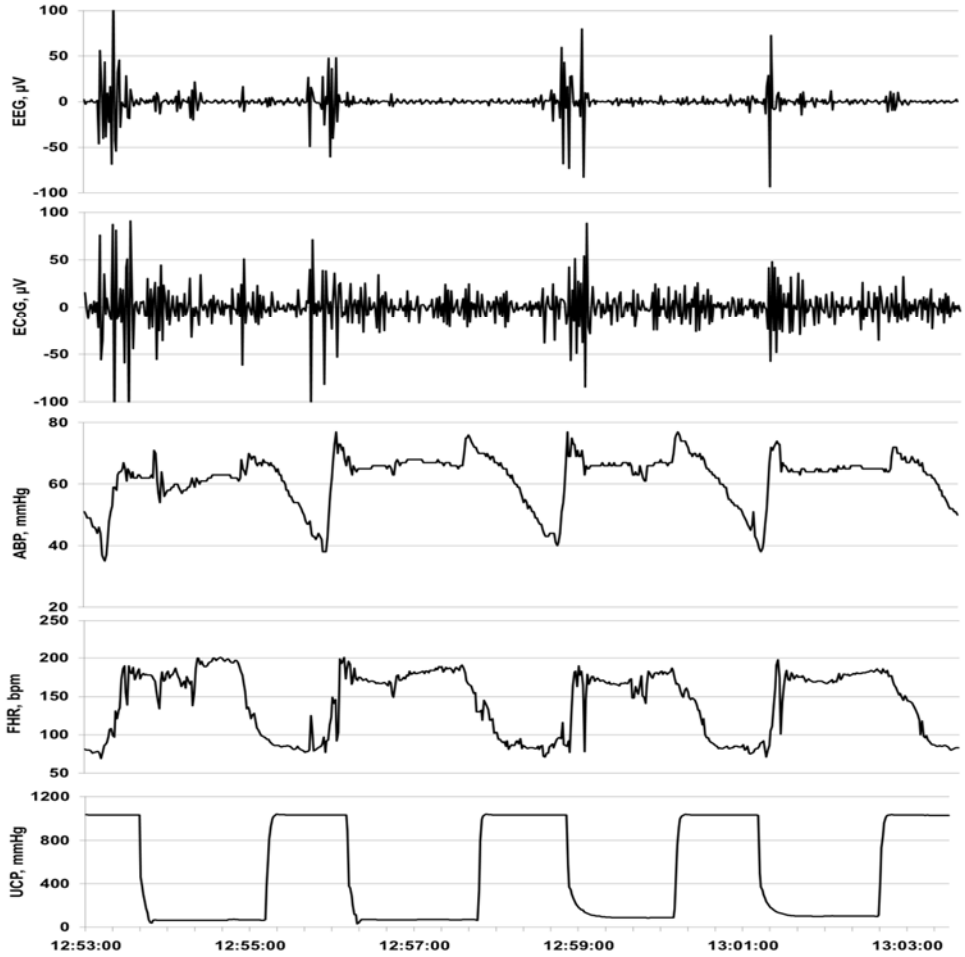

Fig. 1. Exemple d'une réponse ECOG / EEG à des OCO répétitifs. Vue de 10 min d'un patron d'un arrêt cérébral adaptatif visible à l'ECoG et à l'EEG en réponse aux changements de la pression artérielle sanguine (PAS) et du rythme cardiaque fœtal (RCF).

Nous avons montré que le RMSSD est une mesure de maturation de la branche vagale du système nerveux autonome et que cette mesure est réduite par l'atropine (un antagoniste cholinergique) chez le fœtus ovin proche du terme.(13, 16) Le RMSSD augmente également Durant une acidémie sévère (pH ~7.09) induite par 4 minutes d'occlusions du cordon ombilical (OCO) à intervalle de 30 min chez ce même modèle expérimental. (16) Donc le RMSSD est un marqueur potentiel de l'acidémie aggravante.

Dans cette étude, notre objectif est d'évaluer l'impact de taux d'échantillonnage de l'ECG fœtal afin de mesurer le bénéfice d'un monitoring continu de la VRCf dans la prédiction de l'acidémie fœtale. Nous avons testé la performance du RMSSD en tant que mesure de la VRCf et son comportement en présence d'acidémie fœtale quand acquis à un taux d'échantillonnage de 4 Hz, actuellement utilisé dans les moniteurs de RCF, en comparaison au taux d'échantillonnage

expérimental de 1000 Hz. Basé sur des évidences démontrées à partir des études fondamentales chez l'animal et cliniques chez l'homme, nous **proposons que le monitoring longitudinal de la VRCf pendant le travail nous permettra d'améliorer le diagnostic précoce de l'acidémie fœtale , mais influencée par le taux d'échantillonnage de l'ECG.**

1.3. Corréler l'analyse multidimensionnelle de la variabilité du rythme cardiaque fœtal avec l'équilibre acido-basique à la naissance

Les agressions cérébrales prénatales et périnatales restent une cause majeure de troubles neurologique et du développement à long terme.(21) Chez les enfants nés à terme, le contributeur le plus important d'une agression et de paralysie cérébrale est l'hypoxie ou l'asphyxie fœtale en intrapartum avec acidémie conséquente.(22) Bien que le monitoring fœtal électronique durant le travail ait considérablement réduit les décès (23) et les convulsions néonatales, il faillit de détecter avec précision, de manière anticipé, une hypoxie/asphyxie fœtale.(24, 25) Cette lacune a contribué à une épidémie de césariennes non nécessaire accompagnée de coûts élevés et de morbidité maternelle, sans pour autant diminuer le taux de paralysie cérébrale.(26) Selon la tendance, on pourrait dire qu'après 40 ans d'application cliniques extensives dans le monde entier, les limites du monitoring de RCF standard ne peuvent plus être surmontées.

Plusieurs raisons peuvent expliquer les raisons pour lesquelles le monitoring de RCF faillit dans la détection précoce d'une hypoxie associée à une acidémie. Premièrement, l'information provenant de l'analyse visuelle de la fréquence cardiaque (FC) et du mode de survenue des contractions utérines est limitée. Deuxièmement, la technologie actuelle de détection des évènements cardiaques fœtaux bioélectriques est limitée par un enregistrement insuffisant du vrai signal électrique. Les sondes trans -abdominales Doppler fonctionnent sur la moyenne des signaux biophysiques. Les électrodes du scalp, en plus d'être invasives, sont filtrées et échantillonnées à basse fréquence (BF), donc détectant un signal QRS avec le moins de bruit possible.(27) Troisièmement, alors que la VRCf est reconnue pour refléter les modulations par le système nerveux autonome, (13, 15) la perte d'information inhérente à ces méthodes minimise les données utilisables pour l'évaluation. L'échelle de temps de discrets évènements de la VRCf nécessite une résolution temporelle de détection de pics R au sein du complexe QRS en moins d' 1 milliseconde.(15, 28, 29) (30)

Récemment, une approche multidimensionnelle de monitoring au chevet du patient a été développée afin de collecter les signaux cardiaques and respiratoires et en analyser la variabilité. La plateforme CIMVA (continuous individualized multiorgan variability analysis), développée par Seely et coll., est un logiciel basé sur la complexité de la science.(31) Cet outil a démontré son utilité dans les unités de soins intensifs pour adultes, en identifiant une septicémie, approximativement 60 heures, avant le diagnostic clinique (32) et pronostiquant choc et échec de l'extubation. (31) De même, Moorman et coll. ont montré que les moniteurs de VRC au niveau des unités de soins intensifs pédiatriques ont contribué à la détection d'une septicémie imminente par le personnel soignant.(33) Ces techniques ouvrent des avenues prometteuses avec une approche totalement différentes du monitoring fœtal, à condition que les signaux bioélectriques soient échantillonnés à une fréquence appropriée.

Dans cette étude, nous présentons une nouvelle méthode de monitoring en intrapartum monitoring basée sur l'électrocardiographie fœtale (ECGf) transabdominale acquise de manière non invasive à partir de la surface de l'abdomen maternelle, avec une fréquence d'échantillonnage suffisamment élevée pour détecter les modulations autonomiques du RCF. L'analyse repose de préférence sur la VRCf que les performances cardiaques en tant que tel.

Nous avons développé un modèle de prédiction mathématiques, utilisant une matrice multidimensionnelle de 101 mesures de la VRCf et CIMVA, la plateforme standardisée et cliniquement testée,(32) pour prédire le pH et l'excès de base (EB) à la naissance avec seulement une heure de monitoring d'ECGf.

1.4. La variabilité du rythme cardiaque fœtal comme indicateur potentiel de l'inflammation

La principale manifestation pathologique de l'inflammation de l'unité fœto- placentaire, la chorioamniotite, affecte 20% des grossesses à terme et plus de 60% grossesses prématurées; est le plus souvent de trouvaille fortuite. (34, 35) La chorioamniotite symptomatique et asymptomatique sont associées avec un risque d'environ 9-fois plus élevé de paralysie cérébrale. (36) Même une inflammation asymptomatique peut inhiber l'angiogenèse placentaire et ainsi moduler l'issue de la grossesse. (37) Ainsi, un nombre important de fœtus est exposé à des degrés variables d'inflammation qui peut influer sur le développement cérébral. Les méthodes actuelles de

diagnostic de détresse fœtale due à une condition infectieuse ou inflammatoire sont inadéquates. (38, 39) Il est urgent d'identifier les marqueurs précoces de risque foetal d'issues défavorables afin d'intervenir thérapeutiquement. (38, 39)

Via le nerf vague, la voie cholinergique anti inflammatoire (VCA) chez le fœtus entraine une rétroaction négative sur les niveaux systémiques des cytokines inflammatoires (Fig. 2-4). Ce contrôle homéocinétique rapide du milieu inflammatoire est reflété dans de subtiles modifications de la VRCf (Fig. 2).

Les variations de l'activité vagale chez le fœtus peuvent être mesurées de manière non invasive par le monitoring continue de la VRCf. (15, 40) Evidemment, de telles VRCf battements par battements sont plus précises que la moyenne des VRCf calculée dans le temps utilisée actuellement en clinique. Les études périnatales montrent que la VRCf monitorée battement par battement a le potentiel d'être une mesure non invasive, continue, sensible et spécifique de la réponse inflammatoire fœtale. (41-44)

Les mesures de la VRC peuvent dériver de plusieurs domaines analytiques du signal. Le RMSSD (Root Mean Square of Standard Deviation), une mesure à court-terme de la VRC, et d'autres mesures de complexité et de signaux liées à d'autres domaines, reflétant l'échelle de temps à court terme de la VRCf, peuvent servir d'indicateurs de cette modulation vagale complexe de l'activité inflammatoire (Fig. 2).

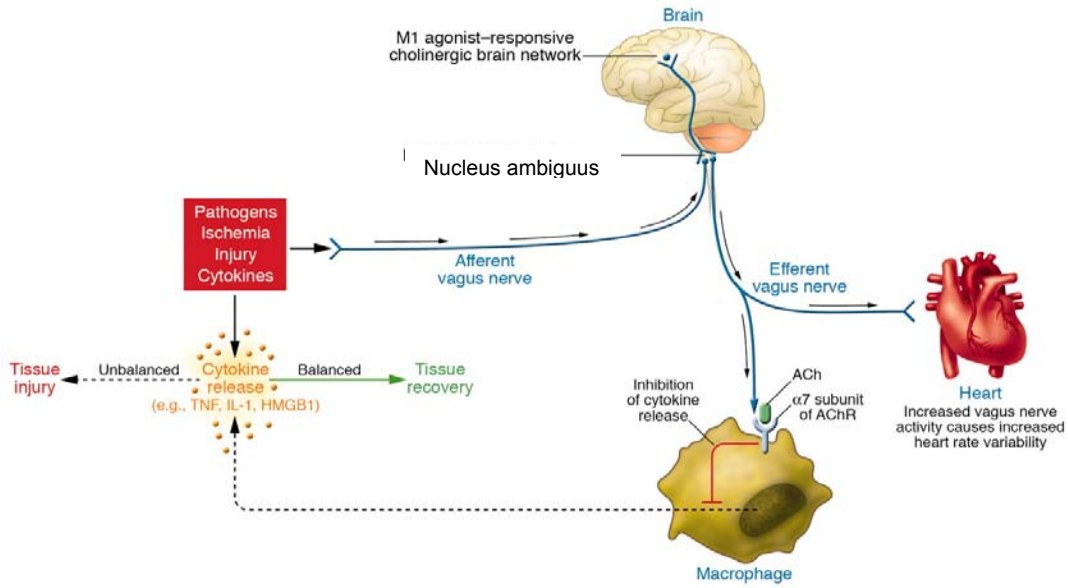

Fig. 2. Réseau de la voie cholinergique anti-inflammatoire (CAP), qui équilibre la production de cytokine. Les pathogènes aussi bien qu'une ischémie et autres formes d'agression activent la production de cytokines, laquelle restaure un état de santé normal. Cependant, si la réponse des cytokines est insuffisante ou excessive, alors ces mêmes

médiateurs causent des maladies. Les signaux efférents provenant du nerf vague inhibent la production de cytokines à travers des voies dépendant de la sous-unité *α7 du récepteur d'*acetylcholine (*AChR*) présent sur les macrophages et d'autres cellules. L'activité efférente du nerf vague augmente également la VRC instantanément (HRV). Les agonistes muscariniques M1 agissant sur le circuit cholinergique peut augmenter l'activité de la VAC et augmente aussi la VRC instantanément. Les signaux afférents transportés par le nerf vague peuvent active une réponse efférente qui inhibe la libération des cytokines, c'est le *réflexe inflammatoire*. (45)

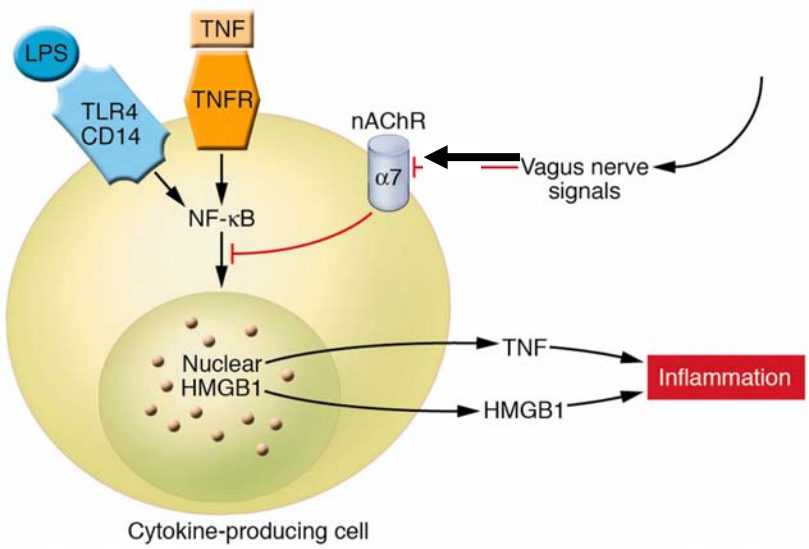

Fig. 3. Les signaux cholinergiques provenant de la stimulation du nerf vague inhibe la liberation de TNF-α, IL-1β, HMGB1, et autres cytokines en encodant un signal cellulaire qui inhibe l'activité nucléaire de NF-κB. Les cellules produisant les cytokines peuvent être le macrophage, la microglie ou l'astrocyte. La famille des récepteurs **nAChR** sont des canaux ioniques liés au ligand qui assurent la médiation de diverses fonctions physiologiques et ont été originellement identifiés au niveau du système nerveux. Ils consistent en différents sous-types formés par un assemblage spécifique de cinq sous-unités polypeptide incluant α1-10, β1-4, γ, δ, et ε. Les sous-unités sont divisées en 2 groupes : les récepteurs nicotiniques neuronaux (formés de α2–10 et β2–4) et des récepteurs nicotiniques musculaires (formés de α1, β1, γ, δ, et ε). Les sous-types neuronaux fonctionnelles de nAChR sont soit homomériques (formés de 5 sous-unités α identiques, telle que α7- ou α9 nAChR) ou hétéromérique (formé des combinaisons de sous-unités α et β, tels que α3β2 nAChR). Remarquablement, c'est le récepteur α7 nAChR qui est requis pour les effets de la VAC sur les cellules sur les cellules immunitaires innées cérébrales et périphériques et les. TNFR est l'abréviation pour le récepteur TNF. (45-48)

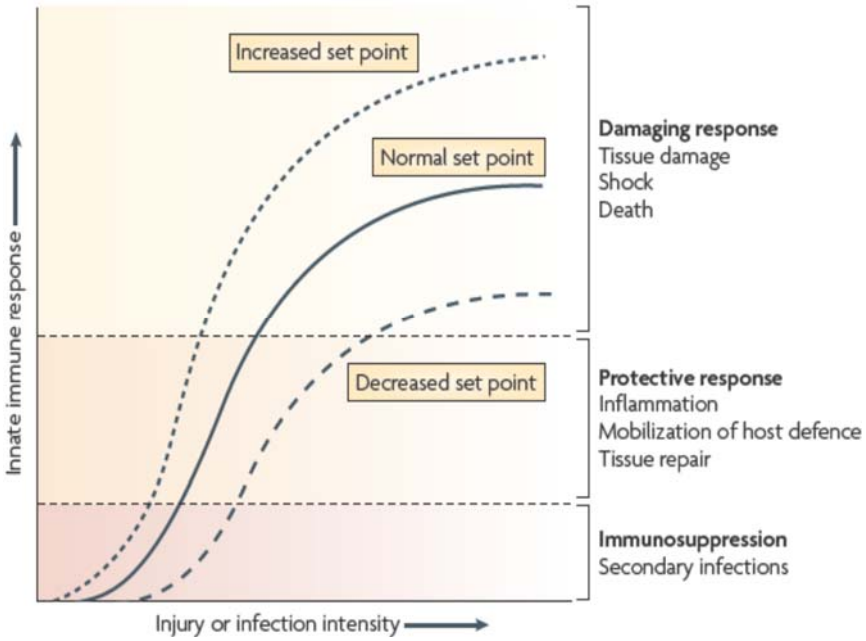

Fig. 4. Le point de réglage de la réponse du système immunitaire est défini par la magnitude de la réponse innée du système immunitaire relative au stimulus à l'infection ou d'une agression quelconque. Augmenter le point de réglage ou déplacer la courbe vers la gauche augmente les chances que le tissue soit endommagé en réponse à une infection ou agression. Diminuer le point de réglage ou déplacer la courbe vers la droite réduit la probabilité qu'un dommage tissulaire puisse arriver. La VCA est le circuit neural qui fournit une entrée compensatoire aigue afin d'ajuster la magnitude de la réponse immunitaire relative au point de réglage. (46)

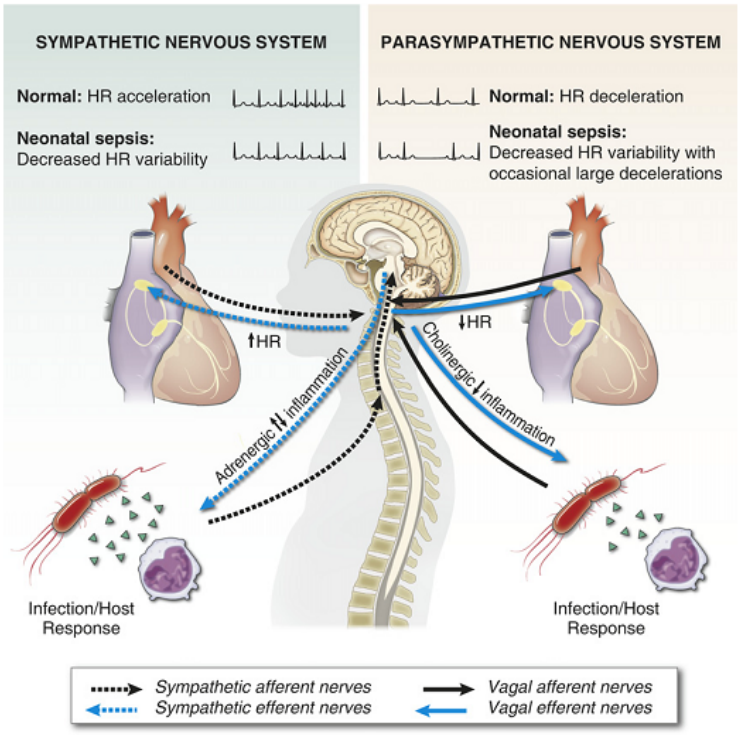

Fig. 5. Interactions entre les systèmes nerveux, immunitaires et cardiaques. Les pathogènes ou cytokines envoient des impulsions au tronc cérébral via les nerfs afférents. Les signaux autonomiques afférents sont aussi déclenchés par les barorécepteurs en réponse aux changements de la pression sanguine. Les nerfs sympathiques et parasympathiques (vague) envoient alors des signaux efférents au niveau du nœud sino auriculaire (SA), menant, respectivement, à des accélérations et décélérations du rythme cardiaque (RC). Dans la septicémie, la VRC diminue avec quelques petites accélérations et décélérations, probablement reflétant une dérégulation des réponses autonomes. Les fœtus ou les nouveau-nés avec septicémie peuvent avoir une VRC diminuée et occasionnellement de larges décélérations. Le système nerveux autonome (SNA), en plus de réguler la VRC, joue également un rôle important dans la défense de l'hôte en envoyant des signaux adrénergiques et cholinergiques (via la voie cholinergique anti-

inflammatoire, VCA) à la périphérie modulant la libération des médiateurs inflammatoires tels que les cytokines. Cf. Fig. 2-4 ci-dessus. (44)

L'inflammation induite par le lipopolysaccharide (LPS) chez le fœtus ovin est un modèle bien établi de la réponse inflammatoire chez le fœtus humain à la septicémie (Fig. 5-6). Cependant, aucune étude n'a utilisé les mesures de VRCf pour décrire le processus inflammatoire. (cf. Fig. 5).

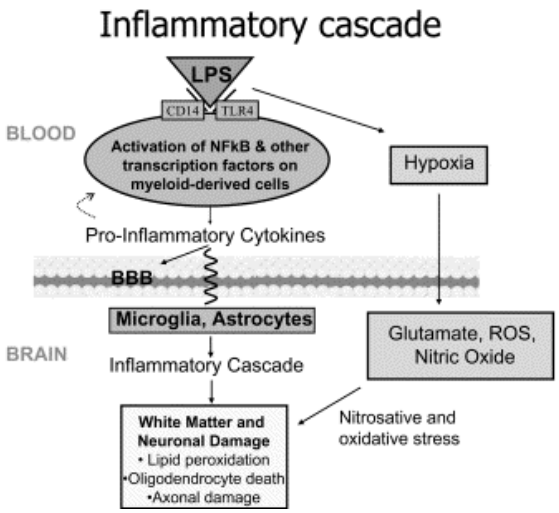

Fig. 6. Cascade inflammatoire en présence du LPS

Nous émettons l'hypothèse que les différents patrons de la corrélation de la VRCf aux cytokines pro-inflammatoires refléteront les états de réponses spontanées versus inflammatoires de la VAC.

2. PUBLICATIONS

2.1 Adaptive shut-down of EEG activity predicts critical acidemia in the near-term ovine fetus

[1]Martin G. FRASCH, MD, PhD, [1]L. Daniel DUROSIER, MD, [1]Mingju CAO, PhD, [2]Brad MATUSHEWSKI, MSc, [3]Lynn KEENLISIDE, [4]Yoram LOUZOUN, PhD, [5]Michael G. ROSS, MD, MPH, [2]Bryan S. RICHARDSON, MD

[1]CHU Ste-Justine Research Center, Dept. of Obstetrics and Gynaecology, Université de Montréal, QC, Canada, [2]Dept. of Obstetrics and Gynecology, Univ. Western Ontario, London, Ontario, Canada, [3]Imaging Program, Lawson Health Research Institute, London, ON, [4]Department of Mathematics, Bar-Ilan University, Ramat-Gan, Israel,

[5]Department of Obstetrics & Gynecology, LA BioMed at Harbor-UCLA Med. Ctr., Torrance, CA

Disclosure: BSR and MGF are inventors of related patent applications entitled "EEG Monitor of Fetal Health" including U.S. Patent Application Serial No. 12/532,874 and CA 2681926 National Stage Entries of PCT/CA08/00580 filed March 28, 2008, with priority to US provisional patent application 60/908,587, filed March 28, 2007. No other disclosures have been made.

Source of Financial Support: Canada Research Chair Tier 1 in Fetal and Neonatal Health and Development (BSR); CIHR and FRSQ (MGF); Women's Development Council, London Health Sciences Centre, London, ON, Canada (BSR, MGR, MGF).

Presentation Information: Presented in part at Society for Gynecologic Investigation Annual Meetings 2012 and 2013.

Short Title: Fetal EEG – HR monitoring predicts fetal acidemia

Please address reprint requests and correspondence to:

Martin G. Frasch

Département d'obstétrique-gynécologie

Université de Montréal

CHU Sainte-Justine Centre de Recherche

3175, chemin de la Côte Ste-Catherine

Montréal, Québec H3T 1C5
Canada
Phone: +1-514-345-4931 x4048
Fax: +1-514-345-4648

ABSTRACT

In fetal sheep, the electrocorticogram (ECOG) recorded directly from the cortex during repetitive heart rate (FHR) decelerations predictably correlates with worsening hypoxic-acidemia. In human fetal monitoring during labour, the equivalent electroenkephalogram (EEG) can be recorded non-invasively from the sculp. We tested the hypothesis that fetal EEG – FHR monitoring allows for early detection of worsening hypoxic-acidemia similar to that shown for ECOG-FHR monitoring. Near term fetal sheep were chronically instrumented with arterial and venous catheters, ECG, ECOG and EEG electrodes and umbilical cord occluder, followed by four days of recovery. Prior to study, fetuses were identified as normoxic (n=9, N/UCO group) or chronically hypoxic (n=5, arterial O2Sat<55%, H/UCO group). One minutes lasting repetitive umbilical cord occlusions (UCO) of increasing strength were induced each 2.5 minutes until pH dropped to <7.00. Repetitive UCOs led to marked acidosis (arterial pH 7.35±0.01 to 7.00±0.01). In all groups, at pH of 7.20, 53 min prior to pH<7.00, both ECOG and EEG amplitudes decreased ~4 fold during each FHR deceleration in a synchronized manner. In the H/UCO group, fetal arterial blood pressure failed to show physiological increases during the repetitive UCOs, while in the N/UCO groups this was only observed once ECOG/EEG amplitude consistently decreased during the FHR decelerations. This suggests an adaptive brain shut-down mechanism that is triggered neurally regardless of preexisting hypoxia. Confirming our hypothesis, these findings provide proof of principle for fetal EEG as a useful adjunct to FHR monitoring during high-risk human labour for early detection of incipient fetal acidemia.

Word count: 247

Key Words: Fetus, ECOG, FHR, monitoring, acidosis, asphyxia, hypoxia

INTRODUCTION

Human clinical studies indicate an increasing risk for neonatal adverse outcome and longer-term sequellae including cerebral palsy with umbilical cord pH values <7.00. ((Liston et al., 2002a, Liston et al., 2002b, Liston et al., 2007) This is supported by studies in the ovine fetus showing that pre-existing hypoxia alters cerebral and cardiovascular responses to labour-like umbilical cord occlusions (UCOs). (Gardner et al., 2002, Fletcher et al., 2006, Wassink et al., 2013) This has led to the use of electronic fetal heart rate (FHR) monitoring as the main stay for the assessment of fetal health during labour. (Liston et al., 2002a, Liston et al., 2002b, Liston et al., 2007) The absence of FHR decelerations along with presence of FHR variability are highly predictive for normal fetal blood gas/pH at birth. (Liston et al., 2002a, Liston et al., 2002b, Liston et al., 2007) However, clinical FHR monitoring has a low positive predictive value for concerning acidemia at birth (~50%) with need for improving existing technologies for the detection of fetal hypoxic-acidemia during labour.(Liston et al., 2002a, Liston et al., 2002b, Liston et al., 2007)

We recently studied patterns of electrocortical activity (ECOG) recorded from the cortex and FHR in the near term ovine fetus in response to repetitive UCOs insults as might be seen in human labour, to delineate the time-course and correlation of ECOG change with worsening acidemia.(Frasch et al., 2011) There were consistent changes in ECOG with amplitude suppression and frequency increase during FHR decelerations accompanied by pathological decreases in fetal arterial blood pressure (ABP). These changes in ECOG suggested an "adaptive brain shutdown" and occurred on average 50 minutes prior to attaining a severe degree of acidemia (*i.e.*, fetal arterial pH<7.00).

As a first step toward implementing this technology in human labour surveillance of fetal well-being we have shown that fetal electroencephalogram (EEG), the clinically available equivalent of the ECOG, can be acquired with a modified FHR scalp electrode. (Frasch et al., 2010); (Frasch et al., 2012) Accordingly, this ancillary surveillance modality during labour could be added easily and cost-effectively to the current electronic FHR monitoring that is widely used. (Liston et al., 2007) We hypothesized that fetal EEG recorded from a modified FHR scalp electrode will allow for early detection of worsening acidemia similar to our previous findings for fetal ECOG (Prout et al., 2010, Frasch et al., 2011) and regardless of preexisting hypoxia. Consequently, in the present study after optimizing EEG signal acquisition using a modified FHR scalp electrode similar to that used during human labour, we subjected near term ovine fetuses to

repetitive UCO insults and compared the fetal ECOG and EEG responses during worsening acidemia.

MATERIALS AND METHODS

Surgical preparation

Fourteen near-term ovine fetuses of 123±1 days gestational age (GA), (term=145 days) of mixed breed were surgically instrumented. The anesthetic and surgical procedures and postoperative care of the animals have been previously described (Kaneko et al., 2003, Frasch et al., 2009). Briefly, polyvinyl catheters were placed in the right and left brachiocephalic arteries and the right cephalic vein. Stainless steel electrodes were sewn onto the fetal chest to monitor the electrocardiogram (ECG). Stainless steel electrodes were additionally implanted biparietally on the dura for the recording of ECOG. A modified double spiral FHR electrode was placed midline just anterior to the ECOG electrodes to acquire EEG as successfully tested(Liston et al., 2007). An inflatable silicon rubber cuff (In Vivo Metric, Healdsburg, CA) for UCO induction was also placed around the proximal portion of the umbilical cord and secured to the abdominal skin. Once the fetus was returned to the uterus, a catheter was placed in the amniotic fluid cavity and another in the maternal femoral vein. Antibiotics were administered intravenously to the mother (0.2 g trimethoprim and 1.2 g sulfadoxine, Schering Canada Inc., Pointe-Claire, Canada) and the fetus and into the amniotic cavity (1 million IU penicillin G sodium, Pharmaceutical Partners of Canada, Richmond Hill, Canada). Amniotic fluid lost during surgery was replaced with warm saline. The uterus and abdominal wall incisions were sutured in layers and the catheters exteriorized through the maternal flank and secured to the back of the ewe in a plastic pouch.

Postoperatively, animals were allowed four days to recover prior to experimentation and daily antibiotic administration was continued. Arterial blood was sampled for evaluation of fetal condition and catheters were flushed with heparinized saline to maintain patency. Animals were 129±1 days GA on the first day of experimental study. Animal care followed the guidelines of the Canadian Council on Animal Care and was approved by the University of Western Ontario Council on Animal Care.

Experimental procedure

The animals were studied over a ~6 hour period in two groups. The first group comprised five fetuses that were found to be spontaneously hypoxic with arterial O2Sat<55% as measured on post-operative days 1 to 3 and at baseline prior to beginning the UCOs and formed an H/UCO group. This is in contrast to the second group of nine fetuses that were normoxic with O2Sat>55% before subjected to UCOs and formed a N/UCO group. After a 1-2 hour baseline control period,

both groups of animals underwent mild, moderate and severe series of repetitive UCOs by graduated inflation of the occluder cuff with a saline solution. During the first hour following the baseline period, mild variable FHR decelerations were performed with a partial UCO for 1 minute duration every 2.5 minutes, with the goal of decreasing fetal heart rate by ~30 bpm, corresponding to an ~50% reduction in umbilical blood flow. (Itskovitz et al., 1983, Richardson et al., 1989) During the second hour, moderate variable FHR decelerations were performed with increased partial UCO for 1 minute duration every 2.5 minutes with the goal of decreasing fetal heart rate by ~60 bpm, corresponding to an ~75% reduction in umbilical blood flow. (Itskovitz et al., 1983, Richardson et al., 1989) Animals then underwent severe variable FHR decelerations with complete UCO for 1 minute duration every 2.5 minutes until the targeted fetal arterial pH of less than 7.0 was detected or 2 hours of severe UCO had been carried out, at which point the repetitive UCOs were terminated. All animals were then allowed to recover for 48 hours following the last UCO. Fetal arterial blood samples were drawn at baseline, at the end of the first UCO of each series (mild, moderate, severe), and at 20 minute intervals (between UCOs) throughout each of the series, as well as at 1, 24 and 48 hours of recovery. For each UCO series blood gas sample and the 24 h recovery sample, 0.7 ml of fetal blood was withdrawn, while 4 ml of fetal blood was withdrawn at baseline, at pH nadir less than 7.00, and at 1 hour and 48 hours of recovery. The amounts of blood withdrawn were documented for each fetus and replaced with an equivalent volume of maternal blood at the end of day 1 of study.

All blood samples were analyzed for blood gas values, pH, glucose, and lactate with an ABL-725 blood gas analyzer (Radiometer Medical, Copenhagen, Denmark) with temperature corrected to 39.0°C. Plasma from the 4 ml blood samples was frozen and stored for cytokine analysis, and will be reported separately.

After the 48 hour recovery blood sample, the ewe and the fetus were killed by an overdose of barbiturate (30mg sodium pentobarbital IV, MTC Pharmaceuticals, Cambridge, Canada). A post mortem was carried out during which fetal sex and weight were determined and the location and function of the umbilical occluder were confirmed. The fetal brain was perfusion fixed and subsequently dissected and processed for later immunohistochemical study (data reported separately) as previously reported. (Keen et al., 2011)

Data acquisition and analysis

A computerized data acquisition system was used to record fetal arterial and amniotic pressures, the ECG, ECOG and EEG electrical signals, as previously described (Richardson and Gagnon, 2008), which were monitored continuously throughout the baseline, UCO series, and first hour of the recovery period. Arterial and amniotic pressures were measured using Statham pressure transducers (P23 ID; Gould Inc., Oxnard, CA). Arterial blood pressure (ABP) was determined as the difference between instantaneous values of arterial and amniotic pressures. A PowerLab system was used for data acquisition and analysis (Chart 7 For Windows, ADInstruments Pty Ltd, Castle Hill, Australia).

Pressures, ECG, ECOG and EEG were recorded and digitized at 1000 Hz for further study. For ECG, a 60 Hz notch filter was applied, while for ECOG and EEG, a band pass 0.3 - 30 Hz filter was used. FHR was triggered and calculated online from arterial pressure systolic peaks.

Averaged values of FHR and ABP were calculated from artifact-free recordings of one hour of baseline, as well as between and during each consecutive variable FHR deceleration induced by the mild, moderate, and severe UCOs as previously reported.(Ross et al., 2013b) FHR_{nadir} was measured as the minimal FHR during a UCO; ABP_{max} was measured as maximal ABP during a UCO; ABP_{min} was measured as the minimal ABP during a UCO; ΔFHR was calculated as FHR deceleration depth during UCO, *i.e.*, the difference between mean FHR between UCO and FHR_{nadir}; ΔABP was calculated as the difference between ABP_{max} and mean ABP between UCO; ΔABP_{UCO} was calculated as the difference between ABP_{max} and ABP_{min} to capture the known biphasic change of ABP during each UCO.

The ECOG and EEG signals were sampled down to 100 Hz prior to the ECOG and EEG analysis. Subsequently, the voltage amplitude and 95% spectral edge frequency (SEF), this being the ECOG/EEG frequency below which 95% of ECOG/EEG spectral power is found, were calculated over 3 second intervals for the duration of the experimental monitoring. For each animal, mean values of the ECOG and EEG amplitudes and SEF were determined at baseline as well as during and between UCO for each of the deceleration series. To track the correlation between the ECOG/EEG and FHR, we determined the cross-correlation function (CCF) between the smoothed ECOG/EEG amplitudes (absolute value of the ECOG/EEG signals) and the smoothed FHR with a square smoothing kernel of 10 seconds with delays of -100 to 100 seconds (Matlab, Mathworks, Natick, MA, USA). CCF analysis tests the spectrographic similarity of ECOG and EEG recordings. The CCF were normalized to 1 and maxima of the normalized CCF were determined. The closer

these maxima (CCFM) are to 1, the higher is the correlation between both signals. We then compared the correlation between the different levels of occlusion (*i.e.*, baseline, mild, moderate and severe UCO) as a function of the delay:

$$C_{xy}(\tau) = \frac{E((x(t) - E(x))(y(t-\tau) - E(y))}{\sigma(x)\sigma(y)}$$

where $\sigma(x)$ is its standard deviation, and E(x) is its expected value.

To further validate the degree of synchronization between ECOG/EEG amplitudes and FHR, we compared the coherence in the 0.01-0.1 Hz band - representing the 10-100 seconds locking period - to all other frequency bands. 0.01-0.1 Hz represents the expected coherence time scale between these two signals (Low et al., 1995) ENREF 13. The spectral coherence is the ratio between the squared Fourier transform of the cross-correlation function divided by the Fourier transform of the correlation function of each signal by itself. Since the correlated ECOG/EEG-FHR activities were consistently observed during the severe UCO series, the above comparisons were made accordingly between the severe UCO series versus all the preceding experimental stages (*i.e.*, baseline, mild and moderate UCO).

Statistical analysis

Normal data distribution was tested using Kolmogorov-Smirnov test followed by parametric or non-parametric tests, as appropriate. Arterial pH and BD measurements in response to repetitive UCOs and associated variable decelerations were compared with the corresponding baseline values by one-way repeated-measures analysis of variance (ANOVA) with Student-Newman-Keuls post hoc analysis. One-way repeated measures ANOVA followed by Holm-Sidak (versus baseline) or Student-Newman-Keuls (pairwise) tests for multiple comparisons have been used to assess differences in ECOG/EEG and cardiovascular responses to UCO within N/UCO and H/UCO groups. Differences between ECOG and EEG within each group were assessed using t-test or signed rank test. Differences in ECOG/EEG and cardiovascular alterations during ECOG/EEG-FHR synchronized pattern were tested using t-test or signed rank test. Differences between the ECOG/EEG and cardiovascular variables of the N/UCO and H/UCO groups at each time point were assessed using rank-sum test. No adjustment for multiple comparison was undertaken at this point.(Rothman, 1990) A two-sided rank sum test was used to detect changes in CCF and spectral coherence between the ECOG/EEG amplitudes and FHR during the severe UCO series versus the preceding stages of the experiment (*i.e.*, baseline, mild and moderate UCO).

All values are expressed as means ± SEM. Statistical significance was assumed for $P < .05$. Pearson or Spearman correlation analysis was performed as appropriate, and R values are presented where $P < .05$ (SPSS 19; IBM, Armonk, NY).

RESULTS

Responses of normoxic and hypoxic fetuses to umbilical cord occlusions

All results are summarized in Table 1 and Fig. 2. We present responses of the N/UCO group and highlight the H/UCO group responses where they were different from the N/UCO group.

In the N/UCO group, during the baseline period, fetal arterial pH (7.35±0.01) as well as FHR (159±5 bpm) and ABP (44±2 mmHg) were within the physiologic range. This was similar in H/UCO group (fetal arterial pH 7.34±0.01, Table 1). Arterial O2Sat measured 65±2% which was higher than in the H/UCO group where it measured 41±6% ($p=0.02$).

In the N/UCO group, baseline EEG amplitude measured 37±4 μV which was 3.5x lower than ECOG amplitude at 127±14 μV ($p=0.01$). Baseline EEG SEF was 4.4±0.3 Hz and 1.5x lower than baseline ECOG SEF at 6.7±0.6 Hz ($p<0.01$). In contrast, in the H/UCO group, ECOG and EEG amplitude and SEF were similar and EEG amplitude at 96±9 μV was ~2.6fold higher than in the N/UCO group (Table 1).

In both, N/UCO and H/UCO groups, repetitive UCO and associated variable FHR decelerations resulted in development of severe fetal acidosis (N/UCO: pH 7.35±0.01 to 7.00±0.03; BD -1.6±0.7 to 13.6±1.1 mEq/l; H/UCO: pH 7.34±0.01 to 7.01±0.02; BD -2.0±0.7 to 15.5±0.3 mEq/l) by the end of the severe UCO series (all $p<0.01$).

In the N/UCO group, ABP increased on average to 75±3 mmHg during each UCO versus 54±2 mmHg between each UCO ($p<0.05$). FHR deceleration depth averaged 66±6 bpm (decreasing to 94±6 during each UCO versus 159±3 bpm between each UCO, $p<0.05$). In contrast, in the H/UCO group, ABP remained unchanged at 59±5 mmHg during and between each UCO. Consequently, throughout the mild, moderate and severe UCO series, that is, well before the ECOG/EEG-FHR synchronized pattern onset, ABP showed pathologically low increases of 3±1 mmHg on average with each UCO-induced FHR deceleration. FHR deceleration responses in the H/UCO group were similar to those in the N/UCO group as intended.

In the N/UCO group, ECOG began to show cyclical behavior correlated with UCO-induced FHR decelerations starting at a pH of 7.22±0.03 (range 7.32 – 7.07), and 48±11 min (range 1h41min - 20 min) prior to the pH dropping <7.00: ECOG SEF began to consistently increase to 11.0±0.4 Hz from 8.6±0.5 Hz ($p<0.01$) and ECOG amplitude began to consistently decrease to 102±17 μV from 209±26 μV during versus between each UCO, respectively ($p<0.001$) (Fig. 1). In the H/UCO group, this dynamics was also observed at a similar pH of 7.23±0.01 (range 7.27 –

7.21), and 59±15 min (range 1h34min - 14 min) prior to the pH dropping <7.00 with similar values for ECOG SEF and amplitude (Table 1).

In both N/UCO and H/UCO groups, EEG behaved similarly to the cyclical ECOG behaviour correlated with UCO-induced FHR decelerations. In the N/UCO group, EEG began to show cyclical behaviour correlated with UCO-induced FHR decelerations at a pH of 7.22±0.03 (range 7.32 – 7.07), and 45±9 min (range 1h33min - 20 min) prior to the pH dropping <7.00, SEF began to consistently increase to 9.0±0.7 Hz from 8.1±0.7 Hz ($p<0.05$) and amplitude began to consistently decrease to 81±8 μV from 138±17 μV during versus between UCO and associated FHR decelerations ($p<0.001$) (Fig. 1). In the H/UCO group, this EEG dynamics was similar for the amplitude occurring at a pH of 7.20±0.03 (range 7.27 – 7.15), and 49±15 min (range 1h18min - 12 min) prior to the pH dropping <7.00; meanwhile EEG SEF did not change during compared to between UCOs averaging 7.4±0.4 Hz. Similar to the observation at the baseline, here we found that in the H/UCO group EEG amplitude between the UCOs was ~1.7fold higher than in the N/UCO group (Table 1). Consequently, while in the N/UCO group EEG measured ~66% of the ECOG amplitude between the UCOs, it was similar to ECOG amplitude at this time in the H/UCO group.

In the N/UCO group, 50±14 min (range 2h06min – 19 min) prior to pH<7.00, ABP began to consistently show pathologically low increases of 4±3 mmHg with each FHR deceleration compared to the dynamics during the mild, moderate and severe UCOs before the ECOG/EEG-FHR synchronized pattern onset ($p<0.05$, ΔABP in Table 1). The timing of the observed ECOG and EEG amplitude and SEF recurring pattern changes was highly correlated to the timing of the onset of the pathological ΔABP (both $R=0.99$, $p<0.001$) (Fig. 1). This cardiovascular behaviour was also observed in the H/UCO group at a similar time of 56±15 min (range 1h32min – 12 min) prior to pH<7.00. Notably, in the H/UCO group – in contrast to the N/UCO group – the pathologically low ABP increases of 3±3 mmHg with each FHR deceleration were similar in magnitude to the ΔABP dynamics during mild, moderate and severe UCO before the ECOG/EEG-FHR synchronized pattern onset (ΔABP in Table 1). That is, in the H/UCO group, the difference of this phenomenon to the ΔABP values before the pattern onset was not in absolute values but in the consistent lack of increase with *each* occlusion and FHR deceleration. Similar to the N/UCO group, the timing of the onset of the observed ECOG and EEG amplitude and SEF recurring pattern

changes was highly correlated to the timing of the onset of the pathological ΔABP pattern (both R=1, $p<0.001$) for individual animals.

Evidence of ECOG/EEG – FHR synchronization in N/UCO and H/UCO groups

To test for the assumption that ECOG/EEG amplitude and FHR show temporal synchronization early prior to the onset of severe acidemia (Frasch et al., 2011) in N/UCO and H/UCO groups, we computed in each group the correlation between the smoothed ECOG/EEG amplitudes and smoothed FHR with a 10 seconds moving average with a delay ranging from -100 seconds to 100 seconds (Figure 2). In both groups, only during the severe UCO series did a clear correlation with a phase lag appear between ECOG/EEG amplitude and FHR. Of note, the result was more pronounced for EEG-FHR cross-correlation function (CCF) than for ECOG-FHR CCF.

If such synchronization exists, we expected the difference between the maximal and minimal correlation as a function of the phase to be maximal. We thus checked the distribution of this difference in all sheep fetuses of the N/UCO and H/UCO groups.

In the N/UCO group, the difference between the maximal and minimal correlation as a function of the phase was significantly larger during the severe UCO series compared to all previous time periods (baseline, mild and moderate UCO series), with an average difference of 0.16±0.08 (ECOG-FHR CCF) and 0.5±0.16 (EEG-FHR CCF) during the severe UCO series *vs.* 0.09±0.07 (ECOG-FHR CCF) and 0.31±0.14 (EEG-FHR CCF) for all previous time periods ($p<0.01$ and $p<0.001$, respectively, Figure 2A). To validate the synchronization (phase locking) between ECOG/EEG amplitude and FHR, we compared the coherence in the 0.01-0.1 Hz band - representing the 10-100 seconds locking period - to all other frequency bands. The average coherence in this band for ECOG-FHR and EEG-FHR was at 0.19±0.02 *vs.* 0.15±0.04 ($p<0.01$) and 0.19±0.04 *vs.* 0.15± 0.05 ($p<0.05$) indeed significantly higher during the severe UCO series than during all previous time periods.

In the H/UCO group, the difference between the maximal and minimal correlation as a function of the phase was significantly larger during the severe UCO series compared to all previous time periods (baseline, mild and moderate UCO series), with an average difference of 0.21±0.02 (ECOG-FHR CCF) and 0.25±0.02 (EEG-FHR CCF) during the severe UCO series *vs.* 0.15±0.01 (ECOG-FHR CCF) and 0.16±0.01 (EEG-FHR CCF) for all previous time periods ($p<0.01$ and $p<0.001$, respectively, Figure 2B). To validate the synchronization (phase locking) between ECOG/EEG amplitude and FHR, we compared the coherence in the 0.01-0.1 Hz band -

representing the 10-100 seconds locking period - to all other frequency bands. The average coherence in this band for ECOG-FHR and EEG-FHR was at 0.21±0.04 *vs.* 0.15±0.02 ($p<0.01$) and 0.25±0.05 *vs.* 0.16±0.02 ($p<0.001$) again significantly higher during the severe UCO series than during all previous time periods.

DISCUSSION

Fetal EEG during labour may permit early detection of acidemia

Our findings provide proof of principle for fetal EEG monitoring during high-risk human labour. EEG recorded from the scalp of near-term fetal sheep shows changes comparable to ECOG during normoxia (Frasch et al., 2010) and during worsening hypoxic-acidemia. (Frasch et al., 2012) Compared to the paradigm of fixed complete UCOs of increasing frequency we tested (Frasch et al., 2011), the frequency of UCOs does not impact on the pattern of the ECOG/EEG amplitude response, but it does impact on the ECOG/EEG frequency characteristics. The next step is to develop reliable online algorithms to detect such variable amplitude and frequency responses of fetal EEG. Overall, this confirms the notion that ECOG activity acquired from supradural electrodes and EEG activity acquired from scalp electrodes should similarly reflect the field potential neuronal activity, albeit with the ECOG amplitude larger than the corresponding EEG signals. Clinical studies with Cerebral Function monitors in newborns with suspected hypoxic-ischemic encephalopathy have demonstrated the feasibility of recording EEG activity from scalp electrodes and predictive value for longer term neurologic sequellae (Thordstein et al., 2004, de Vries and Hellstrom-Westas, 2005). However, this predictive ability relates to existent and evolving injury within the brain with variable degrees of necrotic/apoptotic cell death either primary or delayed (Williams et al., 1991) and the impact on EEG activity, rather than an adaptive suppression of synaptic activity as a protective mechanism. EEG activity as a measure of brain function has also been assessed in the human fetus during labour-related events after rupture of the membranes. Rosen et al. pioneered the human fetal EEG field in the 1970ies by placing two 'suction-cup' EEG electrodes transvaginally on the fetal scalp at some distance apart from each other and were able to acquire brain activity during uterine contractions, epidurals and drug administration. (Borgstedt et al., 1975, Chik et al., 1976, Sokol et al., 1977, Frasch et al., 2011, Prout et al., 2012, Ross et al., 2013a, Ross et al., 2013b) However, these studies were hampered by the lack of advanced computer-based technology for analyzing large data sets and the need for multiple scalp electrodes which made large scale clinical usage impractical. Recently, Thaler et al. used real-time power spectral analysis of fetal EEG during labour to facilitate signal processing and interpretation. (Thaler et al., 2000) However, while clearly demonstrating the presence of sleep state cycles in the human fetus, this study was limited to 14 healthy pregnancies with normal outcomes, and again used multiple scalp electrodes to acquire EEG which is not feasible for large

scale clinical use. As such, there has been continued need to develop a single transvaginal probe capable of acquiring EEG and FHR signals as an essential first step to ensure the clinical feasibility of monitoring both for the assessment of fetal health during labour.

Our findings overcome the limitations discussed above by providing 1) an EEG probe that can be used practically and by every obstetrician trained in placing the spiral FHR scalp probe during labour and 2) proving that use of such EEG probe would permit an early detection of worsening hypoxic-acidemia allowing for intervention. As an ancillary tool for intrapartum FHR monitoring, fetal EEG monitoring should provide additional decision making power to the delivering obstetrician whether to allow a labour to proceed or deliver acutely, thus minimizing the number of babies born with severe acidemia and increased risk for brain injury at one hand and decreasing the number of unnecessary Caesarian sections at the other hand.

Prospective clinical studies are urgently needed to validate this novel approach to electronic fetal monitoring during labour.

Effects of preceding hypoxia on EEG and cardiovascular responses to umbilical cord occlusions

The chief finding is that ECOG amplitude of the H/UCO group fetuses was ~50% that of the N/UCO group for most of the UCO series. This was accompanied by a small but significant decrease in ECOG SEF between the occlusions during the severe UCO series although still remaining within the theta band range. This finding is in line with our previous ECOG findings in this and other laboratories. (Frasch et al., 2011, Wassink et al., 2013) In contrast, EEG amplitude was ~2fold higher in the H/UCO group than in the N/UCO group both at baseline and during the occlusions once the ECOG/EEG – FHR synchronized pattern was observed. This is likely due to artifacts in fetal sheep EEG. We anticipate that human fetal EEG will provide a cleaner signal while retaining the fundamental EEG-FHR pattern we report herein. This is supported by earlier studies that reported well delineated sleep states discernible from fetal EEG acquired during labour. (Thaler et al., 2000)

There was also a pronounced impact of preceding hypoxia on cardiovascular responses to the UCOs. An uncompromised fetus responds with an ABP increase during a UCO, a behaviour that is altered as the occlusions progress and the acidemia increases to the extent that ABP no longer increases during the occlusions. (Frasch et al., 2011) In the present study we observed that this relative change of ABP during each occlusion, ΔABP, was considerably lower throughout all H/UCO series and similar to values seen during the ECOG/EEG-FHR synchronized pattern in

N/UCO and H/UCO groups. Moreover, during the ECOG/EEG-FHR synchronized pattern, H/UCO group fetuses showed ~60% lower FHR deceleration depth than N/UCO group fetuses (cf. ΔFHR in Table 1) due to a ~35% lower mean FHR between UCOs. These findings suggest that the ECOG/EEG-FHR synchronized pattern onset, while correlated in time to the onset of the pathological ΔABP, is not solely secondary to the cardiovascular compromise of cerebral auto-regulation, but instead neurally mediated at an arterial pH around 7.20. Furthermore, chronic hypoxia preceding UCO of increasing severity had no impact on the average timing of ~53 minutes prior to pH drop to <7.00 when adaptive brain shut-down was observed. We discuss possible mechanisms linking systemic pH changes with adaptive brain shut-down elsewhere. (Xu et al., 2014)

Noteworthy, we observed hardly any effect of chronic hypoxia on EEG properties suggesting that EEG will readily track fetal brain electrical activity regardless of pre-existing hypoxia. During ECOG/EEG-FHR synchronized pattern, chronic hypoxia ablated the difference in EEG SEF during compared to between each UCO, seen in the N/UCO group. This suggests that efforts in development of robust automated algorithms for pattern detection should aim at using amplitude properties of EEG rather than its frequency properties. Chronic hypoxia likely resulted in ECOG suppression in the H/UCO group fetuses which thereby is the reason we saw no difference between ECOG and EEG amplitude values in the H/UCO group as we did in the N/UCO group fetuses.

Growth restricted infants with chronic hypoxemia due to placental dysfunction are at a greater risk for concerning acidemia at birth and thereby subsequent adverse neurological outcomes due to superimposed acute hypoxemia during labour. (Kaneko et al., 2003, Liston et al., 2007, Frasch et al., 2009, Frasch et al., 2011) Our findings show that regardless of preceding hypoxia, the EEG-FHR monitoring in IUGR fetuses would allow detection of EEG-FHR synchronization pattern as an early warning for impending acidemia.

Fetal adaptive brain shut-down is a pro-active mechanism that is not impacted by preceding hypoxia

The above considerations lead us to propose that fetal adaptive brain shut-down revealed via ECOG/EEG-FHR synchronized behaviour is a pro-active and likely neuroprotective mechanism. First, there is a remarkable consistency of pH at ~7.20, when the pattern appears in N/UCO and H/UCO groups. This suggests an active mechanism triggering the adaptive brain shutdown. This is in line with literature suggesting an adenosine (A1) receptor mediated process of cerebral

metabolic shut-down in fetal brain. (Blood et al., 2003, Hunter et al., 2003, Pearce, 2006) In addition, using the same animal model with concurrent measurements of cerebral blood flow and metabolic rates we demonstrated that when cerebral oxygen delivery is severely compromised as during the complete UCOs, ECOG flattens reflecting decreasing synaptic activity as a neuroprotective mechanism. (Kaneko et al., 2003) Second, hypoxia effects are seen mostly in cardiovascular responses and ECOG amplitude (decrease in H/UCO group compared to N/UCO group), but not in the pH or average time when we observed the ECOG/EEG-FHR synchronized pattern. This is also consistent with literature in this animal model. (Keunen and Hasaart, 1999, Pulgar et al., 2007, Wassink et al., 2013)

Significance and future directions

The utility of joint EEG-FHR monitoring is based on consistent emergence of synchronized UCO-triggered EEG-FHR changes prior to reaching a severe degree of fetal acidemia at which brain injury might occur. These changes are due to the mechanism of adaptive brain shut-down triggered at pH ~7.20 and do not depend on preceding cardiovascular behavior due to chronic hypoxia. This makes it likely that the mechanism will be observed in a large population of fetuses with or without preceding hypoxia at labour onset. Fetal EEG monitoring during labour has the potential to serve as a valuable ancillary technique of electronic fetal monitoring. Together with FHR, EEG can provide an early, inexpensive and easily implementable and interpretable tool to accurately predict incipient fetal acidemia in fetuses.

Acknowledgements

The authors wish to thank Maria Sinacori, Carmen Movila, Ashley Keen, Jennifer Thompson, Karolina Piorkowska and Dora Siontas for technical assistance. We further gratefully acknowledge the contribution to the research presented thanks to a workshop organized by the Mathematical Biosciences Institute (MBI) at Ohio State University, Columbus, OH, and the Fields Institute at the University of Toronto.

References:

Blood AB, Hunter CJ, Power GG (2003) Adenosine mediates decreased cerebral metabolic rate and increased cerebral blood flow during acute moderate hypoxia in the near-term fetal sheep. J Physiol 553:935-945.

Borgstedt AD, Rosen MG, Chik L, Sokol RJ, Bachelder L, Leo P (1975) Fetal electroencephalography. Relationship to neonatal and one-year developmental neurological examinations in high-risk infants. American Journal of Diseases of Children (1960) 129:35-38.

Chik L, Sokol RJ, Rosen MG, Borgstedt AD (1976) Computer interpreted fetal electroencephalogram. I. Relative frequency of patterns. American Journal of Obstetrics and Gynecology 125:537-540.

de Vries LS, Hellstrom-Westas L (2005) Role of cerebral function monitoring in the newborn. Archives of disease in childhoodFetal and neonatal edition 90:F201-207.

Fletcher AJ, Gardner DS, Edwards CM, Fowden AL, Giussani DA (2006) Development of the ovine fetal cardiovascular defense to hypoxemia towards full term. Am J Physiol Heart Circ Physiol 291:H3023-3034.

Frasch M, Durosier L, Duchatellier C, Richardson B (2012) Fetal sheep electrocorticogram and electroencephalogram changes accompanying variable fetal heart rate decelerations warn early of acidemia. Reprod Sci 19:F-090.

Frasch M, Keen A, Matushewski B, Richardson B (2010) Comparability of electroenkephalogram (EEG) versus electrocorticogram (ECOG) in the ovine fetus near term. Reprod Sci 17:51A.

Frasch MG, Keen AE, Gagnon R, Ross MG, Richardson BS (2011) Monitoring Fetal Electrocortical Activity during Labour for Predicting Worsening Acidemia: A Prospective Study in the Ovine Fetus Near Term. PloS one 6:e22100.

Frasch MG, Mansano RZ, Gagnon R, Richardson BS, Ross MG (2009) Measures of acidosis with repetitive umbilical cord occlusions leading to fetal asphyxia in the near-term ovine fetus. American Journal of Obstetrics and Gynecology 200:200.e201-207.

Gardner DS, Fletcher AJ, Bloomfield MR, Fowden AL, Giussani DA (2002) Effects of prevailing hypoxaemia, acidaemia or hypoglycaemia upon the cardiovascular, endocrine and metabolic responses to acute hypoxaemia in the ovine fetus. J Physiol 540:351-366.

Hunter CJ, Bennet L, Power GG, Roelfsema V, Blood AB, Quaedackers JS, George S, Guan J, Gunn AJ (2003) Key neuroprotective role for endogenous adenosine A1 receptor activation during asphyxia in the fetal sheep. Stroke 34:2240-2245.

Itskovitz J, LaGamma EF, Rudolph AM (1983) Heart rate and blood pressure responses to umbilical cord compression in fetal lambs with special reference to the mechanism of variable deceleration. Am J Obstet Gynecol 147:451-457.

Kaneko M, White S, Homan J, Richardson B (2003) Cerebral blood flow and metabolism in relation to electrocortical activity with severe umbilical cord occlusion in the near-term ovine fetus. Am J Obstet Gynecol 188:961-972.

Keen AE, Frasch MG, Sheehan MA, Matushewski BJ, Richardson BS (2011) Electrocortical activity in the near-term ovine fetus: automated analysis using amplitude frequency components. Brain Res 1402:30-37.

Keunen H, Hasaart TH (1999) Fetal arterial pressure and heart rate changes in surviving and non-surviving immature fetal sheep following brief repeated total umbilical cord occlusions. Eur J Obstet Gynecol Reprod Biol 87:151-157.

Liston R, Crane J, Hamilton E, Hughes O, Kuling S, MacKinnon C, McNamara H, Milne K, Richardson B, Trepanie MJ (2002a) Fetal health surveillance in labour. J Obstet Gynaecol Can 24:250-276; quiz 277-280.

Liston R, Crane J, Hughes O, Kuling S, MacKinnon C, Milne K, Richardson B, Trepanier MJ (2002b) Fetal health surveillance in labour. J Obstet Gynaecol Can 24:342-355.

Liston R, Sawchuck D, Young D (2007) Fetal health surveillance: antepartum and intrapartum consensus guideline. J Obstet Gynaecol Can 29:S3-56.

Low JA, Panagiotopoulos C, Derrick EJ (1995) Newborn complications after intrapartum asphyxia with metabolic acidosis in the preterm fetus. Am J Obstet Gynecol 172:805-810.

Pearce W (2006) Hypoxic regulation of the fetal cerebral circulation. J Appl Physiol (1985) 100:731-738.

Prout AP, Frasch MG, Veldhuizen R, Hammond R, Matushewski B, Richardson BS (2012) The impact of intermittent umbilical cord occlusions on the inflammatory response in pre-term fetal sheep. PLoS One 7:e39043.

Prout AP, Frasch MG, Veldhuizen RA, Hammond R, Ross MG, Richardson BS (2010) Systemic and cerebral inflammatory response to umbilical cord occlusions with worsening acidosis in the ovine fetus. Am J Obstet Gynecol 202:82 e81-89.

Pulgar VM, Zhang J, Massmann GA, Figueroa JP (2007) Mild chronic hypoxia modifies the fetal sheep neural and cardiovascular responses to repeated umbilical cord occlusion. Brain Res 1176:18-26.

Richardson B, Gagnon R (2008) Behavioural state activity and fetal health & development. In: Maternal-Fetal Medicine, vol. 6th (Creasy, R. K. and Resnik, R., eds) Philadelphia: WB Saunders Co.

Richardson BS, Rurak D, Patrick JE, Homan J, Carmichael L (1989) Cerebral oxidative metabolism during sustained hypoxaemia in fetal sheep. Journal of developmental physiology 11:37-43.

Ross MG, Amaya K, Richardson B, Frasch MG (2013a) Association of atypical decelerations with acidemia. Obstet Gynecol 121:1107-1108.

Ross MG, Jessie M, Amaya K, Matushewski B, Durosier LD, Frasch MG, Richardson BS (2013b) Correlation of arterial fetal base deficit and lactate changes with severity of variable heart rate decelerations in the near-term ovine fetus. American journal of obstetrics and gynecology 208:285 e281-286.

Rothman KJ (1990) No adjustments are needed for multiple comparisons. Epidemiology 1:43-46.

Sokol RJ, Rosen MG, Chik L (1977) Fetal electroencephalographic monitoring related to infant outcome. American Journal of Obstetrics and Gynecology 127:329-330.

Thaler I, Boldes R, Timor-Tritsch I (2000) Real-time spectral analysis of the fetal EEG: a new approach to monitoring sleep states and fetal condition during labor. Pediatr Res 48:340-345.

Thordstein M, Flisberg A, Lofgren N, Bagenholm R, Lindecrantz K, Wallin BG, Kjellmer I (2004) Spectral analysis of burst periods in EEG from healthy and post-asphyctic full-term neonates. Clinical neurophysiology : official journal of the International Federation of Clinical Neurophysiology 115:2461-2466.

Wassink G, Bennet L, Davidson JO, Westgate JA, Gunn AJ (2013) Pre-existing hypoxia is associated with greater EEG suppression and early onset of evolving seizure activity during brief repeated asphyxia in near-term fetal sheep. PLoS ONE 8:e73895.

Williams CE, Gunn A, Gluckman PD (1991) Time course of intracellular edema and epileptiform activity following prenatal cerebral ischemia in sheep. Stroke; a journal of cerebral circulation 22:516-521.

Xu A, Durosier L, Ross MG, Hammond R, Richardson BS, Frasch MG (2014) Adaptive brain shut-down counteracts neuroinflammation in the near-term ovine fetus. Front Neurol - Neuropediatrics.

Table 1. Brain and cardiovascular responses to repetitive umbilical cord occlusions (UCOs) in normoxic (N/UCO) and hypoxic (H/UCO) groups.

N/UCO group	baseline	mild UCO		mod UCO		sev UCO		Pattern	
		dur UCO	btw UCO	dur UCO	btw UCO	dur UCO	btw UCO	dur UCO	btw UCO
ECoG amplitude, μV	127 ± 14	130 ± 14	131 ± 14	152 ± 29	152 ± 29	140 ± 24	156 ± 26	102 ± 17$^{\$}$	209 ± 26
ECoG SEF (95%), Hz	6.7 ± 0.6	8.2 ± 0.5*	8.1 ± 0.5*	7.6 ± 0.3	7.5 ± 0.4	6.0 ± 0.4	5.9 ± 0.3	11.0 ± 0.4$^{\$}$	8.6 ± 0.5
EEG amplitude, μV	37 ± 4^{+}	61 ± 13^{+}	66 ± 14^{+}	48 ± 11^{+}	56 ± 12^{+}	73 ± 11^{+}	102 ± 13*	81 ± 8$^{\$}$	138 ± 17^{+}
EEG SEF (95%), Hz	4.4 ± 0.3^{+}	5.2 ± 0.9^{+}	5.0 ± 0.9^{+}	5.4 ± 0.8^{+}	4.3 ± 0.4^{+}	4.7 ± 0.4^{+}	4.4 ± 0.2^{+}	9.0 ± 0.7$^{\$}$	8.1 ± 0.7
FHR, bpm	159 ± 5	165 ± 5	162 ± 3	131 ± 6*	153 ± 2	115 ± 10*	162 ± 3	101 ± 6$^{\$}$	171 ± 8
ABP, mmHg	44 ± 2	48 ± 2*	49 ± 2*	54 ± 2*	53 ± 2*	60 ± 2*	60 ± 1*	57 ± 2	60 ± 2
ABP_{max}, mmHg		64 ± 3$^{\$}$		74 ± 3$^{\$}$		88 ± 2$^{\$}$		65 ± 3	
ABP_{min}, mmHg		32 ± 2		37 ± 2		36 ± 2		33 ± 3	
FHR_{nadir}, bpm		123 ± 8$^{\$}$		95 ± 5$^{\$}$		63 ± 5$^{\$}$		80 ± 6$^{\$}$	
ΔFHR, bpm		39 ± 8$^{\$\S}$		59 ± 4$^{\$\S}$		99 ± 7$^{\$}$		90 ± 11	
ΔABP_{UCO}, mmHg		33 ± 3		37 ± 3		52 ± 2		32 ± 2	
ΔABP, mmHg		16 ± 2$^{\$\S}$		20 ± 2$^{\$\S}$		28 ± 2$^{\$\S}$		4 ± 3	

H/UCO group	baseline	mild UCO		mod UCO		sev UCO		Pattern	
		dur UCO	btw UCO	dur UCO	btw UCO	dur UCO	btw UCO	dur UCO	btw UCO
ECoG amplitude, μV	100 ± 13	86 ± 11	91 ± 11$^{\#}$	79 ± 7$^{\#}$	84 ± 6$^{\#}$	79 ± 14$^{\#}$	110 ± 17	76 ± 10$^{\$}$	173 ± 27
ECoG SEF (95%), Hz	5.7 ± 1.1	7.7 ± 1.4	7.5 ± 1.7	6.7 ± 0.9	6.9 ± 1.0	6.1 ± 0.5	5.0 ± 0.3$^{\#}$	10.1 ± 1.2$^{\$}$	8.5 ± 0.8
EEG amplitude, μV	96 ± 9$^{\#}$	85 ± 18	97 ± 20	94 ± 13	100 ± 15	111 ± 27	135 ± 30	115 ± 18$^{\$}$	230 ± 21$^{\#}$
EEG SEF (95%), Hz	3.9 ± 0.4	5.1 ± 0.9	4.8 ± 0.6	4.5 ± 0.8	4.4 ± 0.7	5.3 ± 0.6	4.9 ± 0.5	7.8 ± 0.6	6.9 ± 0.2
FHR, bpm	168 ± 5	155 ± 9	163 ± 5	125 ± 15*	157 ± 5	98 ± 5*	155 ± 4	85 ± 7	112 ± 10$^{\#}$
ABP, mmHg	48 ± 3	52 ± 3	53 ± 4	59 ± 7*	59 ± 8*	62 ± 3*	67 ± 4*	60 ± 6	63 ± 6
ABP_{max}, mmHg		67 ± 7		81 ± 9		92 ± 5$^{\$}$		66 ± 7	
ABP_{min}, mmHg		37 ± 3		42 ± 3		40 ± 5		40 ± 5	

FHR_{nadir}, bpm	134 ± 13$^{\$}$	103 ± 18	78 ± 16$^{\$}$	81 ± 6$^{\$}$
ΔFHR, bpm	29 ± 13	54 ± 17	77 ± 15$^{\$}$	38 ± 10$^{\#}$
ΔABP_{UCO}, mmHg	30 ± 5	39 ± 2	52 ± 2	26 ± 2
ΔABP, mmHg	15 ± 4	23 ± 6	25 ± 3	3 ± 3

UCO, umbilical cord occlusion; during, during UCO; between, between UCO; ECoG, electrocorticogram; EEG, electroencephalogram; SEF, 95% spectral edge frequency; FHR, fetal heart rate; ABP, mean arterial blood pressure; ABP_{max}, maximal ABP during a UCO; ABP_{min}, minimal ABP during a UCO; FHR_{nadir}, minimal FHR during a UCO; ΔFHR, FHR deceleration depth during UCO; ΔABP_{UCO}, difference between ABP_{max} and ABP_{min} during UCO; ΔABP, difference between ABP_{max} and mean ABP between UCO. Pattern, segment of UCO series when synchronized ECOG/EEG-FHR activities were observed (*i.e.*, adaptive brain shut-down).

Within group: *, versus baseline; $^{\$}$, pairwise (*i.e.*, during *vs.* between UCO or *vs.* another "during UCO" measurement for ABP_{max}, FHR_{nadir}, ΔFHR, ΔABP); $^{\$}$, versus mild UCO only; §, versus the respective variable during Pattern; $^{+}$, EEG versus ECoG at the same time point.

Between groups: $^{\#}$, H/UCO versus N/UCO.

Table 2. Oxygen saturation and glucose during the experiment's baseline and umbilical cord occlusions (UCOs).

Normoxic UCO		
	O_2 Sat	**Glucose**
Baseline	59.0 ± 16.8	1.1 ± 0.3
Mild 20 min	51.4 ± 14.9	1.1 ± 0.2
Mild 40 min	55.5 ± 16.5	1.1 ± 0.3
Mild 60 min	48.6 ± 22.3	1.1 ± 0.3
Moderate 20 min	49.9 ± 13.3	1.3 ± 0.3
Moderate 40 min	45.4 ± 15.6	1.3 ± 0.3
Moderate 60 min	44.5 ± 21.8	1.4 ± 0.3
Severe 20 min	42.3 ± 9.8	1.7 ± 0.3
Severe 40 min	42.7 ± 11.6	1.9 ± 0.2
Severe 60 min	41.4 ± 11.5	2.0 ± 0.2
End Exp	33.1 ± 11.2	2.0 ± 0.4

Hypoxic UCO		
	O_2 Sat	**Glucose**
Baseline	39.3 ± 14.9	1.0 ± 0.2
Mild 20 min interim	36.6 ± 15.6	1.2 ± 0.3
Mild 40 min interim	39.7 ± 14.9	1.2 ± 0.3
Mild 60 min interim	37.9 ± 14.9	1.2 ± 0.3
Moderate 20 min interim	34.4 ± 9.8	1.6 ± 0.5
Moderate 40 min interim	33.8 ± 9.7	1.6 ± 0.4

Moderate 60 min interim	31.9 ± 9.1	1.4 ± 0.4
Severe 20 min interim	25.4 ± 14.8	1.9 ± 0.4
Severe 40 min interim	28.4 ± 3.6	2.3 ± 0.2
Severe 60 min interim	31.1 ± 1.3	2.4 ± 0.1
End Exp	28.5 ± 6.7	2.1 ± 0.5

Blood samples taken between the mild, moderate and severe UCO series as well as at pH<7.00 (End Exp).

Figure Legends

Figure 1. Example of an individual ECOG / EEG response to repetitive UCO.
TOP: 60 min view of the adaptive brain shut-down pattern visible in ECOG and EEG in response to changes in arterial blood pressure (ABP) and fetal heart rate (FHR). BOTTOM: 10 min zoomed-in window of this pattern.

Figure 2. Cross correlation function (CCF) analysis of the ECOG/EEG response to FHR decelerations in **A)** normoxic (N/UCO) and **B)** hypoxic UCO (H/UCO) groups. 'Other', baseline, mild and moderate umbilical cord occlusion (UCO) series analyzed versus 'Severe' UCO series when the adaptive brain shut-down was observed in all fetuses.

1. Cross-correlation function between the smoothed ECOG/EEG amplitude and FHR with a 10 seconds moving average with a delay ranging from -100 seconds to 100 seconds. Different colours denote the individual signals while the thick red line is their average. Note the emergence of a clear correlation between ECOG/EEG amplitude and FHR during the severe UCO series.
2. The significant difference between the maximal and minimal correlation between ECOG/EEG amplitude and FHR measured as a function of the phase ($p<0.01$ and $p<0.001$, respectively). + signifies the outliers of the distributions (beyond the 90 % values).

Figure 3. Changes in arterial blood gases and acid-base status in response to the umbilical cord occlusions (UCOs).
N/UCO, normoxic UCO group; H/UCO, hypoxic UCO group.

Figures

Fig. 1

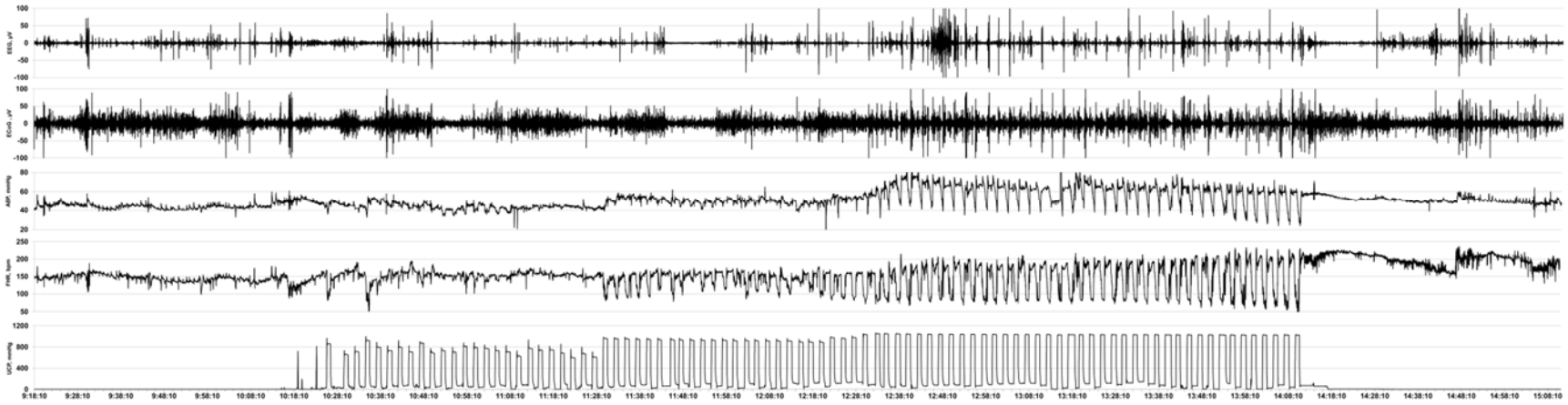

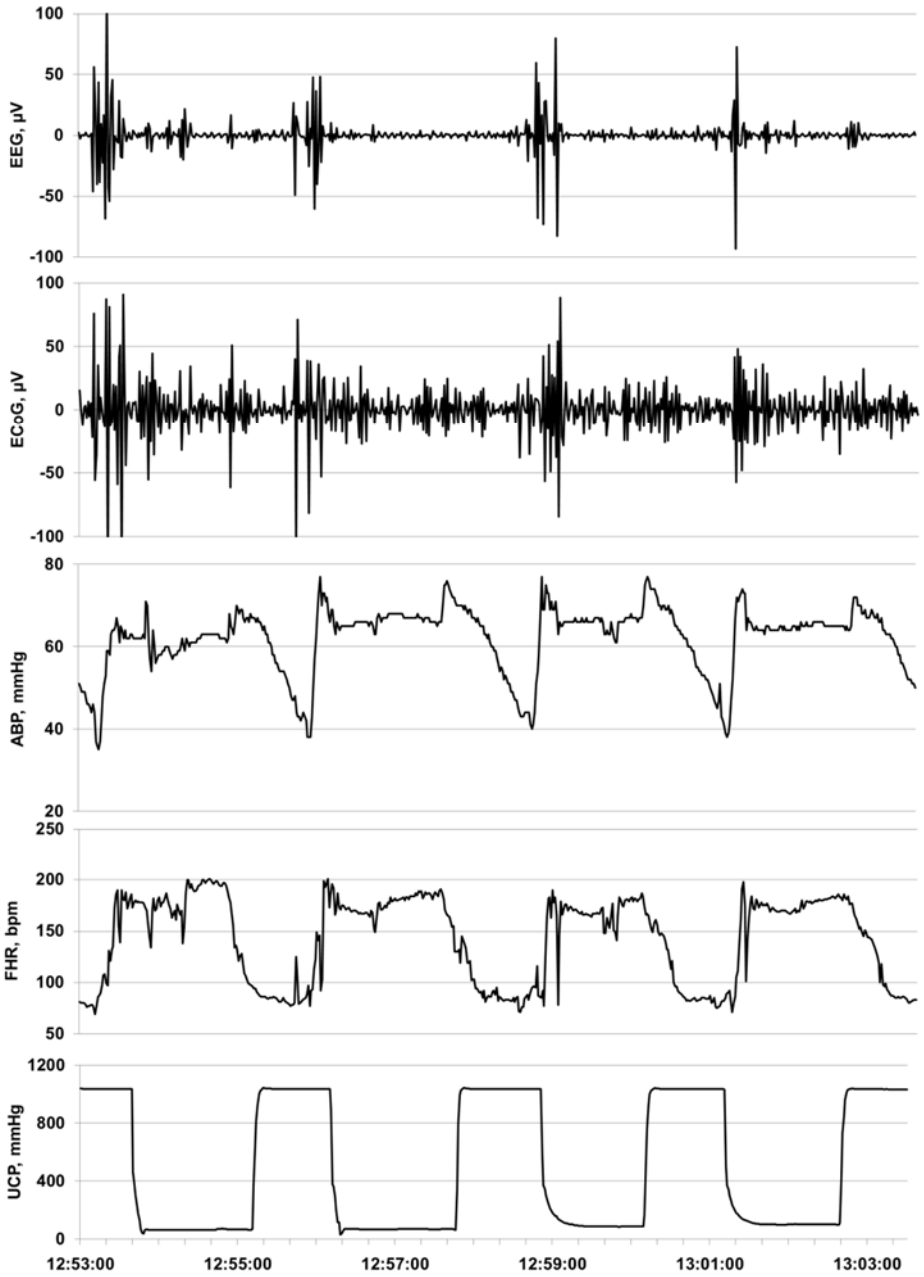
EEG, µV
100
50
0
-50
-100
ECoG, µV
100
50
0
-50
-100
ABP, mmHg
80
60
40
20
FHR, bpm
250
200
150
100
50
UCP, mmHg
1200
800
400
0
12:53:00
12:55:00
12:57:00
12:59:00
13:01:00
13:03:00

Fig. 2

A. Normoxic UCO group.

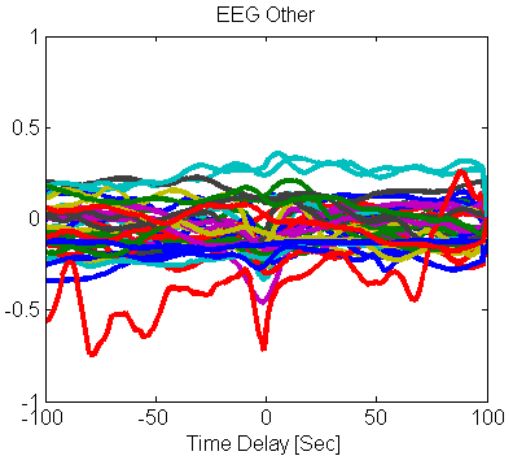

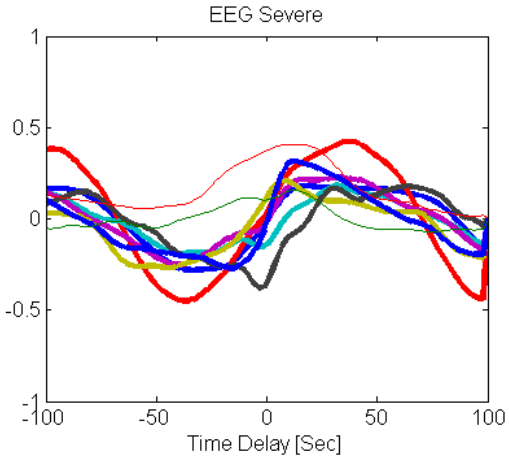

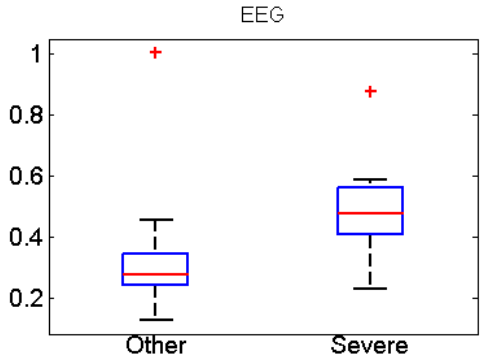

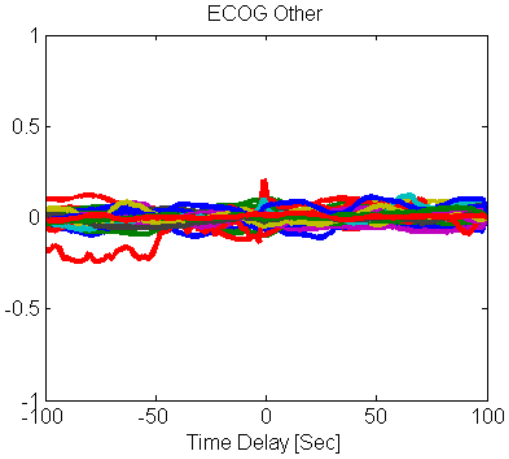

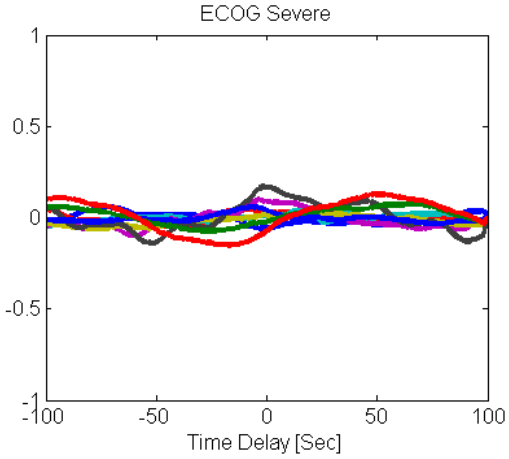

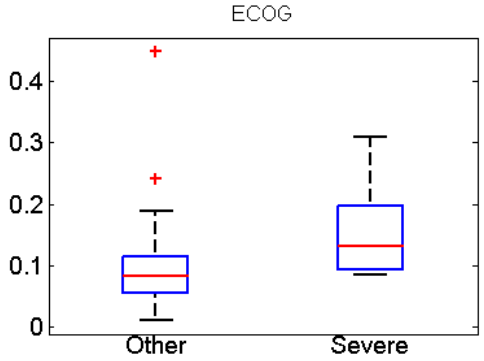

B. Hypoxic UCO group

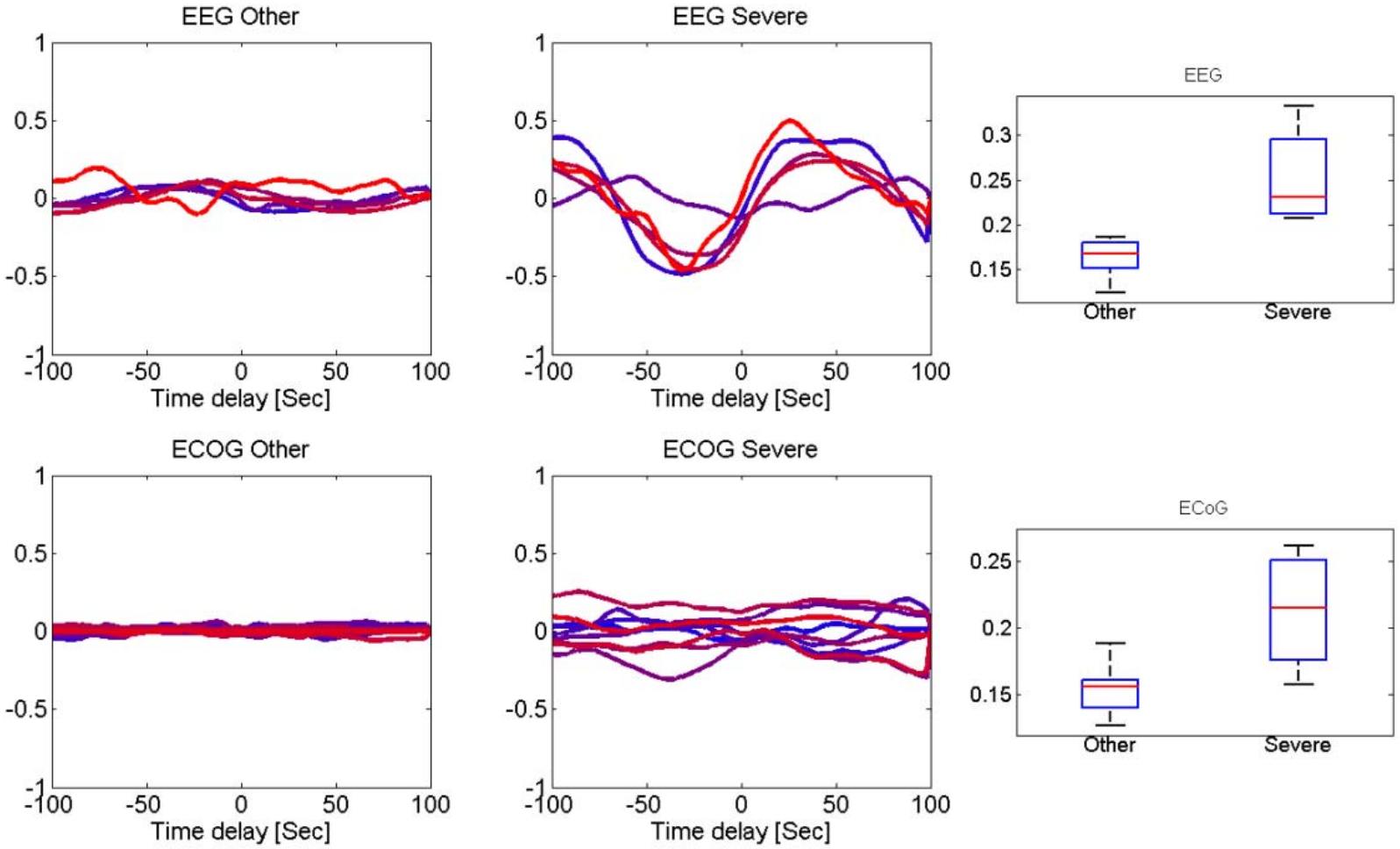

Fig. 3. Arterial blood gas and acid-base status

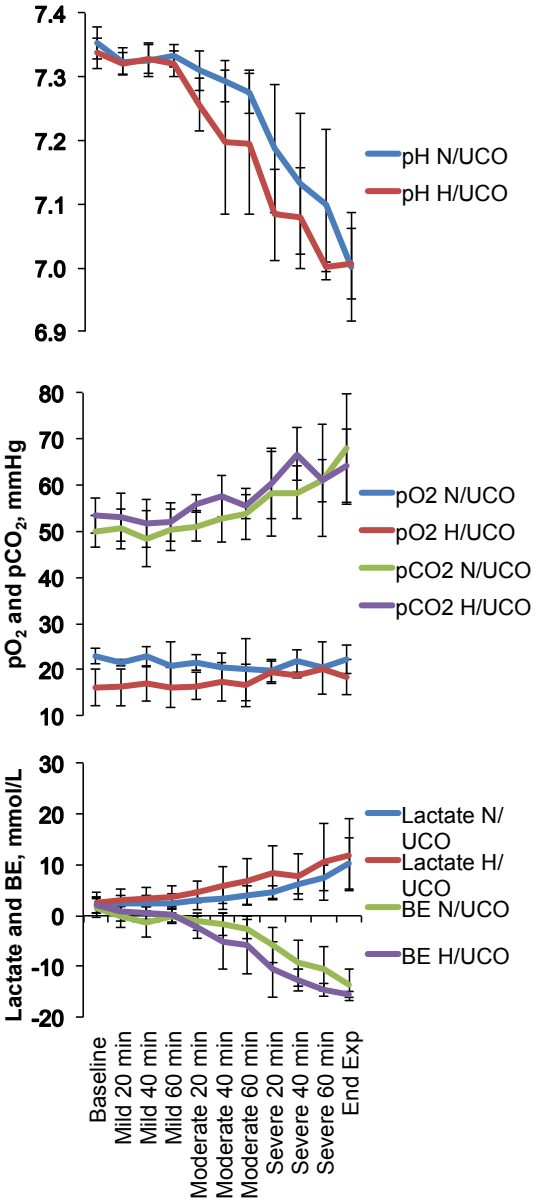

2.2 Sampling rate of heart rate variability impacts the ability to detect acidemia in ovine fetuses near-term

frontiers in PEDIATRICS

ORIGINAL RESEARCH ARTICLE
published: 05 May 2014
doi: 10.3389/fped.2014.00038

Sampling rate of heart rate variability impacts the ability to detect acidemia in ovine fetuses near-term

L. Daniel Durosier[1], Geoffrey Green[2], Izmail Batkin[2], Andrew J. Seely[2], Michael G. Ross[3], Bryan S. Richardson[4] and Martin G. Frasch[1,5]*

[1] Department of Obstetrics and Gynecology, CHU Ste-Justine Research Center, Université de Montréal, Montréal, QC, Canada
[2] Dynamical Analysis Laboratory, Ottawa Hospital Research Institute, University of Ottawa, Ottawa, ON, Canada
[3] Department of Obstetrics and Gynecology, LA BioMed at Harbor-UCLA Medical Center, Torrance, CA, USA
[4] Department of Obstetrics and Gynecology, University of Western Ontario, London, ON, Canada
[5] Faculty of Veterinary Medicine, Animal Reproduction Research Centre (CRRA), Université de Montréal, St-Hyacinthe, QC, Canada

Edited by:
Lewis Phillip Rubin, Texas Tech University Health Sciences Center at El Paso, USA

Reviewed by:
Manigandan Chandrasekaran, Luton and Dunstable University Hospital NHS Trust, UK
Dirk Hoyer, Jena University Hospital, Germany

***Correspondence:**
Martin G. Frasch, Département d'Obstétrique-Gynécologie, CHU Sainte-Justine Centre de Recherche, Université de Montréal, 3175, Chemin de la Côte Ste-Catherine, Montréal, QC H3T 1C5, Canada

Background: To evaluate the impact of sampling rate on the predictive capability of continuous fetal heart rate (FHR) variability (fHRV) monitoring for detecting fetal acidemia during labor, we tested the performance of the root mean square of successive differences (RMSSD) in R–R intervals from the ECG when acquired with the sampling rate of 4 Hz currently available in FHR monitors, in comparison to the gold standard of 1000 Hz.

Methods: Near-term ovine fetuses ($N = 9$) were chronically prepared with precordial electrodes for recording ECG, vascular catheters for blood sampling, and an umbilical cord occluder. For 1 min every 2.5 min, animals underwent mild partial umbilical cord occlusions (UCO) × 1 h, moderate partial UCO × 1 h, then complete UCO × 2 h, or until arterial pH reached <7.00. Arterial blood samples were drawn at baseline and every 20 min during the UCO series. RMSSD was calculated continuously in 5 min windows using an automated, standardized system (CIMVA.com). Results are presented as mean ± SEM with significance assumed for $p < 0.05$.

Results: Repetitive UCO resulted in pH decreasing from 7.35 ± 0.01 to 7.00 ± 0.03. In all nine animals, RMSSD increased from 16.7 ± 1.0 ms at baseline to 44.4 ± 2.3 ms, 70 ± 15 min prior to reaching the pH nadir when sampled at 1000 Hz. When sampled at 4 Hz, RMSSD at baseline measured 36.1 ± 6.0 ms and showed no significant increase during the UCO series until the pH nadir was reached. Consequently, early detection of severe hypoxic-acidemia would have been missed in all fetuses.

Conclusion: RMSSD as a measure of fHRV when calculated from FHR sampled at 1000 Hz allowed for the early detection of worsening hypoxic-acidemia in each fetus. However, when calculated at the low sampling rate of 4 Hz used clinically, RMSSD remained unchanged until terminally when the nadir pH was reached. For early detection of fetal acidemia during labor, more sensitive means of acquiring FHR are therefore recommended than currently deployed, e.g., trans-abdominal fetal ECG.

Keywords: fetus, fHRV, monitoring, acidosis, asphyxia, hypoxia, sampling rate

INTRODUCTION

There is an urgent need to identify early signs of fetal acidemia during labor because severe acidemia is associated with increased risk of lasting neurological deficits and current diagnostic procedures are suboptimal (1–3). Variations in fetal vagal activity can be measured by monitoring fetal heart rate (FHR) variability (fHRV) (4, 5). FHR and fHRV are regulated by a complex interplay of the parasympathetic and sympathetic nervous systems accounting for the baseline FHR as well as short-term and long-term fHRV, which show linear and non-linear properties (6). These fHRV properties are differentially affected by fetal acidemia (7–9).

One pivotal measure of fHRV is the RMSSD, the root mean square of the successive differences of R–R intervals in the ECG (10). Changes in RMSSD reflect modulation of fHRV by parasympathetic (vagal) activity on a beat-to-beat time scale and are more precise in capturing vagal activity than the current short-term FHR variation measures used clinically in electronic FHR monitoring (EFM) (11). However, this precision depends on the sampling rate of the ECG signal from which the R–R intervals and the subsequent fHRV are derived (10).

We have shown that RMSSD is a measure of the maturation of the vagal branch of the autonomic nervous system and that RMSSD is reduced by atropine (a cholinergic antagonist) in fetal sheep near-term (5, 7). RMSSD also increases during severe fetal acidemia (pH ~7.09) induced by 4 min umbilical cord occlusions (UCO) 30 min apart in near-term fetal sheep (7). Therefore, RMSSD is a potential marker for worsening acidemia.

In the present study, we aimed at further evaluating the impact of fetal ECG sampling rate on the benefit of continuous fHRV monitoring in predicting fetal acidemia. We tested the performance of RMSSD as a measure of fHRV and change with worsening fetal acidemia when acquired with the sampling rate of 4 Hz currently available in FHR monitors, in comparison to the gold standard of 1000 Hz. Based on evidence from animal and human clinical studies, we propose that longitudinal fHRV monitoring during labor will allow us to improve early diagnosis of fetal acidemia, but this will be impacted by ECG sampling rate.

MATERIALS AND METHODS

SURGICAL PREPARATION

Nine near-term ovine fetuses [123 ± 2 days gestational age (GA), normal ovine gestation is 145 days] of mixed breed were surgically instrumented. The anesthetic and surgical procedures and postoperative care of the animals have been previously described (3, 12). Briefly, polyvinyl catheters were placed in the right and left brachiocephalic arteries, the cephalic vein, and the amniotic cavity. Stainless steel electrodes were sewn onto the fetal chest to monitor the electrocardiogram (EKG). A polyvinyl catheter was also placed in the maternal femoral vein. In addition, an inflatable silicon rubber cuff (In vivo Metric, Healdsburg, CA, USA) for UCO was placed around the proximal portion of the umbilical cord and secured to the abdominal skin. Antibiotics were administered intravenously to the mother (0.2 g trimethoprim and 1.2 g sulfadoxine, Schering Canada Inc., Pointe-Claire, QC, Canada) and the fetus and into the amniotic cavity (one million IU penicillin G sodium, Pharmaceutical Partners of Canada, Richmond Hill, ON, Canada). Amniotic fluid lost during surgery was replaced with warm saline. The uterus and abdominal wall incisions were sutured in layers and the catheters exteriorized through the maternal flank and secured to the back of the ewe in a plastic pouch.

Postoperatively, animals were allowed 4 days to recover prior to experimentation and daily antibiotic administration was continued. Arterial blood was sampled for evaluation of maternal and fetal condition and catheters were flushed with heparinized saline to maintain patency. Animals were 129 ± 1 days GA on the first day of experimental study. Animal care followed the guidelines of the Canadian Council on Animal Care and was approved by the University of Western Ontario Council on Animal Care.

EXPERIMENTAL PROCEDURE

Fetal animals were studied over a ~6-h period. After a 1–2 h baseline control period, all animals underwent mild, moderate, and severe series of repetitive UCOs by graduated inflation of the occluder cuff with a saline solution. During the first hour following the baseline period, mild variable FHR decelerations were elicited with a partial UCO for 1 min duration every 2.5 min, with the goal of decreasing FHR by ~30 bpm, corresponding to an ~50% reduction in umbilical blood flow (13, 14). During the second hour, moderate variable FHR decelerations were elicited with increased partial UCO for 1 min duration every 2.5 min with the goal of decreasing FHR by ~60 bpm, corresponding to a ~75% reduction in umbilical blood flow (14). Animals then underwent severe variable FHR decelerations with complete UCO for 1 min duration every 2.5 min until the targeted fetal arterial pH of <7.0 was detected or 2 h of severe UCO had been carried out, at which point the repetitive UCOs were terminated. All animals were then allowed to recover for 48 h following the last UCO. Fetal arterial blood samples were drawn at baseline, at the end of the first UCO of each series (mild, moderate, severe), and at 20 min intervals (between UCOs) throughout each of the series, as well as at 1, 24, and 48 h of post-insult recovery. For each UCO series blood gas sample and the 24 h recovery sample, 0.7 ml of fetal blood was withdrawn, while 4 ml of fetal blood was withdrawn at baseline, at pH nadir <7.00, and at 1 and 48 h of recovery. The amounts of blood withdrawn were documented for each fetus and replaced with an equivalent volume of maternal blood at the end of day 1 of study.

All blood samples were analyzed for blood gas values, pH, glucose, and lactate with an ABL-725 blood gas analyzer (Radiometer Medical, Copenhagen, Denmark) with temperature corrected to 39.0°C. Plasma from the 4 ml blood samples was frozen and stored for cytokine analysis, and will be reported separately.

After the 48 h recovery blood sample, the ewe and the fetus were killed by an overdose of barbiturate (30 mg sodium pentobarbital IV, MTC Pharmaceuticals, Cambridge, ON, Canada). A post mortem was carried out during which fetal sex and weight were determined and the location and function of the umbilical occluder were confirmed.

DATA ACQUISITION AND ANALYSIS

A computerized data acquisition system was used to record fetal arterial and amniotic pressures and ECG, which were monitored continuously throughout the baseline and UCO series (15). Arterial and amniotic pressures were measured using Statham pressure transducers (P23 ID; Gould Inc., Oxnard, CA, USA). Arterial blood pressure (ABP) was determined as the difference between instantaneous values of arterial and amniotic pressures. A PowerLab system was used for data acquisition and analysis (Chart 7 for Windows, AD Instruments Pty Ltd., Castle Hill, NSW, Australia).

Pressures and ECG were recorded and digitized at 1000 Hz for further study. For ECG, a 60 Hz notch filter was applied. FHR was additionally triggered and calculated in real time from arterial pressure systolic peaks.

Averaged values of FHR and ABP were calculated from artifact-free recordings of 1 h of baseline, between and during each consecutive variable FHR deceleration induced by UCO (mild, moderate, severe), as reported (16).

R–R intervals sequence was originally generated from ECG sampled at 1000 Hz. For simulation of the 4 Hz sampling rate, the R–R intervals sequence was interpolated at 4 Hz. RMSSD was calculated from the 1000 and 4 Hz sampled R–R intervals continuously in 5 min windows overlapping by 2.5 min using an automated and standardized CIMVA.com system (**Figure 1**). Next, average RMSSD values were determined for the 1 h baseline period and each 20 min interval from the UCO experimental period and correlated to the time-matched pH, lactate, and base excess (BE) values. Accordingly, each 20 min interval included ~8 UCO-induced FHR decelerations and the intervening recovery periods.

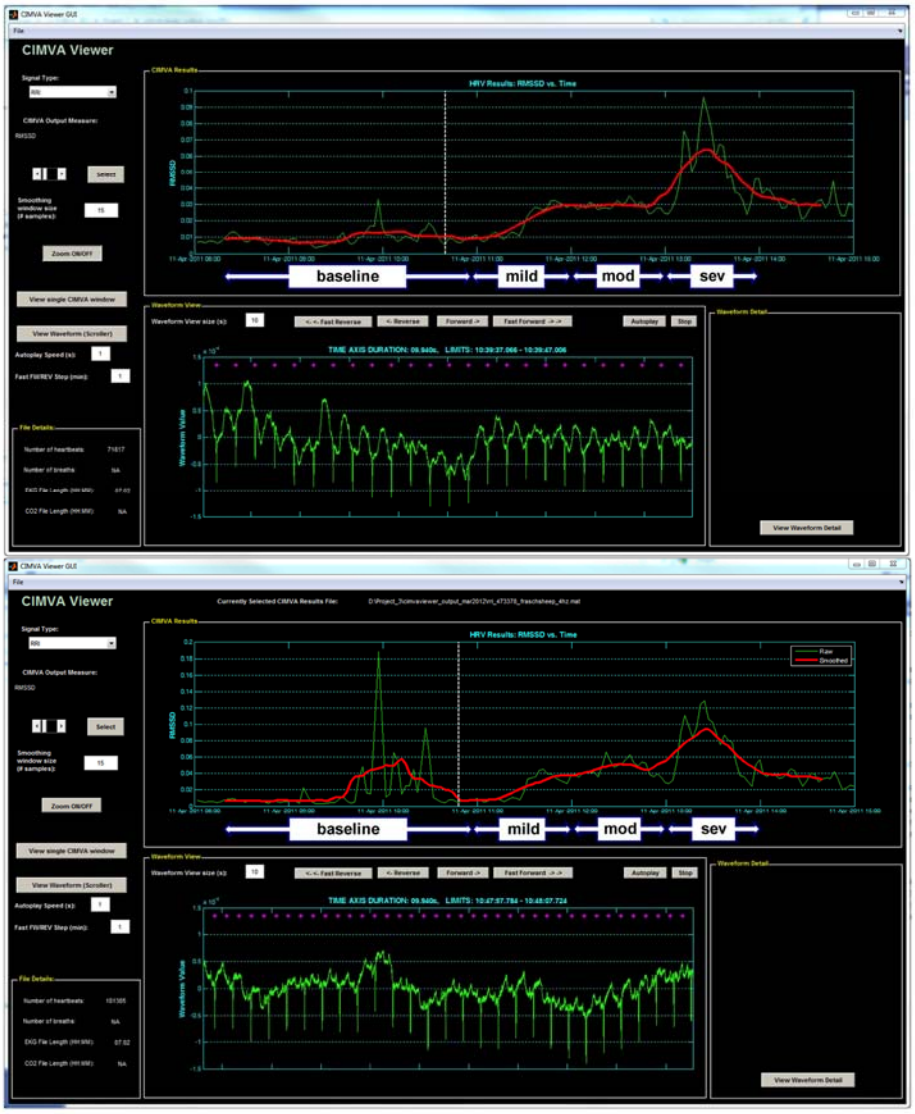

FIGURE 1 | A representative example of the CIMVA fHRV analysis of RMSSD at (top) 1000 Hz and (bottom) 4 Hz. Note the gradual rise of RMSSD with worsening acidemia (pH decreasing) and an overestimation of RMSSD at baseline in 4 Hz sampled fHRV. Mild, mod and sev = mild, moderate, and severe UCO series, respectively.

STATISTICAL ANALYSIS

Normal data distribution was tested using the Kolmogorov–Smirnov test followed by parametric or non-parametric tests, as appropriate. The pH measurements and the temporal change in RMSSD values versus baseline for the 1000 and 4 Hz sampling rates were compared by one-way repeated measures ANOVA followed

by Holm–Sidak or one-way repeated measures ANOVA on ranks (Friedman) followed by correction for multiple comparisons (Dunn's method) as applicable.

All values are expressed as means ± SEM with statistical significance assumed for $p < 0.05$. Pearson or Spearman correlation analysis was performed as appropriate, and R values are presented where $p < 0.05$ (SPSS 19; IBM, Armonk, NY, USA).

RESULTS

Baseline fetal arterial pH (7.35 ± 0.01) as well as FHR (159 ± 5 bpm) and ABP (44 ± 2 mmHg) were within physiological range.

Repetitive fetal UCO resulted in development of marked acidosis with arterial pH decreasing from 7.35 ± 0.01 to 7.00 ± 0.03 and BE from 1.6 ± 0.7 to −13.6 ± 1.1 mEq/l by the end of the UCO study (both $p < 0.01$). ABP increased on average to 75 ± 3 mm Hg during each UCO versus 54 ± 2 mm Hg between each UCO ($p < 0.05$). FHR deceleration depth averaged 66 ± 6 bpm decreasing to 94 ± 6 bpm during each UCO versus 159 ± 3 bpm between each UCO ($p < 0.05$).

The changes in RMSSD with the repetitive UCO are summarized in **Figure 2**. When sampled at 1000 Hz, baseline RMSSD measured 16.7 ± 1.0 ms with all animals, then increased to 44.4 ± 2.3 ms during the repetitive UCO 70 ± 15 min prior to reaching the pH nadir ($p < 0.01$). This increase was evident 20 min into severe UCO series. All subsequent measurements of RMSSD until the UCO were stopped showed similar increases compared to baseline RMSSD values (**Figure 2**, all $p < 0.01$).

When sampled at 4 Hz, baseline RMSSD was found to measure 36.1 ± 6.0 ms. Albeit higher on average, this value was not statistically significantly different from the 1000 Hz sampled baseline measurement (Wilcoxon signed rank $p = 0.3$). During the repetitive UCO, RMSSD showed no definite increase in five of the nine fetuses. In the remaining four fetuses an increase was observed, but only at the time of reaching the pH nadir. Moreover, their RMSSD increase occurred 100 min into the severe UCO series with RMSSD measuring 85.9 ± 9.5 ms ($p < 0.01$) (**Figure 2**).

DISCUSSION

In the present study, RMSSD increased early with worsening hypoxic-acidemia in each fetus when sampled at 1000 Hz. This is in line with previous observations in fetal sheep near-term undergoing repetitive UCO and giving rise to worsening hypoxic-acidemia (7). However, when fetal ECG was instead sampled at 4 Hz simulating the low sampling rate for fHRV used clinically in electronic FHR monitors, RMSSD was not significantly changed in five of the fetal sheep and only increased terminally with severe hypoxic-acidemia in the other four animals. The methodological reason for this finding is overestimation of fHRV due to undersampling (17, 18). As pointed out by Merri et al., this overestimation may be further impacted by the degree of the biological variability itself introducing an additional confounder in the fHRV measures derived from low sampled FHR data.

There are several reasons why FHR monitoring fails to detect fetal hypoxic-acidemia as presently used clinically. First, limited information can be derived by visual analysis of the FHR pattern and uterine contractions. Second, present technology for the detection of fetal heart bioelectric events is limited by poor recording of the true bioelectric signal. Trans-abdominal Doppler probes operate on averaged biophysical signals, and scalp electrodes, either filtered or sampled at low frequency, detect a robust but smoothed QRS signal (19). This results in loss of the information embedded in fHRV (5, 7). The time scale of subtle fHRV events requires the temporal resolution of R peak detection in

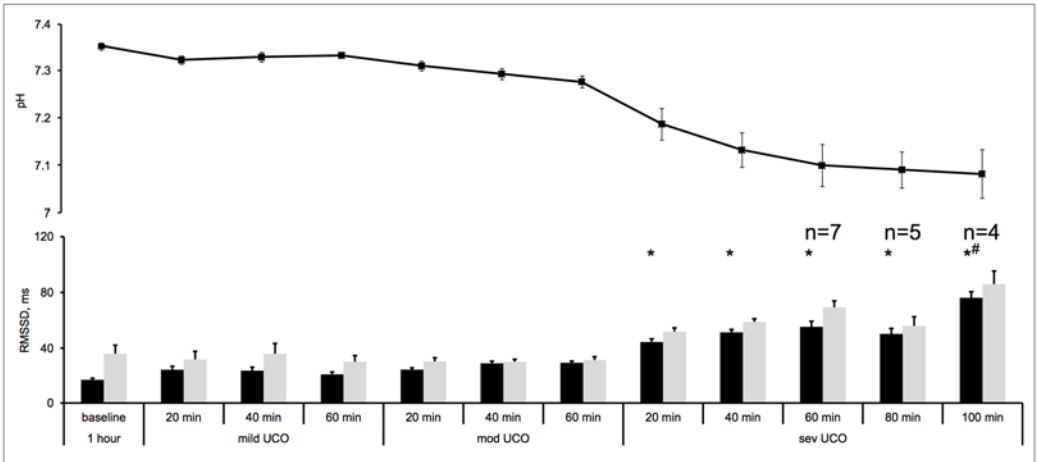

FIGURE 2 | FHRV analysis of RMSSD changes during worsening acidemia (black) at 1000 Hz and (gray) 4 Hz sampling rates. Animals reached pH nadir <7.00 between the time points "severe UCO 40 min" and "severe UCO 100 min." Accordingly, sample sizes of these time points were lower where indicated. For other time points, $N = 9$. Mean ± SEM. *$p < 0.05$ versus baseline for 1000 Hz sampled fHRV; * versus baseline for 4 Hz sampled fHRV.

the QRS complex within <1 ms (6, 20, 21). Our approach and findings in the fetal sheep model are echoed and supported by the recently published prospective study of human fHRV (18). The commercial FHR acquisition software of a conventional cardiotocogram monitor used in that study sampled FHR derived from the Doppler signal every 2.5 s. The researchers modified this algorithm to read the FHR every 0.5 s (corresponding to 2 Hz, still twice as low as the sampling rate simulated in the present study), thus somewhat increasing the precision of fHRV estimation. Despite the still very low fHRV sampling rate, the linear and non-linear fHRV measures determined from this data set allowed the authors to detect differences between the fHRV of the intrauterine growth-restricted fetuses (IUGR) compared to the healthy fetuses. Notably, the authors reported no difference in the high frequency power spectrum estimates of fHRV between the groups. This is consistent with the main finding of this study that low HRV sampling rates likely overestimate HRV, thus obscuring the true change in HRV due to a pathophysiological state.

Thus, for earlier detection of fetal acidemia during labor as herein shown with RMSSD as a measure of fHRV, more sensitive means of acquiring FHR are recommended than currently deployed in EFM. Candidates for alternative means of fetal assessment for detecting the onset of hypoxic-acidemia include transabdominal ECG, already used at the bedside in some jurisdictions, or experimental approaches involving fetal EEG during labor (22–24). Fetal scalp ECG could also be sampled at 1000 Hz, thus permitting true fHRV analyses such as presented here.

Limitations of this study are its small sample size and focus on one particular fHRV measure reflecting vagal modulations of fHRV, the RMSSD. Larger prospective studies in fetal sheep model and human clinical prospective trials of FHR monitoring during labor are needed to provide high resolution R–R data sets with correlated clinical outcomes such as pH and BE at birth. Such data sets could then be studied with a more encompassing panel of fHRV measures to validate their usefulness in intrapartum FHR monitoring for early detection of fetal acidemia. First steps in this direction have been made with respect to sample size, but not yet with respect to the R–R temporal resolution, i.e., sampling rate (25).

SIGNIFICANCE AND NOVELTY

Continuous beat-to-beat fHRV monitoring capable of detecting vagal activation due to fetal acidemia may be a useful tool for early detection of hypoxic-acidemia near term.

PRESENTATION INFORMATION

Presented in part at Society for Gynecologic Investigation Annual Meeting 2012.

ACKNOWLEDGMENTS

The authors gratefully acknowledge the support from the London Health Sciences Centre Women's Developmental Council and technical assistance of Brad Matushewski and Jenifer Thompson. We also thank Carmen Movila for skillful secretarial assistance. Financial support: Canada Research Chair Tier 1 in Fetal and Neonatal Health and Development (Bryan S. Richardson); CIHR and FRSQ (Martin G. Frasch); Women's Development Council, London Health Sciences Centre, London, ON, Canada (Bryan S. Richardson, Michael G. Ross, Martin G. Frasch).

REFERENCES

1. Rees S, Inder T. Fetal and neonatal origins of altered brain development. *Early Hum Dev* (2005) **81**:753–61. doi:10.1016/j.earlhumdev.2005.07.004
2. Liston R, Sawchuck D, Young D; Society of Obstetrics and Gynaecologists of Canada; British Columbia Perinatal Health Program. Fetal health surveillance: antepartum and intrapartum consensus guideline. *J Obstet Gynaecol Can* (2007) **29**:S3–56. Erratum in: *J Obstet Gynaecol Can* (2007) **29**(11):909.
3. Frasch MG, Mansano RZ, Gagnon R, Richardson BS, Ross MG. Measures of acidosis with repetitive umbilical cord occlusions leading to fetal asphyxia in the near-term ovine fetus. *Am J Obstet Gynecol* (2009) **200**:e201–7. doi:10.1016/j.ajog.2008.10.022
4. Van Leeuwen P, Lange S, Bettermann H, Gronemeyer D, Hatzmann W. Fetal heart rate variability and complexity in the course of pregnancy. *Early Hum Dev* (1999) **54**:259–69. doi:10.1016/S0378-3782(98)00102-9
5. Frasch MG, Muller T, Wicher C, Weiss C, Lohle M, Schwab K, et al. Fetal body weight and the development of the control of the cardiovascular system in fetal sheep. *J Physiol* (2007) **579**:893–907. doi:10.1113/jphysiol.2006.124800
6. Frasch MG, Muller T, Hoyer D, Weiss C, Schubert H, Schwab M. Nonlinear properties of vagal and sympathetic modulations of heart rate variability in ovine fetus near term. *Am J Physiol Regul Integr Comp Physiol* (2009) **296**:R702–7. doi:10.1152/ajpregu.90474.2008
7. Frasch MG, Muller T, Weiss C, Schwab K, Schubert H, Schwab M. Heart rate variability analysis allows early asphyxia detection in ovine fetus. *Reprod Sci* (2009) **16**:509–17. doi:10.1177/1933719108327597
8. Kwon JY, Park IY, Shin JC, Song J, Tafreshi R, Lim J. Specific change in spectral power of fetal heart rate variability related to fetal acidemia during labor: comparison between preterm and term fetuses. *Early Hum Dev* (2012) **88**:203–7. doi:10.1016/j.earlhumdev.2011.08.007
9. Siira SM, Ojala TH, Vahlberg TJ, Rosen KG, Ekholm EM. Do spectral bands of fetal heart rate variability associate with concomitant fetal scalp pH? *Early Hum Dev* (2013) **89**:739–42. doi:10.1016/j.earlhumdev.2013.05.007
10. Task Force of the European Society of Cardiology and the North American Society of Pacing and Electrophysiology. Heart rate variability: standards of measurement, physiological interpretation and clinical use. *Circulation* (1996) **93**:1043–65. doi:10.1161/01.CIR.93.5.1043
11. Frasch MG. Monitoring of fetal heart rate variability. *J Critical Care* (2011) **26**(3):e24. doi:10.1016/j.jcrc.2011.02.033
12. Kaneko M, White S, Homan J, Richardson B. Cerebral blood flow and metabolism in relation to electrocortical activity with severe umbilical cord occlusion in the near-term ovine fetus. *Am J Obstet Gynecol* (2003) **188**:961–72. doi:10.1067/mob.2003.219
13. Itskovitz J, Lagamma EF, Rudolph AM. Heart rate and blood pressure responses to umbilical cord compression in fetal lambs with special reference to the mechanism of variable deceleration. *Am J Obstet Gynecol* (1983) **147**:451–7.
14. Richardson BS, Rurak D, Patrick JE, Homan J, Carmichael L. Cerebral oxidative metabolism during sustained hypoxaemia in fetal sheep. *J Dev Physiol* (1989) **11**:37–43.
15. Richardson B, Gagnon R. Behavioural state activity and fetal health & development. In: Creasy RK, Resnik R, editors. *Maternal-Fetal Medicine.* Philadelphia: WB Saunders Co. (2008). p. 171–9.
16. Ross MG, Jessie M, Amaya K, Matushewski B, Durosier LD, Frasch MG, et al. Correlation of arterial fetal base deficit and lactate changes with severity of variable heart rate decelerations in the near-term ovine fetus. *Am J Obstet Gynecol* (2012) **208**(4):285.e1–6. doi:10.1016/j.ajog.2012.10.883
17. Merri M, Farden DC, Mottley JG, Titlebaum EL. Sampling frequency of the electrocardiogram for spectral analysis of the heart rate variability. *IEEE Trans Biomed Eng* (1990) **37**:99–106. doi:10.1109/10.43621
18. Signorini MG, Fanelli A, Magenes G. Monitoring fetal heart rate during pregnancy: contributions from advanced signal processing and wearable technology. *Comput Math Methods Med* (2014) **2014**:707581. doi:10.1155/2014/707581
19. Durosier DL, Cao M, Batkin I, Matushewski BJ, Keenliside L, Herry C, et al. Continuous multivariate electronic fetal monitoring during labor detects early onset of acidemia: prospective study in fetal sheep model. *J Critical Care* (2013) **28**(1)e5–6. doi:10.1016/j.jcrc.2012.10.026
20. Warner HR, Cox A. A mathematical model of heart rate control by sympathetic and vagus efferent information. *J Appl Physiol* (1962) **17**:349–55.

21. Akselrod S, Gordon D, Ubel FA, Shannon DC, Berger AC, Cohen RJ. Power spectrum analysis of heart rate fluctuation: a quantitative probe of beat-to-beat cardiovascular control. *Science* (1981) **213**:220–2. doi:10.1126/science.6166045
22. Patrick J, Campbell K, Carmichael L, Natale R, Richardson B. Daily relationships between fetal and maternal heart rates at 38 to 40 weeks of pregnancy. *Can Med Assoc J* (1981) **124**:1177–8.
23. Graatsma EM, Jacod BC, Van Egmond LA, Mulder EJ, Visser GH. Fetal electrocardiography: feasibility of long-term fetal heart rate recordings. *BJOG* (2009) **116**:334–7. doi:10.1111/j.1471-0528.2008.01951.x
24. Frasch MG, Keen AE, Gagnon R, Ross MG, Richardson BS. Monitoring fetal electrocortical activity during labour for predicting worsening acidemia: a prospective study in the ovine fetus near term. *PLoS One* (2011) **6**:e22100. doi:10.1371/journal.pone.0022100
25. Chudacek V, Spilka J, Bursa M, Janku P, Hruban L, Huptych M, et al. Open access intrapartum CTG database. *BMC Pregnancy Childbirth* (2014) **14**:16. doi:10.1186/1471-2393-14-16

Conflict of Interest Statement: The authors declare that the research was conducted in the absence of any commercial or financial relationships that could be construed as a potential conflict of interest.

Received: 04 December 2013; accepted: 18 April 2014; published online: 05 May 2014. Citation: Durosier LD, Green G, Batkin I, Seely AJ, Ross MG, Richardson BS and Frasch MG (2014) Sampling rate of heart rate variability impacts the ability to detect acidemia in ovine fetuses near-term. Front. Pediatr. **2**:*38. doi: 10.3389/fped.2014.00038 This article was submitted to Neonatology, a section of the journal Frontiers in Pediatrics.*

2.3 Does heart rate variability provide a signature of fetal systemic inflammatory response in a fetal sheep model of lipopolysaccharide-induced sepsis?

Lucien D. Durosier MD[1*], Christophe Herry PhD[2*], Mingju Cao PhD[1], Patrick Burns BVSs[3], André Desrochers DVM[3], Gilles Fecteau DVM[3], Andrew J.E. Seely MD PhD[4] and Martin G. Frasch MD PhD[1,5]

[1] Dept. of OBGYN and Dept. of Neurosciences, CHU Ste-Justine Research Centre, l'Université de Montréal, Montréal, QC, Canada

[2] Dynamical Analysis Laboratory, Ottawa Hospital Research Institute, Clinical Epidemiology Program, Ottawa, Canada

[3] Clinical Sciences, CHUV, l'Université de Montréal, St-Hyacinthe, QC, Canada

[4] Dynamical Analysis Laboratory, Ottawa Hospital Research Institute, University of Ottawa, Ottawa, Canada

[5] Centre de recherche en reproduction animale, l'Université de Montréal, St-Hyacinthe, QC, Canada

*LDD and CH contributed equally to this manuscript.

The work was **performed at** l'Université de Montréal and University of Ottawa

Coresponding author's address:

Martin G. Frasch

Département d'obstétrique-gynécologie

Université de Montréal

CHU Sainte-Justine Centre de Recherche

3175, chemin de la Côte Ste-Catherine

Montréal, Québec H3T 1C5

Canada
Phone: +1-514-345-4931 x4048
Fax: +1-514-345-4648

Funded by CIHR (to MGF and AJES), FRQS, MITACS/NeuroDevNet, Molly Towell Perinatal Research Foundation and CHU Ste-Justine Research Center (to MGF) and CIHR-funded QTNPR and NeuroDevNet/MITACS (to LDD).

Keywords: sepsis; monitoring; HRV; fetus; LPS; sheep; heat map; inflammation; bioinformatics

ABSTRACT

OBJECTIVE:

Fetal inflammatory response occurs during chorioamnionitis, a frequent and often subclinical fetal inflammation associated with increased risk for brain injury and life-lasting neurological deficits. No means of early detection exist. We hypothesized that systemic fetal inflammation without overt septic shock will be reflected in alterations of fetal heart rate (FHR) variability (fHRV) distinguishing fetal baseline versus inflammatory response states.

DESIGN:

Animal study.

SETTING:

University research laboratory.

SUBJECTS:

Chronically instrumented near-term fetal sheep (n=24).

INTERVENTIONS:

We induced a moderate inflammatory response with lipopolysaccharide (LPS) injected intravenously (n=14). Ten additional fetuses served as controls. 102 fHRV measures were determined continuously every 5 min using CIMVA (Continuous Individualized Multi-organ Variability Analysis). CIMVA creates an fHRV measures matrix across five signal-analytical domains, thus describing complementary properties of fHRV. We generated and quantitatively compared the CIMVA fHRV heat map signatures time-matched with the sampling for inflammatory cytokines IL-6 and TNF-α at baseline, 1, 3, 6, 24 and 48 h.

MEASUREMENTS AND MAIN RESULTS:

In the LPS group, IL-6, but not TNF-α, peaked at 3 hours. In parallel, fHRV heat map analysis revealed a significant difference in the medians between LPS and control group at different time points. For the LPS group, a sharp increase in standardized difference in variability with respect to baseline levels was observed between 3h and 6h abating to baseline levels, thus tracking closely the IL-6 inflammatory profile. This pattern was not observed in the control group. We identified a subset of 16 fHRV measures reflecting the fetal inflammatory response state and originating from the statistical, geometric, energetic, informational and invariant domains.

CONCLUSIONS:

Distinctive subsets of fHRV measures can be identified that correlate with levels of inflammation and track its temporal profile. This highlights the potential role of HRV to study and monitor inflammatory response as a function of neuroimmunological behaviour.

INTRODUCTION

The main manifestation of pathologic inflammation in the feto-placental unit, chorioamnionitis, affects 20% of term pregnancies and up to 60% of preterm pregnancies; notably, it is often an occult finding.[1] Both symptomatic and asymptomatic chorioamnionitis are associated with a ~9-fold increased risk of cerebral palsy.[2] Even asymptomatic inflammation may inhibit placental angiogenesis and thus modulate the course of the pregnancy.[3] Thus, a significant number of fetuses are exposed to variable degrees of inflammation that may impact on their brain development. Current methods to diagnose fetal compromise due to an infectious or inflammatory condition are inadequate.[4] Hence, an urgent need exists to identify early signs of the fetus at risk of adverse outcome and intervene therapeutically.[4]

Via the vagus nerve, the fetal cholinergic anti-inflammatory pathway's (CAP) provides negative feedback on systemic levels of inflammatory cytokines. [5] This rapid homeokinetic control of inflammatory milieu is reflected in subtle alterations of fetal heart rate (FHR) variability (fHRV).[5] Variations in fetal vagal activity can be measured non-invasively by monitoring the beat-to-beat fHRV.[6] Importantly, derived from fetal EKG sampled at 1000 Hz, such beat-to-beat fHRV is more precise than the time-averaged fHRV used currently clinically, for which a sampling rate of less than 4 Hz is used.[6] Perinatal studies show that beat-to beat fHRV has potential as a non-invasive, continuous, sensitive and specific measure of the fetal inflammatory response.[7] HRV measures can be derived from various signal-analytical domains. RMSSD (Root Mean Square of Standard Deviation), a measure of short-term HRV, certain complexity and other signal domain measures reflecting short term time scale fHRV may serve as a indicators of this complex vagal modulation of inflammatory activity.

Lipopolysaccharide (LPS)-induced inflammation in fetal sheep is a well-established model of the human fetal inflammatory response to sepsis.[8] However, whether this process can be tracked via fHRV monitoring has not been studied. We hypothesized that distinct patterns of fHRV correlation to pro-inflammatory cytokines will reflect CAP’s spontaneous versus inflammatory response states.

METHODS

Animal care followed the guidelines of the Canadian Council on Animal Care and the approval by the University of Montreal Council on Animal Care (protocol #10-Rech-1560).

Anesthesia and surgical procedure

Briefly, we instrumented 24 pregnant time-dated ewes at 126 days of gestation (dGA, ~0.86 gestation) with arterial, venous and amniotic catheters and ECG electrodes.

Anesthesia and surgical procedure

Intravenous access was achieved using a single-lumen catheter (Arrow Jugular Catheterization Set; Arrow International, Inc., 2400 Bernville Road, Reading, PA 19605 USA) via a jugular vein. All the ewes were sedated with acepromazine (Atravet 10 mg/mL) 0.03 mg/kg body weight intravenously approximately 30 minutes prior to the induction of anesthesia. Diazepam (Diazepam 5mg/mL) 5-7 mg/kg, ketamine (Ketalar 100mg/mL) 4-5mg/kg and propofol (Propofol 10mg/mL) 0.5 to 1mg/kg were given intravenously to induce general anesthesia. The ewes were then intubated with a silicon tracheal tube (SurgiVeT, Endotracheal Tubes; Smiths Medical ASD, Inc. St. Paul, MN 55112, USA) 9 to 12 mm ID. An airway exchange catheter (Cook Airway Exchange Catheter with RAPI-FIT Adapters; Cook Critical Care 750, Bloomington IN 47402-0489 USA) was used to aid with the intubation. Mechanical ventilation (Dispomed Ventilator; Dispomed Ltd., 745 Nazaire-Laurin, Joliette, Quebec J6E 0L6) was used to maintain a PaCO2 within normal limits. An auricular artery was catheterized (BD Insyte-W; Becton Dickinson, Infusion Therapy Systems Inc., 9450 S State St, Sandy Utah 84070 USA, 22 to 20 G; 1 in [0.9 x 25 mm] to 1.16 in [1.1 x 30 mm]) and connected to non-compliant tubing to monitor direct arterial blood pressure (Edwards Lifesciences Ref: PX272 Pressure monitoring kit with TruWave Disposable Pressure). A multi-parameter physiologic monitor (LifeWindow LW6000; Digicare Biomedical Technology 107 Commerce Road, Boynton Beach, FL 33426-9365 USA) was used to record the electrocardiogram, direct arterial blood pressure, oxygen saturation (SpO_2), capnography ($P_{ET}CO_2$), and temperature every five minutes. Normal body temperature was maintained using a circulating water blanket (Gaymar).

Ovine singleton fetuses of mixed breed were surgically instrumented with sterile technique under general anesthesia (both ewe and fetus). In case of twin pregnancy the larger fetus was chosen based on palpating and estimating the intertemporal diameter. The total

duration of the procedure was ca. 2 hours. A 20 cm midline incision was made starting from the umbilicus caudally. The uterus was then palpated to determine fetal position and numbers. A 2 cm full thickness left paracostal incision was then made to pre-pass all the catheters through the abdominal wall and into the abdominal incision. After determining the largest fetus, the uterus was partially exteriorized, the uterine wall was incised on the greater curvature leaving the amnion intact. The amnion was incised and the upper body was exteriorized. A sterile rubber glove filled with warm sterile saline was put over the fetus head. The uterine wall and fetal membranes were maintained exteriorized by clamping them to the ewe skin with Babcock forceps. The thoracic limbs were abducted and the brachial artery and vein carefully dissected by medial approach along the antebrachium. Polyvinyl catheters were inserted in the right and left brachial arteries and the left cephalic vein. Briefly, the vessel to be catheterized was ligatured distally with a 2-0 Vicryl. Castroviejo scissors were used to incise vessel wall. A polyvinyl catheter was inserted up to 8 cm proximally or until a resistance was felt. The catheter was secured temporally with vascular clamp, while the assistant was checking patency. Then the catheter was secured with 2-0 Vicryl. The fetal skin was sutured with Vicryl 2-0 in a continuous pattern fashion. Four copper electrodes (LIFYY, Metrofunk Kabel-Union, Berlin, Germany) were sewn onto the fetal chest to monitor the electrocardiogram (ECG): right and left shoulder, manubrium and xyphoid process. The amniotic catheter was finally sutured to the sternum. This catheter had a fenestrated extremity. All the catheters were secured by suturing them on the dorsum of the fetus with 2-O Vicryl. The fetus was returned in the uterus, the gloves over his head removed and the fetal membranes were sutured with a 4-0 Vicryl in a continuous fashion making sure all the catheters were individually exteriorized through the incision. The uterine wall was sutured with a 0 Vicryl with a double layer Cushing pattern. The midline was sutured with PDS II USP 1 in a continuous fashion. Subcutaneous tissues were sutured with 2-0 Vicryl in a continuous fashion and the skin closed with surgical staples.

Antibiotics were administered to the mother intravenously (3.9 mL per 45 kg body weight Trimethoprim sulfadoxine) as well as to the fetus intravenously and into the amniotic cavity (250 mg sodium ampicillin). Amniotic fluid lost during surgery was replaced with warm saline. The flank incision was partially closed with a purse string suture with PDS II USP1 to allow some movement of the catheters. The exteriorized catheters through the

maternal flank were secured to the back of the ewe in a plastic pouch. For the duration of the experiment the ewe was returned to the metabolic cage, where she could stand, lie and eat *ad libitum* while we monitored the non-anesthetized fetus without sedating the mother. During postoperative recovery antibiotic administration was continued for 3 days. Arterial blood was sampled for evaluation of maternal and fetal condition and catheters were flushed with heparinized saline to maintain patency.

Cytokine analyses

Cytokine concentrations (IL-6, TNF-α) in plasma were determined by using an ovine-specific sandwich ELISA. Mouse anti sheep monoclonal antibodies (capture antibody IL-6, MCA1659, Bio Rad AbD Serotec) or mouse anti-bovine monoclonal antibody (TNF-α, MCA2335X, Bio Rad AbD Serotec) were pre-coated at a concentration 4 µg/ml on ELISA plate at 4°C for overnight, after 3 times wash with washing buffer (0.05% Tween 20 in PBS, PBST), plates were then blocked for 1h with 1% BSA in PBST. Following 3 times washing, 50 µl of serial diluted protein standards and samples were loaded per well and incubated for 2 hours at room temperature. All standards and samples were run in duplicate. Recombinant sheep proteins (IL-6, Protein Express Cat. no 968-305; TNF-α, Cat. no 968-105) were used as ELISA standard. Plates were then washed for 3 times. Rabbit anti sheep polyclonal antibodies (detection antibody IL-6, AHP424, Bio Rad AbD Serotec) or rabbit anti-bovine polyclonal antibody (TNF-α, AHP852Z, Bio Rad AbD Serotec) at a dilution of 1:250 were applied in wells and incubated for 30 min at room temperature. Plates were then washed with washing buffer for 5 times. Detection was accomplished by assessing the conjugated enzyme activity (goat anti-rabbit IgG-HRP, dilution 1:5000, Jackson ImmunoResearch, Cat. No 111-035-144) via incubation with TMB substrate solution (BD OptEIA TMB substrate Reagent Set, BD Biosciences Cat. No 555214), colour development reaction was stopped with 25 µl of 2N sulphuric acid. Plates were read on ELISA plate reader at 450 nm, with 570 nm wavelength correction (EnVision 2104 Multilabel Reader, Perkin Elmer). The sensitivity of IL-6 ELISA was 16 pg/ml, the sensitivity of TNFα ELISA was 13.9 pg/ml, respectively. For all assays, the intra-assay and inter-assay coefficients of variance was <5% and <10%, respectively.

Antibiotics were administered to the mother intravenously (3.9 mL per 45 kg body weight Trimethoprim sulfadoxine) as well as to the fetus intravenously and into the amniotic cavity (250 mg sodium ampicillin). The exteriorized catheters through the maternal flank were

secured to the back of the ewe in a plastic pouch. For the duration of the experiment the ewe was returned to the metabolic cage, where she could stand, lie and eat *ad libitum* while we monitored the non-anesthetized fetus without sedating the mother. During postoperative recovery antibiotic administration was continued for 3 days. Arterial blood was sampled for evaluation of maternal and fetal condition and catheters were flushed with heparinized saline to maintain patency.

Experimental protocol

Postoperatively, all animals were allowed 3 days to recover before starting the experiments. On these 3 days, at 9.00 am 3 mL arterial plasma sample were taken for blood gases and cytokine analysis. Each experiment commenced at 9.00 am with a 1 h baseline measurement followed by the respective intervention as outlined below. FHR and arterial blood pressure was monitored continuously (CED, Cambridge, U.K., and NeuroLog, Digitimer, Hertfordshire, U.K). Blood and amniotic fluid samples (3 mL) were taken for arterial blood gases, lactate, glucose and base excess (in plasma, ABL800Flex, Radiometer) and cytokines (in plasma and amniotic fluid) at the time points 0 (baseline), +1 (*i.e.*, 1 h after LPS administration), +3, +6, +24, +48 and +54 h (*i.e.*, before sacrifice at day 3). For the cytokine analysis, plasma was spun at 4°C (4 min, 4000g force, Eppendorf 5804R, Mississauga, ON), decanted and stored at -80°C for subsequent ELISAs. After the +54 hours (Day 3) sampling, the animals were sacrificed. Fetal growth was assessed by body, brain, liver and maternal weights.

Ten fetuses were used as controls receiving NaCl 0.9%. Fourteen fetuses received LPS (400 ng/fetus/day) (Sigma L5293, from E coli O111:B4, readymade solution containing 1mg/ml of LPS) intravenously on days 1 and 2 at 10.00 am to mimic high levels of endotoxin in fetal circulation over several days as it may occur in chorioamnionitis. CAP activation was measured by changes in CIMVA-derived fHRV measures as explained below.

Cardiovascular analysis

Mean ABP (mABP) and FHR were calculated for each animal, at each time point (baseline, 1h, 3h, 6h, 24h, 48h and 54h), as an average of the artifact-free 30 preceding minutes (60 preceding minutes for the baseline) using Spike 2 (Version 7.13, CED, Cambridge, U.K.).

FHRV analysis

The CIMVA (continuous individualized multiorgan variability analysis, Table 1, Supplemental Digital Content - Table S1) server platform was used to develop comprehensive continuous fHRV measures analysis. The complete fetal ECG was uploaded onto the CIMVA server to generate continuous fHRV. Output of the CIMVA software was a matrix of fHRV measures along with measures of data quality for every interval evaluated linked to the timing of blood sampling for arterial blood gases and pH as well as LPS administrations. By offering a standardized, comprehensive and validated linear and nonlinear fHRV analysis software platform, CIMVA allowed us to assess the temporal relation of multiple fHRV measures to manipulations of the CAP and the potential clinical value of linear and nonlinear fHRV measures for monitoring fetal inflammatory response. Importantly, data generated with such standardized approach allow comparison to future studies.

For each animal, at each time point (baseline, 1h, 3h, 6h, 24h and 48h) and for each fHRV measure, an average of the 30 preceding minutes (60 preceding minutes for the baseline) was calculated. Not all animals for which fHRV was to be calculated had data at 54 h time point, so this time point was not included in the heat map analysis. The median baseline contribution was removed for each animal and for each measure, to emphasize the expected loss of fHRV as inflammation sets in and to allow a fair comparison between animals. The resulting difference in fHRV was then standardized for each measure, by removing the median of a measure and dividing by the Median Absolute Deviation (MAD), yielding an array of standardized variability for each time point and visualized as heat maps (Matlab, MathWorks, Natick, MA). In order to compare the two groups fairly, we chose to use the same color scale indicative of the standardized relative change with respect to baseline, which we assume is due to LPS-induced inflammation. The heat map underlying values are standardized scores.

Cytokine analyses

Cytokine concentrations (IL-6, TNF-α) in plasma were determined by using an ovine-specific sandwich ELISA. Details are provided as the supplementary material (Methods).

Statistical analysis

Generalized estimating equations (GEE) modeling approach was used to assess the effects of LPS while accounting for repeated measurements on fetal blood gases and acid-base status, plasma cytokines (IL-6 and TNF-α) and cardiovascular responses. We used a linear scale response model with time and LPS as predicting factors to assess their interactions using

maximum likelihood estimate and Type III analysis with Wald Chi-square statistics. SPSS Version 21 was used for these analyses (IBM SPSS Statistics, IBM Corporation, Armonk, NY). The median change of fHRV (across fHRV measures) at each time point was compared across groups using a Wilcoxon rank-sum test on the medians. For the heat map analyses, we assessed the global statistical significance of the difference in medians between time point and groups using a Quasi-Least Squares approach within the framework of generalized estimating equations, with a Markov Correlation structure and normal distribution assumption. We used Ratcliffe and Shults' Matlab implementation. [9] All results are presented as Mean±SD for $P<0.05$.

RESULTS

Cohorts' characteristics

Maternal weight averaged 77±10 kg. Maternal venous blood gases, pH and lactate did not significantly change during the experiments and were within physiological range throughout the experiment for both groups. Averaged over all measurement time points, they were: pO_2 53.7 ± 6.2 mmHg; pCO_2 40.9 ± 1.5 mmHg, pH 7.44 ± 0.01; lactate 0.66 ±0.15 mmol/l.

Fetal body weights averaged was 3.6 ± 0.8 kg. Gestational age at time of the experimental day 1 averaged 130 days ± 0.7 dGA (term 145 dGA). In the control group 4/7 fetuses were male and 5/7 singletons. In the LPS group 4/10 fetuses were male and 2/10 singletons.

Clinical-chemical data

Basal fetal arterial blood gases, pH (7.37 ± 0.04), BE (3.3 ±2.3 mmol/l) and lactate (1.5 ± 0.9 mmol/l) were within physiological range during the baseline in both groups (Fig. 1). We found significant time-LPS interactions for pH ($P=0.03$), pO_2, pCO_2, lactate and BE (all $P<0.001$) (Figure 1A).

Cardiovascular analysis

We found time-LPS interactions for mABP and FHR responses ($P=0.015$ and $P<0.001$, respectively, Fig. 1B). This was significant for FHR at 6 hours ($P=0.008$). While we did not perform a formal cardiology review, studying all raw fetal EKG recordings on the experimental day 1 following NaCl (control group) or LPS injections revealed no pronounced differences (Fig. S1).

Plasma cytokines response to LPS

We detected time-LPS interaction for IL-6 ($P<0.001$) and for TNF-α ($P=0.002$) (Fig. 1C). The LPS group showed a peak of IL-6 at 3 h and an overall 45% drop in TNF-α levels.

Analysis of CIMVA fHRV signature of fetal inflammatory response: Heat maps approach

Since the fHRV measures reported either increase or decrease with the loss of physiological variability, we looked at absolute change rather than linear decrease. We compared the changes in the median of fHRV (across measures) at each time point across the groups. The results are summarized in Fig. 2 and Fig. 3. The effect of LPS at 3 h is consistent with the IL-6 peak at 3 h following the LPS injection. The statistical summary of the results is

shown in Table 2 and indicates that the Time and Group effects are statistically significant at the 0.05 level.

Identification of the inflammatory signature in fHRV

Next, to identify an fHRV inflammatory signature we selected a subset of measures correlated with a piecewise linear function consisting of a flat portion until 3 h, followed by a linear decrease of unit slope based on following considerations. First, a simple prototype function was designed to embody the hypothesized change in fHRV from the inflammatory process based on our *a priori* assumption for the prototypical inflammatory response of LPS animals with the observed systemic peak response of IL-6 to LPS exposure at 3 h (cf. Fig. 1C). Second, the correlation was assessed using Spearman rank correlation coefficient between the time responses of each fHRV measure synchronized across LPS animals and that piecewise linear prototype function.

71 measures had a statistically significant correlation coefficient but only the measures whose absolute correlation coefficient was greater than 0.3 were retained, yielding a subset of 16 measures (Table 3).

The results are presented in Fig. 3, where the difference between the LPS group and the control group is more pronounced than in Fig. 2, particularly at 6 h post-injection. Results shown in Table 4 indicate that both Time and Group effects are statistically significant at the 0.05 level. The effect of LPS at 3 h is consistent with the IL-6 peak at 3 h following the LPS injection.

DISCUSSION

We demonstrate that multidimensional fHRV analysis identifies distinctive subsets of fHRV measures tracking the temporal profile of fetal inflammation. Our findings may eventually lead to design of bedside fetal monitors for early detection of subclinical inflammation.

Our experimental cohort's morphometric, arterial blood gases, acid-base status and cardiovascular characteristics were within physiological range and representative for a late-gestation fetal sheep as a model of human fetal development near term.[10] The effect of the low LPS dose on the arterial blood gases, acid-base status and cardiovascular responses is compatible with a mild septicemia (mild compensated metabolic acidemia and hypoxia) evidenced by a transient rise of IL-6 at 3 hours without overt shock with cardiovascular decompensation. Noteworthy, the cytokine rise was accompanied by a slight drop of mABP and a rise in FHR. This explains why mean FHR was selected as one of the fHRV measures profiling the inflammation. The selective rise of IL-6, but not TNF-α is in line with literature at this developmental stage. [11, 12] Here we report that despite the lack of zero-moment change in TNF-α concentration over time, LPS caused an overall decrease in TNF-α concentration. This is a novel observation, since the clinical studies reporting no change in TNF-α in perinatal inflammation or labour usually sample only once from the cord blood. Our finding is in line with the general notion that sepsis may suppress hormone secretion variability.[13, 14] Further studies are needed to test whether similar pattern applies to other hormones such as IL-8 and IL-10.

Fairchild *et al.* showed how pathogen-induced sepsis and inflammatory response in adult mice are impacting the higher order heart rate (HR) characteristics that can be derived from HRV.[15] Such HR characteristics can be monitored non-invasively and continuously providing insights into the activity of autonomic nervous system (ANS), vagus nerve in particular, and its control of innate immune responses to infection via CAP.[16] The authors hypothesized that HRV should increase following the CAP activation in response to infection. Their findings seemingly reject the initial hypothesis and support the clinically known phenomenon of "suppressed HRV", rather than of an increased HRV. CAP has been identified in adult animals and humans.[5] Multiple epidemiologic studies have shown that low HRV, as reflected in root mean square of the successive differences of R-R intervals of ECG (RMSSD) or High Frequency

(HF) band spectral power, may serve as a marker of vagal modulation of inflammatory activity in adults.[17, 18] Clinico-pathologic studies indicate that loss of CAP's inhibitory influence unleashes innate immunity, producing higher levels of pro-inflammatory mediators that exacerbate tissue damage, and decreases short-term time scale HRV.[17] Fairchild *et al.* focused on long-term time scale HRV only, while the authors' hypothesis and the wiring of the CAP both imply that infection and sepsis will modulate vagal signaling. That is, short-term time scale HRV would increase, but not necessarily the long-term time scale HRV. Classic examples of short-term HRV are RMSSD and HF band spectral power.[19] The relation of these HRV measures to CAP is now well documented by the above cited clinical studies, at least in the adult organism. RMSSD and HF band spectral power are also decreased in fetal sheep near-term following atropine blockade.[20] This identifies such short-term fHRV measures as reflecting vagal modulations of fHRV.

Furukawa *et al.* demonstrated that CAP is active in neonatal rats and decreases hypoxic-ischemic brain damage.[21] We have shown in fetal sheep that atropine blockade has no effect on SDNN[20], while others demonstrated an SDNN decrease in adult mice.[22] Both studies report a significant tachycardia as a result. These differences suggest that subtle, but relevant species variations may exist in the HRV time scales at which vagal activity operates. Moreover, ANS development depends on the individual *in utero* growth trajectories[10] and is also species-dependent with regard to sympathetic and vagal activation patterns.[23] The very notion of sympathetic versus parasympathetic activation has been challenged laying foundation for the concept of sympatho-vagal co-activation as evidenced in different studies, species and developmental stages.[23, 24] This translates into the requirement to presume and seek for more complex signatures of intrinsic and challenged ANS behaviour reflected in HRV than mere states of sympathetic or vagal dominance.

Thus, further integrative studies in neonatal models of sepsis are needed to elucidate the authors' driving clinical observation of bradycardia and long-term time scale HRV depression during sepsis and how this phenomenon relates to CAP activity. We suggest that such studies should not seek for HRV depression *per se*, but rather for patterns of HRV represented by its multidimensional characteristics, for example as this is done by the CIMVA system we deployed in the present study. Such approach permitted us to avoid limiting ourselves *a priori* to particular fHRV measures, but, rather, seeking for HRV measures signatures reflective of unchallenged,

baseline and inflammation states. To achieve this goal we have deployed heat map-driven visualization and statistical analysis.[25, 26] Since the fHRV measures reported either increased or decreased with the loss of physiological variability measured at baseline, prior to LPS exposure, heat map representation required that we looked at absolute change rather than linear decrease over time. Noteworthy, the heat map in Fig. 2 shows a high degree of variability in responses at all time points. This variability is larger in comparison to heat maps patterns we are used to from genomics studies for a two of reasons: 1) the number of fHRV measures reported; we demonstrate that not all of these fHRV measures are relevant to detect and track the LPS-induced inflammation and 2) by the fact that the heat map we deploy is not a conventional heat map, *i.e.*, no clustering is performed; as a result, it looks very fragmented. Fig. 3 then shows that the fHRV responses are more homogeneous when fewer key features are used. A larger sample size would be needed to confirm the findings and further reduce the variability of responses between animals of the same group.

Our understanding of the dynamics of fHRV in human and ovine fetuses during physiologic (*e.g.*, sleep states) and pathophysiologic (*e.g.*, asphyxia, sepsis) conditions has evolved over the past two decades.[7, 27-29] Late gestation human fetuses exhibit nonlinear cardiac dynamics and higher vagal tone is associated with more efficient regulation of homeostasis.[30, 31] FHR and fHRV are regulated by a complex interplay of the parasympathetic and sympathetic nervous systems accounting for the baseline FHR as well as short-term and long-term fHRV showing linear and nonlinear properties.[32] These fHRV properties are differentially affected by LPS-induced fetal and neonatal inflammatory response.[33, 34] Decreased fetal and neonatal HRV and transient repetitive heart rate decelerations coincide with or precede clinical signs of sepsis.[7, 35, 36] This may be due to an altered vagal tone with intermittent vagal firing in the setting of a systemic fetal inflammatory response during sepsis.[7] In an experimental model of sepsis in adults, sympathetic activation by infusion of epinephrine before administration of endotoxin reduced high-frequency HRV, suggesting vagal hyporesponsiveness.[17] Severe sepsis could induce a state of generally decreased vagal efferent firing or responsiveness, leading to fewer normal small FHR decelerations. On the other hand, CAP activation in sepsis via vagal efferent signaling would decrease FHR and increase fHRV.[7] Based on this animal and human clinical perinatal body of evidence, we propose that developing longitudinal and comprehensive fHRV monitoring in

a model of LPS-induced inflammation will allow us to build algorithms to improve early diagnosis of infection. Such monitoring would capture both linear and nonlinear fHRV properties, a strategy that has proven effective in septic adult and neonatal patients.[37-39]

Our studies in near-term fetal sheep further suggest that continuous assessment of fHRV between and during the FHR decelerations at precision levels higher than currently deployed clinically with non-stress tests/CTG can provide further insights into the dynamics of autonomic nervous system responses to acidemia due to umbilical cord compressions. Measures derived from fHRV show the potential to serve as indicators of incipient fetal acidemia as early as 60 min in advance of pH drop to less than 7.00.[6, 20]

Significance and perspectives

We identified a subset of HRV measures that seem to best characterize the inflammatory state either individually (highest correlation with expected temporal inflammatory profile) or when used as a group (heat map statistical analysis). This subset of HRV measures belongs to different domains of HRV which suggests that such multidimensional representation of HRV reflects an underlying code carrying information about neuroimmunological, and possibly intrinsic cardiac, interactions modulated by system's state. Hence, future work will focus on more detailed delineation of the intrinsic versus ANS-modulated HRV signatures in the physiological and pathophysiological contexts. The physiological context will include linking different signal-analytical domains of HRV such as fractal variability and complexity to the underlying processes characteristic of any living organism, such as metabolism and entropy production. [40]

Enhancing the pathophysiological context will provide the framework to increase the basic and clinical understanding of the signatures presented herein and drive the development of bedside algorithms for detection of fetal inflammation.

ACKNOWLEDGEMENTS

Funded by CIHR (to MGF and AJES), FRQS, MITACS/NeuroDevNet, Molly Towell Perinatal Research Foundation (to MGF) and CIHR-funded QTNPR and NeuroDevNet/MITACS (to LDD).

References

1. Gotsch F, Romero R, Kusanovic JP, Mazaki-Tovi S, Pineles BL, Erez O, Espinoza J, Hassan SS: **The fetal inflammatory response syndrome**. *Clinical obstetrics and gynecology* 2007, **50**(3):652-683.
2. Grether JK, Nelson KB: **Maternal infection and cerebral palsy in infants of normal birth weight**. *JAMA : the journal of the American Medical Association* 1997, **278**(3):207-211.
3. Garnier Y, Kadyrov M, Gantert M, Einig A, Rath W, Huppertz B: **Proliferative responses in the placenta after endotoxin exposure in preterm fetal sheep**. *European journal of obstetrics, gynecology, and reproductive biology* 2008, **138**(2):152-157.
4. Garite TJ: **Management of premature rupture of membranes**. *Clinics in perinatology* 2001, **28**(4):837-847.
5. Tracey KJ: **Reflex control of immunity**. *Nature reviewsImmunology* 2009, **9**(6):418-428.
6. Durosier LD, Green G, Batkin I, Seely AJ, Ross MG, Richardson BS, Frasch MG: **Sampling rate of heart rate variability impacts the ability to detect acidemia in ovine fetuses near-term**. *Frontiers in pediatrics* 2014, **2**:38.
7. Fairchild KD, O'Shea TM: **Heart Rate Characteristics: Physiomarkers for Detection of Late-Onset Neonatal Sepsis**. *Clinics in perinatology* 2010, **37**(3):581-598.
8. Rees S, Inder T: **Fetal and neonatal origins of altered brain development**. *Early human development* 2005, **81**(9):753-761.
9. Ratcliffe SJ, Shults J: **GEEQBOX: A Matlab toolbox for generalized estimating equations and quasi-least squares**. *J Stat Soft* 2008, **25**(14):1-14.
10. Frasch MG, Muller T, Wicher C, Weiss C, Lohle M, Schwab K, Schubert H, Nathanielsz PW, Witte OW, Schwab M: **Fetal body weight and the development of the control of the cardiovascular system in fetal sheep**. *The Journal of physiology* 2007, **579**(Pt 3):893-907.

11. Duncombe G, Veldhuizen RA, Gratton RJ, Han VK, Richardson BS: **IL-6 and TNFalpha across the umbilical circulation in term pregnancies: relationship with labour events**. *Early Hum Dev* 2010, **86**(2):113-117.
12. Chan CJ, Summers KL, Chan NG, Hardy DB, Richardson BS: **Cytokines in umbilical cord blood and the impact of labor events in low-risk term pregnancies**. *Early Hum Dev* 2013, **89**(12):1005-1010.
13. Rassias AJ, Holzberger PT, Givan AL, Fahrner SL, Yeager MP: **Decreased physiologic variability as a generalized response to human endotoxemia**. *Crit Care Med* 2005, **33**(3):512-519.
14. Scheff JD, Mavroudis PD, Calvano SE, Androulakis IP: **Translational applications of evaluating physiologic variability in human endotoxemia**. *Journal of clinical monitoring and computing* 2013, **27**(4):405-415.
15. Fairchild KD, Srinivasan V, Moorman JR, Gaykema RP, Goehler LE: **Pathogen-induced heart rate changes associated with cholinergic nervous system activation**. *American journal of physiologyRegulatory, integrative and comparative physiology* 2011, **300**(2):R330-339.
16. Olofsson PS, Rosas-Ballina M, Levine YA, Tracey KJ: **Rethinking inflammation: neural circuits in the regulation of immunity**. *Immunol Rev* 2012, **248**(1):188-204.
17. Haensel A, Mills PJ, Nelesen RA, Ziegler MG, Dimsdale JE: **The relationship between heart rate variability and inflammatory markers in cardiovascular diseases**. *Psychoneuroendocrinology* 2008, **33**(10):1305-1312.
18. von Kanel R, Nelesen RA, Mills PJ, Ziegler MG, Dimsdale JE: **Relationship between heart rate variability, interleukin-6, and soluble tissue factor in healthy subjects**. *Brain, behavior, and immunity* 2008, **22**(4):461-468.
19. **Heart rate variability: standards of measurement, physiological interpretation and clinical use. Task Force of the European Society of Cardiology and the North American Society of Pacing and Electrophysiology**. *Circulation* 1996, **93**(5):1043-1065.
20. Frasch MG, Mueller T, Weiss C, Schwab K, Schubert H, Schwab M: **Heart Rate Variability Analysis Allows Early Asphyxia Detection in Ovine Fetus**. *Reproductive sciences (Thousand Oaks, Calif)* 2009.

21. Furukawa S, Sameshima H, Yang L, Ikenoue T: **Activation of acetylcholine receptors and microglia in hypoxic-ischemic brain damage in newborn rats**. *Brain Dev* 2013, **35**(7):607-613.
22. Laude D, Baudrie V, Elghozi JL: **Effects of atropine on the time and frequency domain estimates of blood pressure and heart rate variability in mice**. *Clin Exp Pharmacol Physiol* 2008, **35**(4):454-457.
23. Frasch MG, Frank B, Last M, Muller T: **Time scales of autonomic information flow in near-term fetal sheep**. *Frontiers in physiology* 2012, **3**:378.
24. Beuchee A, Hernandez AI, Duvareille C, Daniel D, Samson N, Pladys P, Praud JP: **Influence of hypoxia and hypercapnia on sleep state-dependent heart rate variability behavior in newborn lambs**. *Sleep* 2012, **35**(11):1541-1549.
25. Hemphill JC, Andrews P, De Georgia M: **Multimodal monitoring and neurocritical care bioinformatics**. *Nature reviews Neurology* 2011, **7**(8):451-460.
26. Sorani MD, Hemphill JC, 3rd, Morabito D, Rosenthal G, Manley GT: **New approaches to physiological informatics in neurocritical care**. *Neurocritical care* 2007, **7**(1):45-52.
27. Karin J, Hirsch M, Akselrod S: **An estimate of fetal autonomic state by spectral analysis of fetal heart rate fluctuations**. *Pediatr Res* 1993, **34**(2):134-138.
28. Lake DE, Griffin MP, Moorman JR: **New mathematical thinking about fetal heart rate characteristics**. *Pediatr Res* 2003, **53**(6):889-890.
29. Frank B, Frasch MG, Schneider U, Roedel M, Schwab M, Hoyer D: **Complexity of heart rate fluctuations in near-term fetal sheep during sleep**. *Biomed Tech (Berl)* 2006, **51**(4):233-236.
30. Groome LJ, Loizou PC, Holland SB, Smith LA, Hoff C: **High vagal tone is associated with more efficient regulation of homeostasis in low-risk human fetuses**. *Dev Psychobiol* 1999, **35**(1):25-34.
31. Groome LJ, Mooney DM, Holland SB, Smith LA, Atterbury JL, Loizou PC: **Human fetuses have nonlinear cardiac dynamics**. *J Appl Physiol* 1999, **87**(2):530-537.
32. Frasch MG, Muller T, Weiss C, Schwab K, Schubert H, Schwab M: **Heart rate variability analysis allows early asphyxia detection in ovine fetus**. *Reprod Sci* 2009, **16**(5):509-517.

33. Lake DE, Richman JS, Griffin MP, Moorman JR: **Sample entropy analysis of neonatal heart rate variability**. *Am J Physiol Regul Integr Comp Physiol* 2002, **283**(3):R789-797.
34. Stone ML, Tatum PM, Weitkamp JH, Mukherjee AB, Attridge J, McGahren ED, Rodgers BM, Lake DE, Moorman JR, Fairchild KD: **Abnormal heart rate characteristics before clinical diagnosis of necrotizing enterocolitis**. *J Perinatol* 2013, **33**(11):847-850.
35. Rudolph AJ, Vallbona C, Desmond MM: **Cardiodynamic studies in the newborn. 3. Heart rate patterns in infants with idiopathic respiratory distress syndrome**. *Pediatrics* 1965, **36**(4):551-559.
36. Cabal LA, Siassi B, Zanini B, Hodgman JE, Hon EE: **Factors affecting heart rate variability in preterm infants**. *Pediatrics* 1980, **65**(1):50-56.
37. Seely AJ, Macklem PT: **Complex systems and the technology of variability analysis**. *Critical care (London, England)* 2004, **8**(6):R367-384.
38. Ahmad S, Ramsay T, Huebsch L, Flanagan S, McDiarmid S, Batkin I, McIntyre L, Sundaresan SR, Maziak DE, Shamji FM: **Continuous Multi-Parameter Heart Rate Variability Analysis Heralds Onset of Sepsis in Adults**. *PLoS One* 2009, **4**(8):e6642.
39. Fairchild KD, Schelonka RL, Kaufman DA, Carlo WA, Kattwinkel J, Porcelli PJ, Navarrete CT, Bancalari E, Aschner JL, Walker MW *et al*: **Septicemia mortality reduction in neonates in a heart rate characteristics monitoring trial**. *Pediatr Res* 2013, **74**(5):570-575.
40. Seely AJ, Macklem P: **Fractal variability: an emergent property of complex dissipative systems**. *Chaos* 2012, **22**(1):013108.

Figure legends

Figure 1A. Arterial blood gas and acid-base responses to lipopolysaccharide.

Blue, control group (n=5); red, LPS group (n=10) at baseline, 1h, 3h, 6h, 24h, 48h and 54h after start of the experiment. Mean ± SD. We found a significant time-LPS interactions for pH ($P=0.03$), pO_2, pCO_2, lactate and BE (all $P<0.001$).

Figure 1B. Cardiovascular responses to lipopolysaccharide.

Blue, control group (n=6); red, LPS group (n=10); mABP, fetal mean arterial blood pressure in mmHg; FHR, fetal heart rate at baseline in beats per minute (bpm), 1h, 3h, 6h, 24h, 48h and 54h after start of the experiment. Mean ± SD. We found time-LPS interaction for mABP and FHR responses ($P=0.015$ and $P<0.001$, respectively). This was significant for FHR at 6 hours ($P=0.008$).

Figure 1C. Fetal inflammatory response to lipopolysaccharide.

Blue, control group (n=5); red, LPS group (n=10); Mean ± SD. *, $P=0.001$ versus control.

Figure 2A. Heat map representation of the fetal heart rate variability response to inflammation.

Heat maps representing standardized variability measures adjusted for the baseline contribution for different time-points for LPS (TOP) and Control (Bottom). Numbers at the bottom of X-axis indicate animals. Left Y-axis labels indicate keywords for variability measures. Each row corresponds to a variability measure.

Figure 2B. Statistical representation of the fetal heart rate variability response to inflammation (cf. Figure 4).

Median of standardized variability measures (adjusted for the baseline contribution) across animals and variability measures at each time point, corresponding to the heat maps from Control and LPS group. (*) indicates p-values<0.05. (**) indicates p-values< 0.01. (***) indicates p-values<0.001, using a Wilcoxon rank-sum test on the medians.

Figure 3A. **Heat map representation of the fetal heart rate variability signature of inflammation.**

Heat maps representing standardized variability measures adjusted for the baseline contribution, for different time-points for LPS (TOP) and Control (Bottom), using features highly correlated with expected drop in variability. Numbers at the bottom of X-axis indicate animals. Left Y-axis labels indicate keywords for variability measures. Each row corresponds to a variability measure.

Figure 3B. **Statistical representation of the fetal heart rate variability signature of inflammation (cf. Figure 2).**

Median of standardized variability measures (adjusted for the baseline contribution) across animals and selected variability measures (11) at each time point, corresponding to the heat maps from Control and LPS group. (*) indicates p-values<0.05. (**) indicates p-values< 0.01. (***) indicates p-values<0.001, using a Wilcoxon rank-sum test on the medians. The effect of LPS at 3 hours is consistent with the IL-6 peak at 3 hours following the LPS injection.

Figure S1. Representative fetal EKG recordings from the Control and LPS groups.

TOP: Fetal ECG, diastolic, systolic, mean and raw arterial blood pressure signals (Dbp, Sbp, Mnbp, BP, fetal heart rate (HR).

BOTTOM: Atrioventricular blocks seen in both one control and two LPS sheep fetuses. Notably, in the LPS fetus the AV block was observed intermittently throughout the post LPS period on Day 1, while it was seen only once in the control fetus. Three control fetuses showed brief episodes of premature ventricular contraction (PVC) with what may be a subsequent ventricular block (VB). One LPS fetus showed also a series of intermittent premature ventricular contractions with a block. Please note that no formal cardiology review was performed.

Table 1. Description of heart rate variability domains.*

Domain	Features
Statistical	The statistical domain consists of statistical measures (mean, standard deviation, Gaussian, and so on) describing the data distribution. It assumes the data originates from a stochastic process.
Geometric	The geometric domain describes the properties related to the shape of the dataset in space. This includes, in a deterministic system, grid counting, heart rate turbulence, spatial filling index, and Poincaré and recurrence plots.
Energetic	The energetic domain describes the features related to the energy or the power of the data, such as frequency, periodicity, and irreversibility in time.
Informational	The informational domain describes the degree of complexity and irregularity in the elements of a time series, such as distance from periodicity or from a reference model. It includes various measures of entropy (compression, fuzzy, multiscale, and so on).
Invariant	The invariant domain describes the properties of a system that demonstrate fractality or other attributes that do not change over either space or time. Included are scaling exponents, fluctuation analysis, and multifractal exponents.

* Domains suggested for continuous individualized multiorgan variability analysis (CIMVA platform). After Bravi *et al.*, 2011.

Table 2. Statistical significance of time and group effects* on the median change of fetal heart rate variability corresponding to the heat maps (cf. Fig. 2) from Control and LPS group.

Variable	Beta	Std. Error	z value	p-value	95% CI
Time	-0.0030	0.0013	-2.2780	0.0227	[-0.0055 -0.0004]
Group	0.1560	0.0778	2.0056	0.0449	[0.0035 -0.3085]
Constant	-0.0105	0.0646	-0.1620	0.8709	[-0.1372 -0.1162]

* using a Quasi Least Squares method within the framework of Generalized Estimating Equations, with a Markov Correlation structure. The standard errors, 95% confidence intervals, and p-values are for the tests Beta = 0. Both Time and Group effects are statistically significant at the 0.05 level.

Table 3. fHRV measures correlating to the LPS-induced* inflammation

Domains	fHRV measures	R**
Statistical	Mean heart rate	0.60
	Interquartile range	0.31
	Symbolic dynamics: modified conditional entropy, non-uniform case	0.42
	Symbolic dynamics: forbidden words, non-uniform case	0.38
	Symbolic dynamics: Shannon entropy, non-uniform case	0.44
	Symbolic dynamics: percentage of 1 variations sequences, non-uniform case	0.45
	Symbolic dynamics: percentage of 0 variations sequences, non-uniform case	0.45
Geometric	Grid transformation feature: grid count	0.34
Energetic	LF Power	0.34
	Multifractal spectrum cumulant of the second order	0.47
	Multiscale time irreversibility asymmetry index	0.46
Informational	Grid transformation feature: AND similarity index	0.34
	Fano factor distance from a Poisson distribution	0.30
	Allan factor distance from a Poisson distribution	0.49
Invariant	Correlation dimension (Global exponent)	0.32
	Scaled windowed variance	0.40

* *i.e.*, during inflammatory response induced by LPS injections

** Spearman correlation coefficient, p-values <<0.01

Note that the correlation we report here is not a correlation with the levels of the actual inflammatory cytokine IL-6. Rather, it is the (absolute) Spearman correlation between the time responses of each fHRV measure synchronized across LPS animals and a piecewise linear prototype function with a peak at 3h, which was our *a priori* assumption for the prototypical inflammatory response of LPS animals based on the systemic peak response of IL-6 to LPS exposure.

Table 4. Statistical significance of time and group effects* on the median change of the selected fetal heart rate variability representing the "inflammatory signature" (cf. Fig. 3) from Control and LPS group.

Variable	Beta	Std. Error	z value	p-value	95% CI
Time	-0.0069	0.0019	-3.6885	0.0002	[-0.0105 -0.0032]
Group	0.5461	0.2345	2.3284	0.0199	[0.0864 -1.0058]
Constant	-0.1945	0.2279	-0.8537	0.3932	[-0.6412 -0.2521]

* using a Quasi Least Squares method within the framework of Generalized Estimating Equations, with a Markov Correlation structure. The standard errors, 95% confidence intervals, and p-values are for the tests Beta = 0. Both Time and Group effects are statistically significant at the 0.05 level.

Fig. 1A

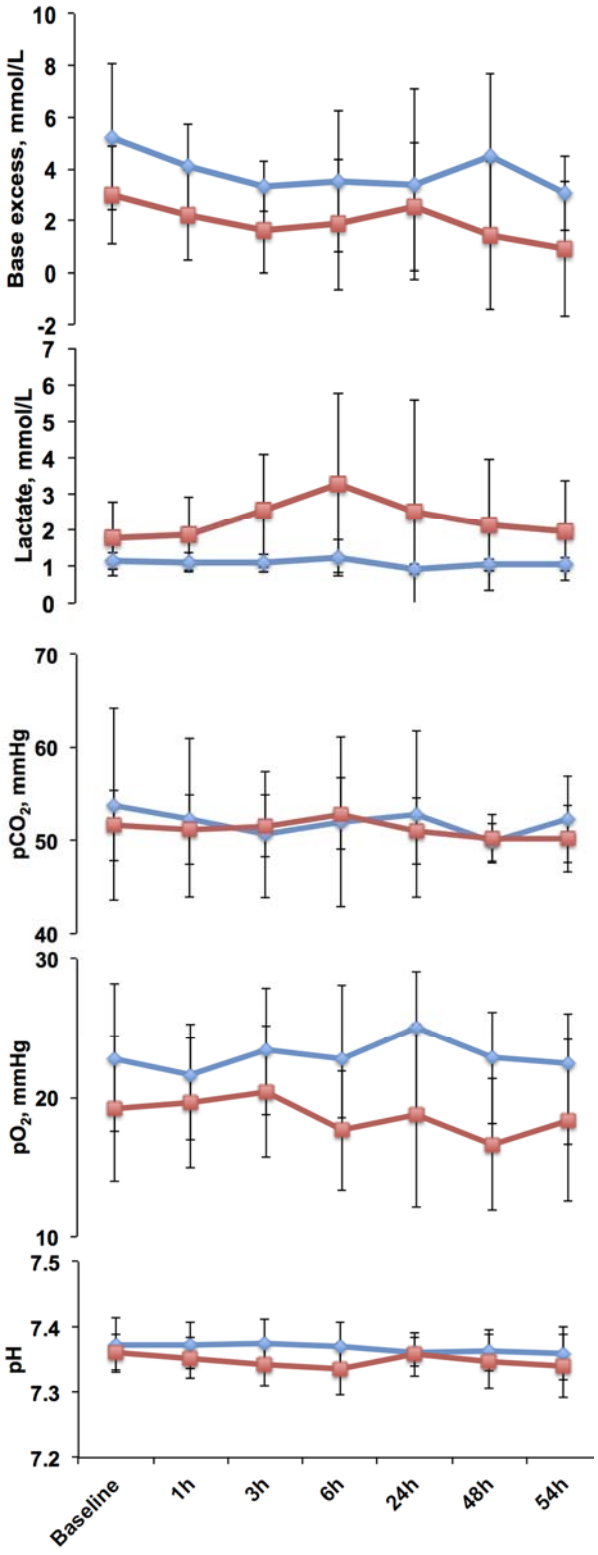
Base excess, mmol/L
10
8
6
4
2
0
-2
Lactate, mmol/L
7
6
5
4
3
2
1
0
pCO2, mmHg
70
60
50
40
pO2, mmHg
30
20
10
pH
7.5
7.4
7.3
7.2
Baseline
1h
3h
6h
24h
48h
54h

Fig. 1B

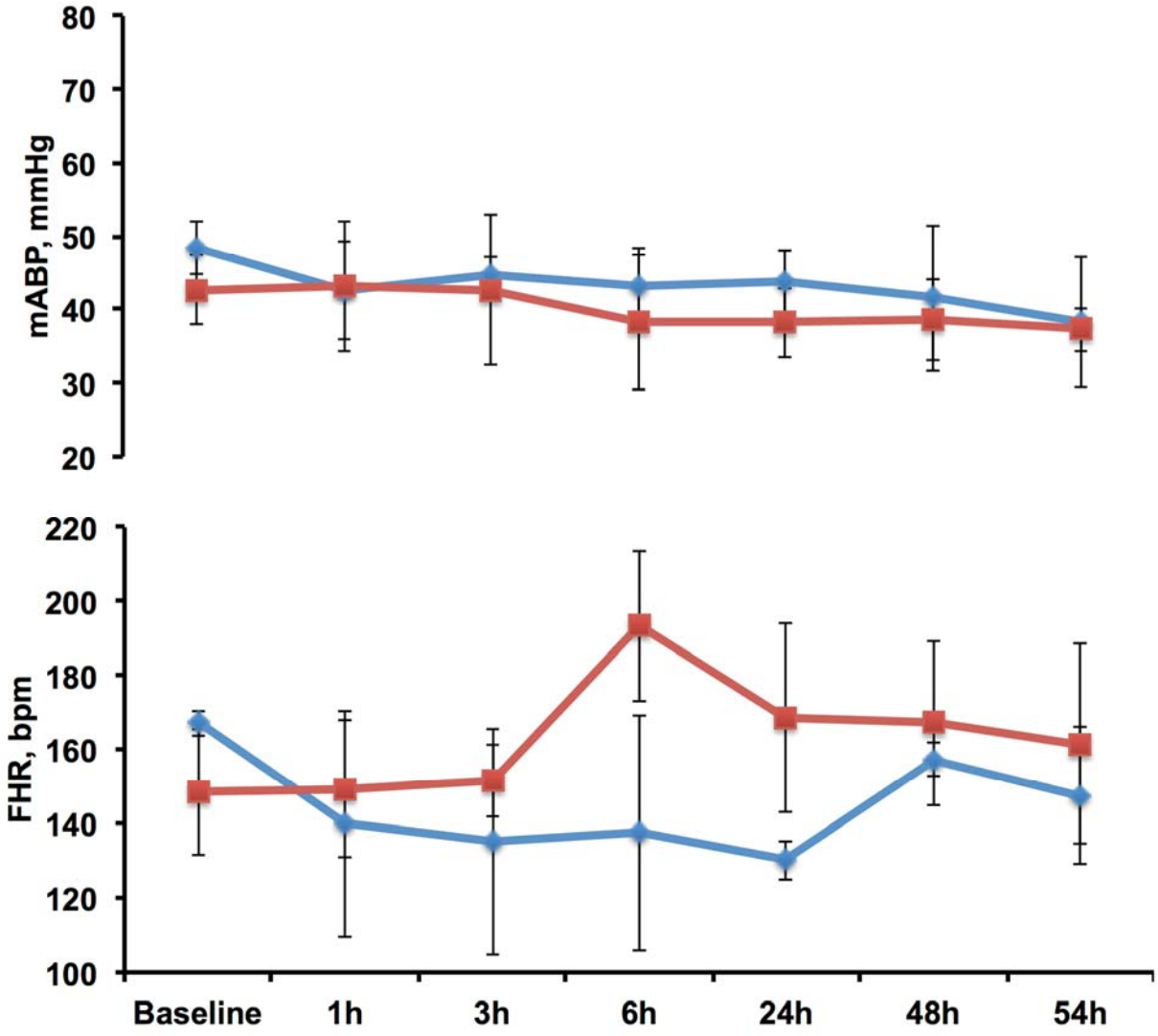
mABP, mmHg
80
70
60
50
40
30
20
FHR, bpm
220
200
180
160
140
120
100
Baseline
1h
3h
6h
24h
48h
54h

Fig. 1C

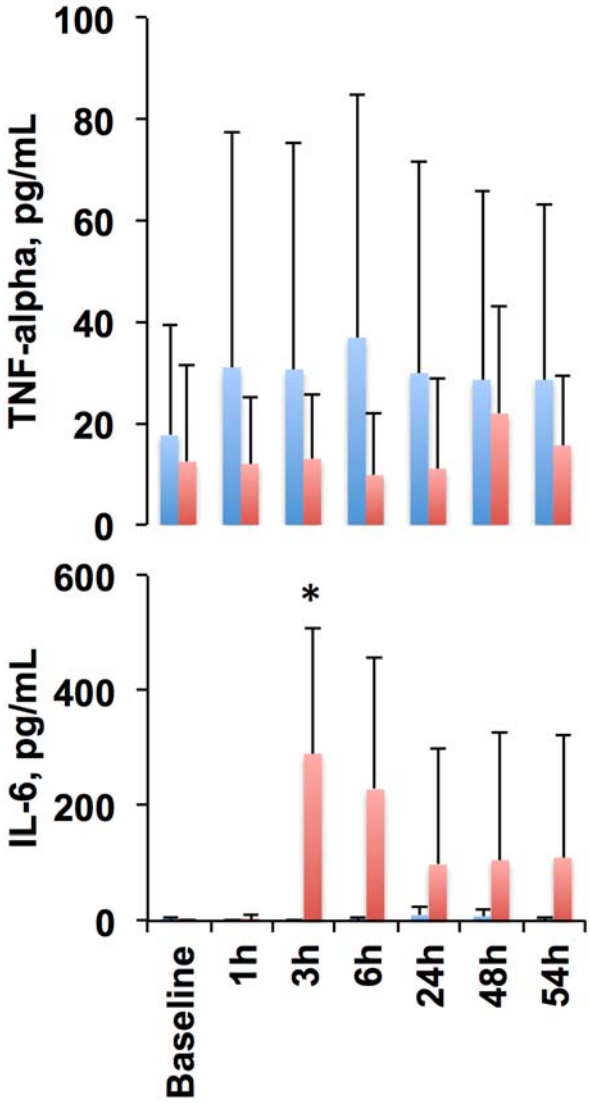
TNF-alpha, pg/mL
100
80
60
40
20
0
IL-6, pg/mL
600
400
200
0
*
Baseline
1h
3h
6h
24h
48h
54h

Fig. 2A

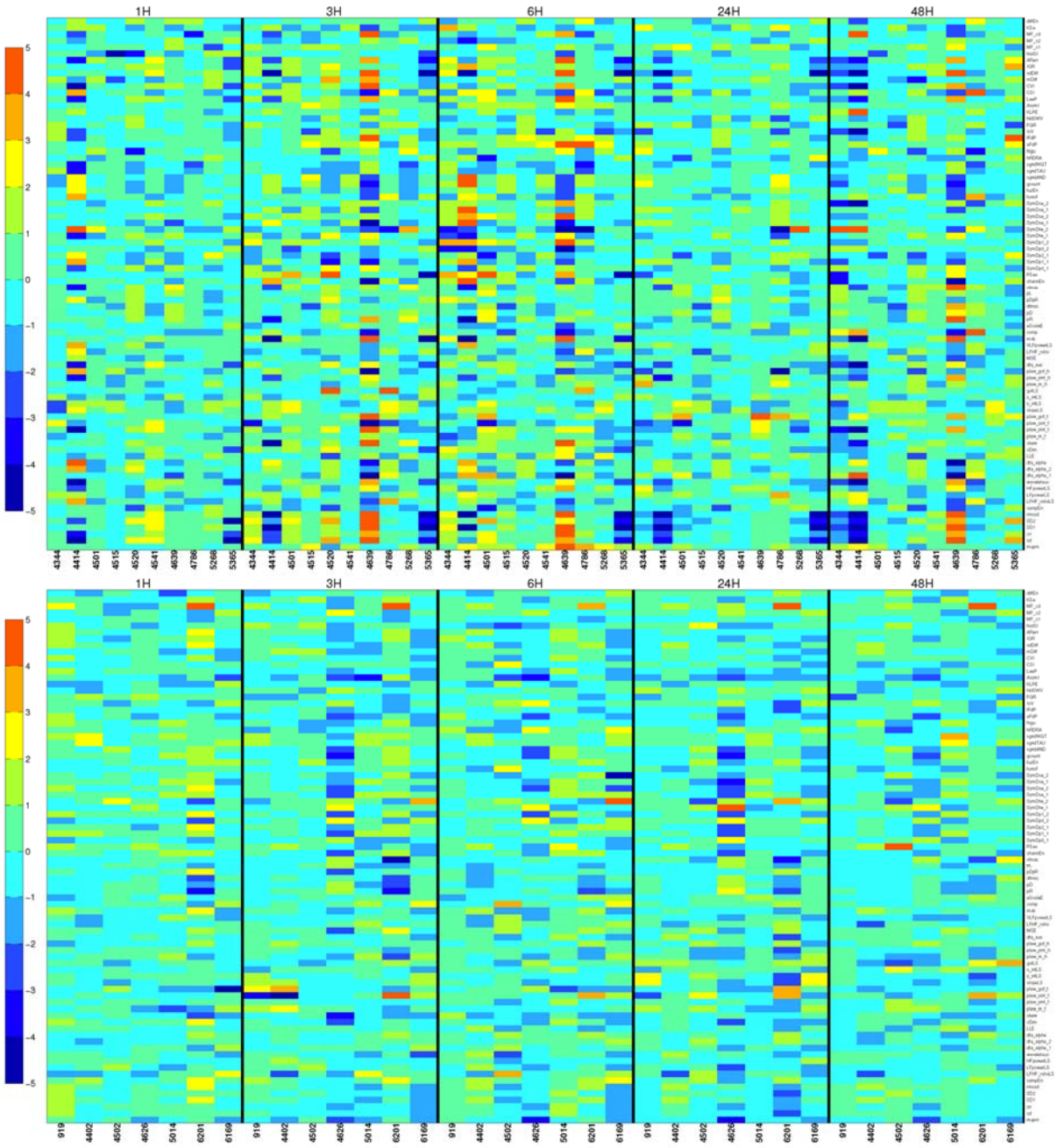
1H
3H
6H
24H
48H
5
4
3
2
1
0
−1
−2
−3
−4
−5
4344 4414 4501 4515 4520 4541 4639 4786 5268 5365
919 4402 4502 4626 5014 6201 6169

Fig. 2B

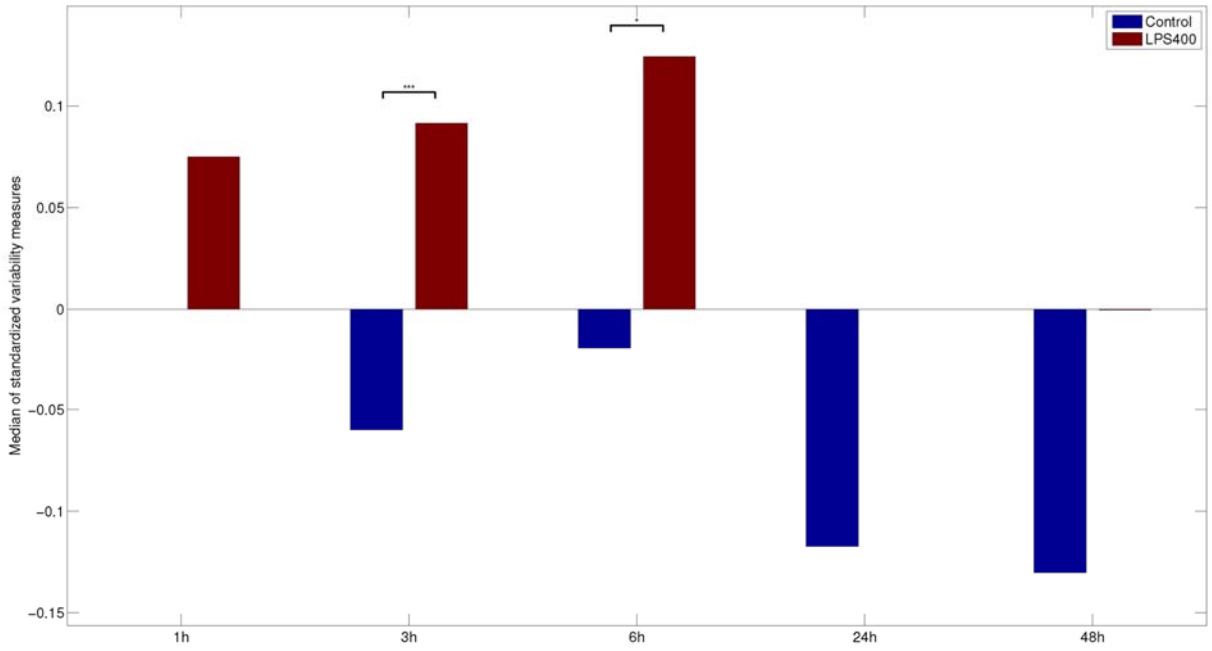
Control
LPS400
Median of standardized variability measures
0.1
0.05
0
−0.05
−0.1
−0.15
1h
3h
6h
24h
48h

Fig. 3A

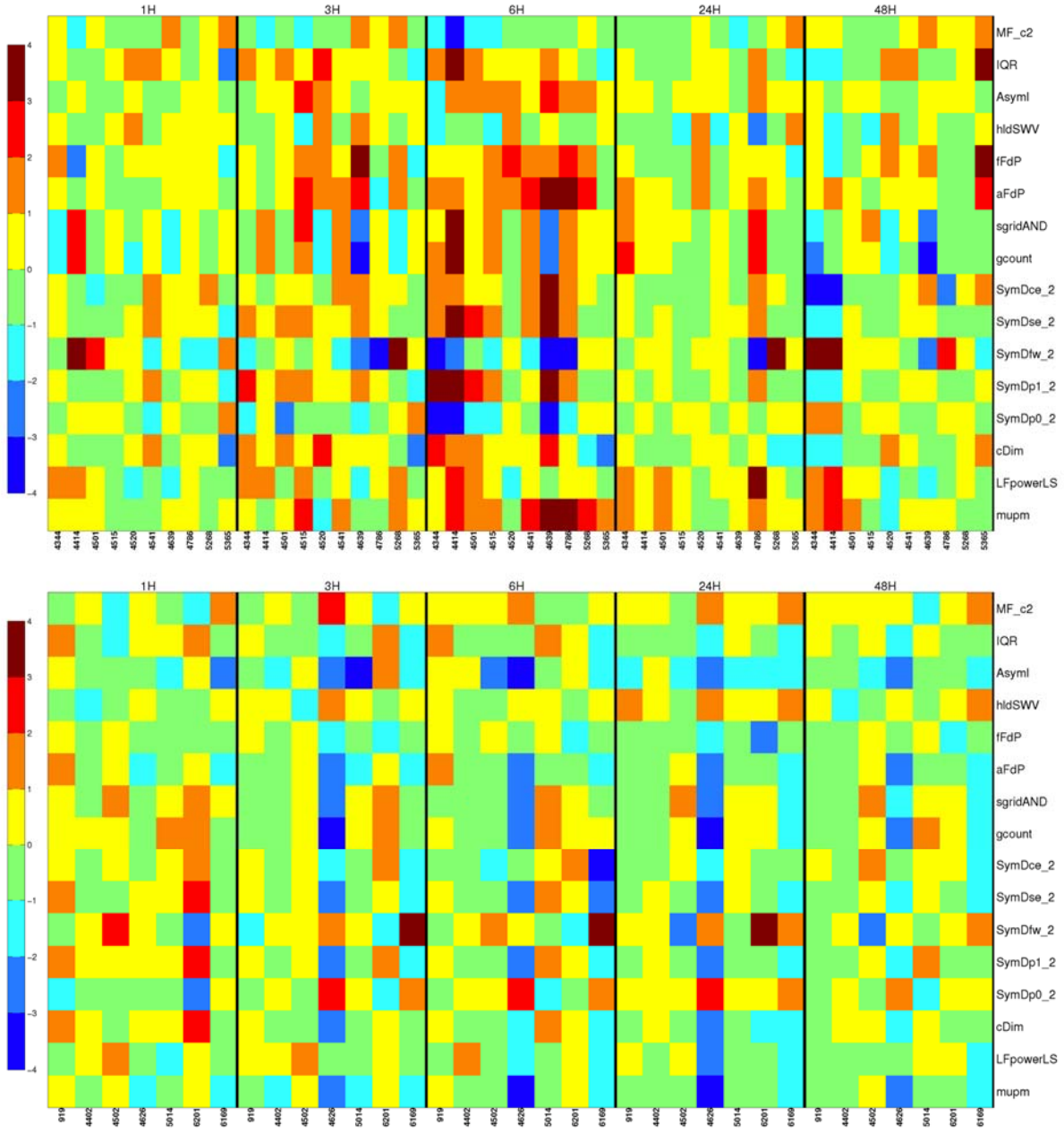
1H
3H
6H
24H
48H
MF_c2
IQR
Asyml
hldSWV
fFdP
aFdP
sgridAND
gcount
SymDce_2
SymDse_2
SymDfw_2
SymDp1_2
SymDp0_2
cDim
LFpowerLS
mupm

Fig. 3B

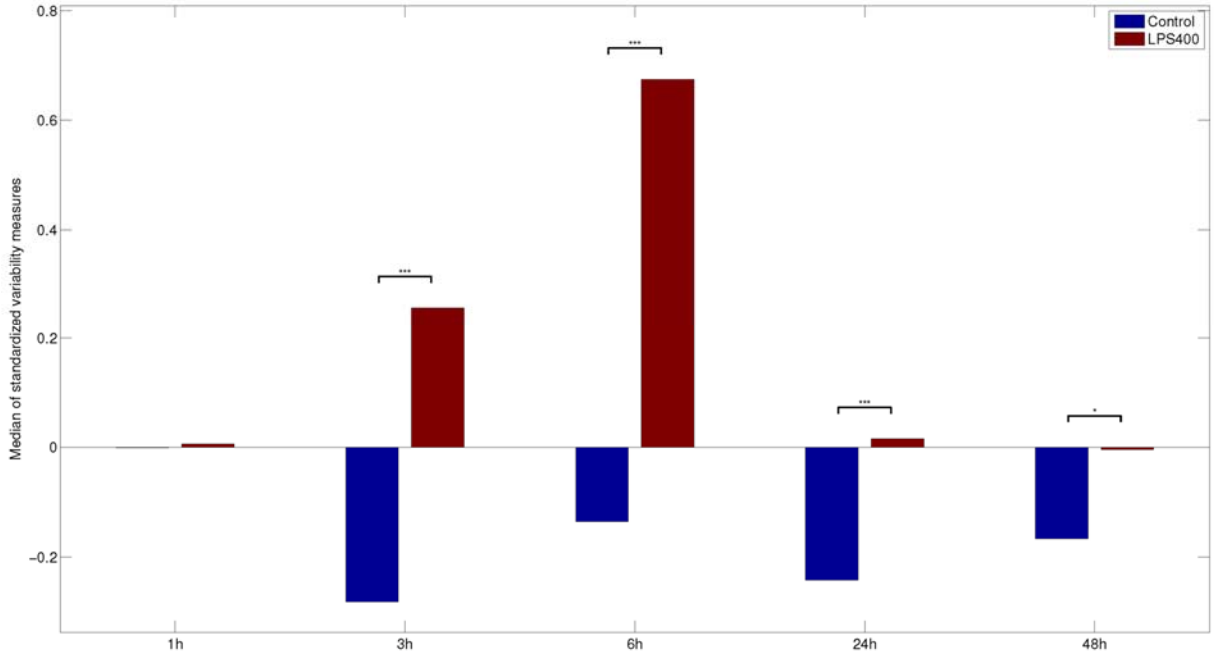
Control
LPS400
Median of standardized variability measures
0.8
0.6
0.4
0.2
0
−0.2
***
***
***
*
1h
3h
6h
24h
48h

Supplemental Digital Content

Table S1. Measures included in each domain of fetal heart rate variability for continuous individualized multiorgan variability analysis.

Domain	Fetal heart rate variability measure	CIMVA ID[#]
Statistical	Coefficient of variation (based on intervals)	**cv_interval**
	Form factor	**formF**
	Interquartile range	**IQR**
	Kurtosis	**kurt**
	Lee parameter	**LeeP**
	Mean value	**mu**
	Mean rate	**mupm**
	Mean of the differences	**mDiff**
	Root mean square of successive differences of R-R intervals	**rmssd**
	Skewness	**skew**
	Standard deviation	**sd**
	Standard deviation of the differences	**sdDiff**
	Symbolic dynamics: modified conditional entropy, non-uniform case	**SymDce_2**
	Symbolic dynamics: modified conditional entropy, uniform case	**SymDce_1**
	Symbolic dynamics: forbidden words, non-uniform case	**SymDfw_2**
	Symbolic dynamics: forbidden words, uniform case	**SymDfw_1**
	Symbolic dynamics: Shannon entropy, non-uniform case	**SymDse_2**
	Symbolic dynamics: Shannon entropy, uniform case	**SymDse_1**
	Symbolic dynamics: percentage of 0 variations sequences, non-uniform case	**SymDp0_2**
	Symbolic dynamics: percentage of 0 variations sequences, uniform case	**SymDp0_1**
	Symbolic dynamics: percentage of 1 variations sequences, non-uniform case	**SymDp1_2**
	Symbolic dynamics: percentage of 1 variations sequences, uniform case	**SymDp1_1**
	Symbolic dynamics: percentage of 2 variations sequences, non-uniform case	**SymDp2_2**
	Symbolic dynamics: percentage of 2 variations sequences, uniform case	**SymDp2_1**
Geometric	Dynamic moment of the second order	**DM2**
	Dynamical moment of the third order along the principal bisector	**DM3pb**
	Dynamical moment of the third order along the secondary bisector	**DM3sb**
	Dynamical moment of the third order along the x-axis	**DM3x**
	Dynamical moment of the third order along the y-axis	**DM3y**
	Finite growth rates	**avFGR**

	Grid transformation feature: grid count	**gcount**
	Poincaré plot SD1	**SD1**
	Poincaré plot SD2	**SD2**
	Poincaré plot cardiac sympathetic index	**CSI**
	Poincaré plot cardiac vagal index	**CVI**
	Recurrence quantification analysis: average diagonal line	**dlmean**
	Recurrence quantification analysis: maximum diagonal line	**dlmax**
	Recurrence quantification analysis: maximum vertical line	**vlmax**
	Recurrence quantification analysis: determinism/recurrences	**pDpR**
	Recurrence quantification analysis: percentage of determinism	**pD**
	Recurrence quantification analysis: percentage of laminarity	**pL**
	Recurrence quantification analysis: percentage of recurrences	**pR**
	Recurrence quantification analysis: Shannon entropy of the diagonals	**sedl**
	Recurrence quantification analysis: Shannon entropy of the vertical lines	**sevl**
	Recurrence quantification analysis: trapping time	**tTime**
Energetic	Low frequency/high frequency ratio	**LFHF_ratio**
	Low frequency (LF) power	**LFpower***
	High frequency (HF) power	**HFpower****
	Hjorth parameters: activity	**act**
	Hjorth parameters: complexity	**comp**
	Hjorth parameters: mobility	**mob**
	Multifractal spectrum cumulant of the first order	**Multifractal_c1**
	Multifractal spectrum cumulant of the second order	**Multifractal_c2**
	Multifractal spectrum cumulant of the third order	**Multifractal_c3**
	Multiscale time irreversibility asymmetry index	**AsymI**
	Plotkin and Swamy energy operator: average energy	**PSeo**
	Teager energy operator: average energy	**Teo**
	Very low frequency power	**VLFpower*****
	Wavelet area under the curve	**waveletauc**
Informational	Allan factor distance from a Poisson distribution	**aFdP**
	Fano factor distance from a Poisson distribution	**fFdP**
	Fuzzy entropy	**fuzEn**
	Grid transformation feature: AND similarity index	**sgridAND**
	Grid transformation feature: time delay similarity index	**sgridTAU**
	Grid transformation feature: weighted similarity index	**sgridWGT**
	Index of variability distance from a Poisson distribution	**IoVdP**

	Kullback-Leibler permutation entropy	**KLPEn**
	Multiscale entropy	**MSE**
	Predictive feature: error from an autoregressive model	**ARerr**
	Sample entropy	**SampEn**
	Shannon entropy	**shannEn**
	Similarity index of the distributions	**histSI**
Invariant	Correlation dimension global exponent	**cDimG**
	Detrended fluctuation analysis: a1	**dfa_alpha**
	Detrended fluctuation analysis: a2	**dfa_alpha2**
	Detrended fluctuation analysis: area under the curve	**dfa_auc**
	Detrended fluctuation analysis: overall a	**dfa_alpha**
	Diffusion entropy	**diffEn**
	Embedding scaling exponent	**eScaleE**
	Kolmogorov-Sinai entropy	**KSe**
	Higuchi scaling exponent	**Higu**
	Largest Lyapunov exponent	**LLE**
	Power Law (based on frequency) slope x2	**plaw_m_f**
	Power Law (based on frequency) y-intercept x2	**plaw_yint_f**
	Power Law (based on frequency) x-intercept x2	**plaw_xint_f**
	Power Law (based on frequency) goodness of fit x2	**plaw_gof_f**
	Power Law (based on histogram) slope	**plaw_m_h**
	Power Law (based on histogram) y-intercept	**plaw_yint_h**
	Power Law (based on histogram) x-intercept	**plaw_xint_h**
	Power Law (based on histogram) goodness of fit	**plaw_gof_h**
	Rescaled detrended range analysis	**hRDRA**
	Scale-dependent Lyapunov exponent slope	**SDLEalpha**
	Scale-dependent Lyapunov exponent mean value	**SDLEmean**
	Scaled windowed variance	**hldSWV**

*, LF =[0.04-0.2 Hz]; **, HF=[0.2-2 Hz]; ***, VLF=[0.001-0.04 Hz].

#, CIMVA= continuous individualized multiorgan variability analysis.

2.4 Correlating multidimensional fetal heart rate variability analysis with acid-base balance at birth

Fast Track Communications

IOP Publishing | Institute of Physics and Engineering in Medicine Physiological Measurement

Physiol. Meas. 35 (2014) L1–L12 doi:10.1088/0967-3334/35/12/L1

Fast Track Communication

Correlating multidimensional fetal heart rate variability analysis with acid-base balance at birth

Martin G Frasch[1], Yawen Xu[2], Tamara Stampalija[3], Lucien D Durosier[1], Christophe Herry[4], Xiaogang Wang[2], Daniela Casati[5], Andrew JE Seely[4], Zarko Alfirevic[6], Xin Gao[2] and Enrico Ferrazzi[5]

[1] Department of Obstetrics and Gynecology and Department of Neuroscience, CHU Sainte-Justine Research Centre, University of Montreal, Montreal, Quebec, Canada
[2] Department of Mathematics and Statistics, York University, Toronto, Ontario, Canada
[3] Unit of Prenatal Diagnosis, Institute for Maternal and Child Health, IRCCS Burlo Garofolo, Trieste, Italy
[4] Dynamical Analysis Laboratory, Ottawa Hospital Research Institute, University of Ottawa, Ottawa, Canada
[5] Department of Obstetrics and Gynecology, Vittore Buzzi Children's Hospital, Biomedical and Clinical Sciences, Faculty of Medicine, University of Milan, Italy
[6] Department of Women's and Children's Health, University of Liverpool, Liverpool Women's Hospital, Liverpool, UK

E-mail:

Received 21 October 2014
Accepted for publication 31 October 2014
Published 19 November 2014

Abstract

Fetal monitoring during labour currently fails to accurately detect acidemia. We developed a method to assess the multidimensional properties of fetal heart rate variability (fHRV) from trans-abdominal fetal electrocardiogram (fECG) during labour. We aimed to assess this novel bioinformatics approach for correlation between fHRV and neonatal pH or base excess (BE) at birth.

We enrolled a prospective pilot cohort of uncomplicated singleton pregnancies at 38–42 weeks' gestation in Milan, Italy, and Liverpool, UK. Fetal monitoring was performed by standard cardiotocography. Simultaneously, with fECG (high sampling frequency) was recorded. To ensure clinician blinding, fECG information was not displayed. Data from the last 60 min preceding onset of second-stage labour were analyzed using clinically validated continuous individualized multiorgan variability analysis (CIMVA) software in 5 min overlapping windows. CIMVA allows simultaneous calculation of 101 fHRV measures across five fHRV signal analysis domains.

0967-3334/14/1200L1+12$33.00

We validated our mathematical prediction model internally with 80:20 cross-validation split, comparing results to cord pH and BE at birth.

The cohort consisted of 60 women with neonatal pH values at birth ranging from 7.44 to 6.99 and BE from −0.3 to −18.7 mmol L^{-1}. Our model predicted pH from 30 fHRV measures ($R^2 = 0.90$, $P < 0.001$) and BE from 21 fHRV measures ($R^2 = 0.77$, $P < 0.001$).

Novel bioinformatics approach (CIMVA) applied to fHRV derived from trans-abdominal fECG during labor correlated well with acid-base balance at birth. Further refinement and validation in larger cohorts are needed. These new measurements of fHRV might offer a new opportunity to predict fetal acid-base balance at birth.

Keywords: fetus, labour, monitoring, statistics, prediction, acidemia

S Online supplementary data available from stacks.iop.org/PM/35/1200L1

(Some figures may appear in colour only in the online journal)

1. Introduction

Prenatal and perinatal brain injury remain major causes of long-term neurodevelopmental disorders (Saigal and Doyle 2008). In full-term births, an important contributor to brain injury and cerebral palsy is intrapartum fetal hypoxia or asphyxia with consequent acidemia (Graham *et al* 2008). Although electronic fetal monitoring during labour has successfully reduced deaths (Chen *et al* 2011) and neonatal seizures, it has failed to accurately detect early fetal hypoxia/asphyxia (Nelson *et al* 1996, Grimes and Peipert 2010). This deficiency has contributed to an epidemic of unnecessary cesarean sections with ensuing maternal morbidity and costs, without, however, decreasing the rate of cerebral palsy.(Graham *et al* 2006) It is likely that after 40 years of extensive worldwide clinical application, the limits of standard fetal heart rate monitoring cannot be overcome.

There are several reasons why fetal heart rate monitoring fails to detect early hypoxia-associated acidemia. First, limited information can be derived from visual analysis of heart rate and uterine contraction patterns. Second, present technology for the detection of fetal heart bioelectric events is limited by poor recording of the true bioelectric signal. Trans-abdominal Doppler probes operate on averaged biophysical signals. Scalp electrodes, besides being invasive, are filtered or sampled at low frequency, thus detecting a smoothed QRS signal (Durosier *et al* 2013). Third, while fetal heart rate variability (fHRV) is known to reflect modulation by the autonomic nervous system (Frasch *et al* 2007 2009b), the loss of information inherent in these methods minimizes usable data for assessment. The time scale of subtle fHRV events requires temporal resolution of R peak detection in the QRS complex within less than 1 ms (Warner and Cox 1962, Akselrod *et al* 1981, Frasch *et al* 2009b, Durosier *et al* 2014a).

Recently, a multidimensional bedside monitoring approach has been developed to collect cardiac and respiratory signals and analyze variability. Seely *et al*'s continuous individualized multiorgan variability analysis (CIMVA) platform includes software based on complexity science (Green *et al* 2013). It has shown promise in adult intensive care units, identifying sepsis about 60 h before clinical diagnosis (Bravi *et al* 2012) and predicting shock and extubation failure (Green *et al* 2013). Similarly, Moorman *et al*'s displays of HRV monitors in the neonatal intensive care unit contributed to detection of impending sepsis by staff (Moorman *et al* 2011).

These techniques open exciting avenues to a completely different approach to fetal monitoring, given bioelectric events sampled at an appropriate frequency (Durosier *et al* 2014a).

In this study, we present a new method of intrapartum monitoring based on trans-abdominal fetal electrocardiography (fECG) acquired noninvasively from the surface of the maternal abdomen, with sampling frequency high enough to detect autonomic modulation of the fetal heart rate. The analysis relies on fHRV rather than focusing on cardiac performance as such. We developed a mathematical prediction model, using a multidimensional matrix of 101 fHRV measures and the clinically tested and standardized CIMVA platform (Bravi *et al* 2012), to predict pH and base excess (BE) at birth, with only one hour of fECG monitoring.

2. Materials and methods

2.1. Participants and data acquisition

This is a prospective cohort study. Women in labour were recruited at Vittore Buzzi Children's Hospital, University of Milan, Italy, and Liverpool Women's Hospital, United Kingdom. Data were analyzed in Canada at: 1) Sainte-Justine Research Centre, University of Montreal; 2) Ottawa Hospital Research Institute; and 3) Department of Mathematics, York University, Toronto.

The study was approved by the institutional research ethics boards in Milan and Liverpool. All participants signed informed consent. All women in labour with uncomplicated singleton pregnancies at full-term or beyond (38–42 weeks' gestation) were enrolled. Both vaginal and operative abdominal deliveries were included. Pregnancies with maternal or fetal complications, twin gestations, or non-vertex presentations were excluded. At the beginning of active labour, women were interviewed and informed of the possible different methodology of fetal heart rate monitoring, continuous rather than intermittent, as it is usual in low risk women, and requested to allow the additional non-invasive technology. Active labour was defined as cervical dilatation ≥3 cm and the presence of ≥6 uterine contractions in 20 min.

Fetal monitoring during labour was performed simultaneously with standard cardiotocography and trans-abdominal fECG (Monica AN24, Monica Healthcare, Nottingham, UK). To ensure blinding of clinicians and midwives, no trans-abdominal fECG information was displayed. Obstetric management proceeded according to local standard protocol. Acid-base balance was assessed at birth on the umbilical arterial blood for pH and BE as per standard protocol.

The fECG signal was recorded at 900 Hz, downloaded, and stored for later offline analysis. Time intervals between R waves of consecutive QRS complexes (R-R intervals) were extracted for CIMVA analysis. To simulate a practical scenario during labour we analyzed the last 60 min before the start of active pushing.

2.2. Data analysis and modelling

The unique feature of the CIMVA platform is that it allows simultaneous and standardized calculation of 101 fHRV measures across five domains (table 1; for the detailed break-down see table S1, supplementary appendix (stacks.iop.org/PM/35/1200L1)) (Bravi *et al* 2011 2012). Thus, the dataset contained 101 fHRV measures determined in 5 min sliding windows with a 2.5 min overlap. We averaged each fHRV measure over a 60 min period.

Briefly, we selected relevant variables by using least absolute shrinkage and selection operator (lasso) regression and the Bayesian information criterion (figure 1). To verify results, we randomly selected 80% of the cohort as a training set and 20% as a test set (80:20 cross-validation split).

Table 1. Description of heart rate variability domains[a].

Domain	Features
Statistical	The statistical domain consists of statistical measures (mean, standard deviation, Gaussian, and so on) describing the data distribution. It assumes the data originates from a stochastic process.
Geometric	The geometric domain describes the properties related to the shape of the dataset in space. This includes, in a deterministic system, grid counting, heart rate turbulence, spatial filling index, and Poincaré and recurrence plots.
Energetic	The energetic domain describes the features related to the energy or the power of the data, such as frequency, periodicity, and irreversibility in time.
Informational	The informational domain describes the degree of complexity and irregularity in the elements of a time series, such as distance from periodicity or from a reference model. It includes various measures of entropy (compression, fuzzy, multiscale, and so on).
Invariant	The invariant domain describes the properties of a system that demonstrate fractality or other attributes that do not change over either space or time. Included are scaling exponents, fluctuation analysis, and multifractal exponents.

[a] Domains suggested for continuous individualized multiorgan variability analysis (CIMVA platform).(16)

The prediction model was fitted by multiple linear regression analysis. Our dataset is high-dimensional with a larger number of variables (v) than the number of observations (n). Not unexpectedly, given that fHRV measures describe different but partially overlapping aspects of fHRV properties within and across signal analysis domains (table 1), some variables were highly correlated. The least absolute shrinkage and selection operator (lasso) proposed by Tibshirani (Tibshirani 1996) is a promising variable selection technique to handle this type of data; it is a penalized least squares method, imposing a constraint on the L_1 norm of the regression coefficients. We used least angle regression (LARS) from the R statistical package to obtain regression coefficients $\widehat{\beta}_{\text{lasso}}$ (Hornik 2014).

We used the minimum Bayesian information criterion (BIC) combined with the minimum sum of squared errors, $\text{SSE} = \sum(Y - X\widehat{\beta}_{\text{lasso}})^2$, to select the best subset model (Schwarz 1978). We then used multiple linear regressions to predict response variables (pH and BE at birth) based on the selected subset of independent variables (fHRV measures). This multiple linear regression analysis identified several 'redundant' variables with very small β regression coefficients and large P values. We therefore pruned the multiple linear regression model by eliminating these 'redundant' variables. Such elimination of independent variables resulted in only a moderate reduction of cross-validation prediction error (CVPE) in the model. After obtaining the pruned model, we tested it for accuracy, by using an 80:20 cross-validation split within the cohort. For cross-validation, we randomly selected 80% of the data as a training set and 20% as a test set. The CVPE was calculated to predict the confidence interval and was defined as $\text{CVPE} = \sqrt{\|Y_{\text{test}} - X_{\text{test}}\beta_{\text{train}}\|^2 / n_{\text{test}}}$, where Y_{test}, X_{test} and n are from the test data and β_{train} is the regression coefficient from the training data. The 95% prediction interval for $\hat{y}$ is $[\hat{y} + 1.96 * \text{CVPE}, \hat{y} - 1.96 * \text{CVPE}]$. The performance of the models was quantified as root mean squared error (RMSE) and visualized for each case via residual plots.

2.3. Statistical analysis

Since this is a pilot, proof-of-principle study, no sample size assessment was undertaken. A P value < 0.05 was considered significant. Statistical analysis was performed using SPSS, version 19 (IBM, Armonk, NY).

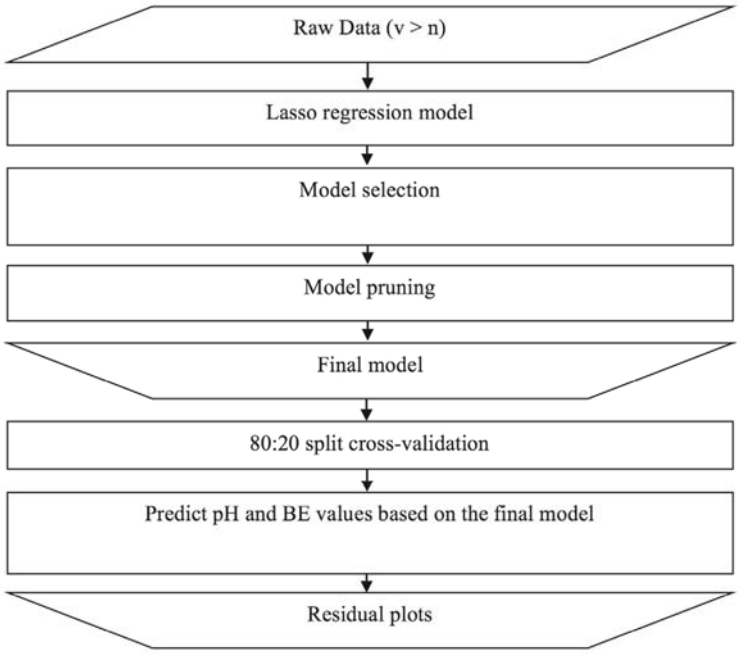

Figure 1. Steps in model building. The model was constructed using the least absolute shrinkage and selection operator (lasso) regression and the Bayesian information criterion for selection of variables, following steps outlined in the figure. Abbreviations: *n*, number of observations; *v*, number of variables. The 80:20 cross-validation split was performed; we randomly selected 80% of the data as a training set and 20% as a test set.

3. Results

3.1. Participant characteristics

The cohort consisted of 60 women (47 from Milan, 13 from Liverpool) of whom 3.3% (2 women) went on to have a cesarean section while the all the others have had a vaginal delivery. Of the vaginal deliveries, 18.3% (11 babies) were delivered by vacuum extraction and none by forceps extraction. Characteristics of the participants are summarized in table 2.

3.2. Model performance and validation

37 (19–60) min elapsed between the completion of the one hour fECG monitoring and the fetal blood gas and acid-base assessment at delivery (table 2). The models showed good fit for predicting pH and BE at birth: $R^2 = 0.77–0.90$ (figure 2, table 3). Gender and gestational age did not contribute significantly to the models. Neither variable was statistically significant

Table 2. Characteristics of participants included in the analysis[a].

Characteristic	
Maternal BMI, kg/m^2	26 ± 4
Maternal body weight, kg	70 ± 11
Maternal height, m	1.63 ± 0.05
Gravida	2 ± 1
Nulliparous—no. (%)	39 (65%)
Gestational age, days	281 ± 8
Gender, male (%)	28 (47%)
Weight, kg	3.47 ± 0.45
Serum pH	7.24 ± 0.09
Base excess, mmol/L	−6.3 ± 3.6
1 min Apgar score	8.7 ± 1.2
5 min Apgar score	9.7 ± 0.5
1st stage duration, hh:mm	4:23 (2:49–5:34)
Pushing duration, hh:mm	0:35 (0:18–1:00)
Recording end-delivery, hh:mm	00:37 (00:19–1:00)

Plus–minus values are means ± standard deviation.
Recording durations are provided as means (ranges).
BMI, body mass index; umbilical arterial blood values are provided for pH and base excess.
[a] Cohort size $N = 60$

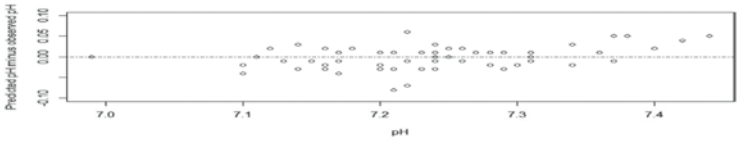

pH:
RMSE = 0.03
Pred. error range = [-0.08, 0.05]

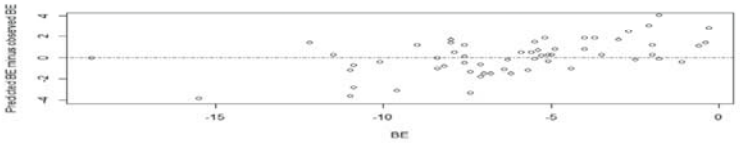

BE:
RMSE = 1.70
Pred. error range = [-3.6, 2.9]

Figure 2. Predictive power of the models. Residual plots for predicting pH and base excess (BE). RMSE, root mean squared error. The model made highly accurate predictions across a wide spectrum of pH and BE values observed as evidenced by the low RMSE.

for pH prediction. For BE, only gestational age was significant ($P = 0.04$). Nonetheless, R^2 values were hardly decreased when gestational age was removed: $R^2 = 0.79$ versus 0.77 with and without gestational age, respectively. The model selected 30 of the original

Table 3. Predicted values as compared to measured values for pH and base excess at birth[a].

	pH as response	BE as response
Goodness of fit (R^2)[b]	0.90	0.77
Sum of squared errors	0.05	174.26
Degrees of freedom	30	21
Predicted range of response variable (min, max)[a]	(6.99, 7.39)	(−18.74, −0.37)
True range of response variable (min, max)	(6.99, 7.44)	(−18.70, −0.40)
Cross-validation prediction error[c]	0.07	2.81

BE, base excess.
[a] Cohort size $N = 60$.
[b] Predicted range of response variables is based on cross-validation prediction error following an 80:20 cross-validation split at 95% confidence level.
[c] Cross-validation prediction error is the average of 1000 iterations.

Table 4. Distribution of fetal heart rate variability measures predicting pH and BE across signal-analytical domains.

fHRV domains[a]	Number of pH measures	Number of BE[b] measures	Number of measures common to both pH and BE
Statistical	5	6	1
Geometric	2	3	0
Energetic	4	3	1
Informational	9	3	2
Invariant	10	6	1

[a] Fetal heart rate variability (fHRV) domains, as suggested for continuous individualized multiorgan variability analysis (CIMVA).(16) see tables 1, S2 and S3 (stacks.iop.org/PM/35/1200L1).
[b] BE, base excess.

101 variables as useful predictors of pH ($R^2 = 0.90$) (table 3; for the detailed break-down of the fHRV measures selected see table S2, supplementary appendix (stacks.iop.org/PM/35/1200L1)). Cross-validation (80:20 split) confirmed accuracy of the model. Cross-validation prediction error was 0.0735, meaning that the predicted pH value had a range of ±0.144 at the 95% confidence level. The model for predicting BE had 21 variables. Cross-validation prediction error for BE was 2.81, meaning a range of ±5.498 at the 95% confidence level (table 3; for the detailed break-down of the fHRV measures selected see table S3, supplementary appendix (stacks.iop.org/PM/35/1200L1)).

3.3. Individual observations

The two babies delivered by cesarian section had a measured pH of 7.22 and 7.16 with BE of −7.6 mmol L^{-1} in both cases. Our model predicted the respective values of pH 7.16 and 7.19 with BE of −7.1 mmol L^{-1} and −8.8 mmol L^{-1}. Noteworthy, among the remaining babies, all delivered vaginally, one was born with pH of 6.99 and BE of −18.7 mmol L^{-1} and predicted pH of 6.99 and BE of −18.7 mmol L^{-1} (vacuum extraction); another baby was born without any surgical intervention with pH of 7.1 and BE of −15.5 (predicted pH of 7.14 and BE of −11.7 mmol L^{-1}). Overall, the model made highly accurate predictions across a wide spectrum of pH (6.99; 7.44) and BE (−18.7; −0.4 mmol L^{-1}) values observed as evidenced by the low cross-validation prediction error (figure 2, table 3).

3.4. Do pH and BE predictions reflect distinct physiological mechanisms?

We assessed the distribution of fHRV measures selected for the pH and BE prediction models, respectively, across the fHRV analytical domains (table 4). We found only 5 fHRV measures in common for the prediction of pH and BE at birth.

4. Discussion

4.1. Main findings

This study presents new insights on continuous fetal heart rate monitoring during labour using noninvasive fECG at sampling rates far exceeding those currently used for standard cardiotocographic monitoring (Durosier *et al* 2014a). We have developed a model for predicting pH and BE at birth based on fHRV in the hour preceding second-stage labour. The model using data from this last hour performed well across a wide range of physiological and pathological pH and BE values. Our findings build on previous results in a fetal sheep model of human labour where worsening fetal acidemia could be predicted early (1–2 h ahead of the pH drop to ≤ 7.00) using measures of true beat-to-beat heart rate variability such as root mean square of successive differences or sample entropy (Frasch *et al* 2009c, Durosier *et al* 2013 2014b). In the present study, we expanded the scope of fHRV analysis to include the most extensive currently available and clinically validated HRV analysis tool, the CIMVA platform. Our results indicate that acid-base status at birth can be predicted before the onset of active labour, *i.e.* before pushing begins.

4.2. Strengths and limitations

The strengths of the present study are two-fold. First, it is a proof-of-concept study on adapting and extending a CIMVA-type platform to the obstetric setting. Current results suggest that fHRV monitoring on a CIMVA platform is a potentially valuable instrument for improving intrapartum fetal surveillance. Second, the present study can be instructive as a prototype for the kind of analysis that can be applied to other realms of clinical care. Just as bioinformatics furthers an understanding of gene expression patterns, we have developed and deployed a novel approach that uses complex signal bioinformatics to predict fetal acidemia at birth. This approach confers advantages over existing methods: it takes physiological considerations into account, which we discuss below, and is validated within a pilot cohort using an 80:20 cross-validation split. The methodology developed here is widely generalizable within and well beyond obstetrics and fetal health diagnostics. It can be applied to any prediction of clinical outcome related to neurocardiovascular or neuroimmunological stimulation that involves afferent and efferent stimulation of sympathetic and parasympathetic branches of the autonomic nervous system and affects HRV properties. We anticipate that it can be deployed in a variety of clinical research challenges such as predicting degree of inflammation (pre-, peri-, and postnatally), intrauterine growth restriction, or early onset of preeclampsia or sepsis, because all these conditions are associated with responses of the autonomic nervous system via the cholinergic anti-inflammatory pathway or hypothalamic-pituitary-adrenal axis activation (Shapiro *et al* 2013).

Nevertheless, there are several limitations. Our sample size was relatively small. Consequently, there were only 2 cases of fetal acidemia in the cohort (pH < 7.00 or BE < − 12 mmol L^{-1}; one with both pH and BE fulfilling the criteria and another with BE only), insufficient to test for acidemia as a binary outcome (present or absent). Larger cohorts

cerebral metabolism and responsiveness (Amer-Wahlin and Marsal 2011). This assumption may explain the controversial clinical data so far reported by computerized ST-analysis trials (Salmelin *et al* 2013). Similarly, the method and results presented here need validation in larger trials.

5. Conclusion

The development of new technologies, such as combined trans-abdominal fetal ECG and bioinformatics (such as the CIMVA platform), gives grounds for revisiting the usefulness of intrapartum fetal heart rate monitoring. Our findings, validated across a wide range of physiological and pathophysiological pH and BE values, suggest that it is feasible to predict acid-base status at birth through the analysis of fHRV variables before the onset of second-stage labour. Larger clinical cohorts are needed to further validate these findings, refine the prediction models, and evaluate the clinical performance of the model as a novel tool to predict acid-base status at birth and hence its potential to provide early guidance to obstetrical labour management and prediction of neonatal well-being.

Acknowledgments

The authors are grateful to Danielle Buch, medical writer/editor at the Applied Clinical Research Unit of the CHU Sainte-Justine Research Center for critical revision of the manuscript, substantive editing, and rewrites. The authors also thank Carmen Movila for excellent secretarial support.

Disclosure of interests

No conflicts of interests to declare.

Contribution to authorship

YX, TS, LDD, CH and DC performed the actual experiments, analysed the initial results, and contributed to the final article. TS, DC, ZA and EF obtained all patient samples, collected all clinical data, and contributed to the final article. MGF, TS, XW, AJES, ZA, XG and EF conceived of the study design, analysed the final data, wrote the initial draft of the article, and contributed to the final version.

Details of ethics approval

The study was approved by the institutional research ethics boards of the University of Milan and the University of Liverpool, and written informed consent was obtained from all participants.

Funding

Le Fonds de recherche du Québec—Santé (FRQS) salary support to MGF. Réseau de formation en recherche périnatale du Québec (QTNPR) scholarship to LDD. No further financial support was received by the authors for the research, authorship, and publication of this article.

References

Akselrod S, Gordon D, Ubel F A, Shannon D C, Berger A C and Cohen R J 1981 Power spectrum analysis of heart rate fluctuation: a quantitative probe of beat-to-beat cardiovascular control. *Science* **213** 220–2

Amer-Wahlin I and Marsal K 2011 ST analysis of fetal electrocardiography in labor *Semin. Fetal Neonatal Med.* **16** 29–35

Bravi A, Green G, Longtin A and Seely A J 2012 Monitoring and identification of sepsis development through a composite measure of heart rate variability *PLoS One* **7** e45666

Bravi A, Longtin A and Seely A J 2011 Review and classification of variability analysis techniques with clinical applications *Biomed. Eng. Online* **10** 90

Chen H Y, Chauhan S P, Ananth C V, Vintzileos A M and Abuhamad A Z 2011 Electronic fetal heart rate monitoring and its relationship to neonatal and infant mortality in the United States *Am. J. Obstet. Gynecol.* **204** 491.e1–10

Durosier L, Cao M, Batkin I, Matushewski B J, Keenliside L, Herry C, Green G, Seely A, Richardson B and M.G F 2013 Continuous multivariate electronic fetal monitoring during labor detects early onset of acidemia: Prospective study in fetalsheep model *(11th Annual Int. Conf. on Complexity in Acute Illness (ICCAI)). J. Critical Care* **28** e5–6

Durosier L D, Green G, Batkin I, Seely A J, Ross M G, Richardson B S and Frasch M G 2014a Sampling rate of heart rate variability impacts the ability to detect acidemia in ovine fetuses near-term *Front. Pediatr.* **2** 38

Frasch M G, Mansano R Z, Gagnon R, Richardson B S and Ross M G 2009a Measures of acidosis with repetitive umbilical cord occlusions leading to fetal asphyxia in the near-term ovine fetus *Am. J. Obstet. Gynecol.* **200** e1–7

Frasch M G, Muller T, Hoyer D, Weiss C, Schubert H and Schwab M 2009b Nonlinear properties of vagal and sympathetic modulations of heart rate variability in ovine fetus near term *Am. J. Physiol. Regul. Integr. Comp. Physiol.* **296** R702–7

Frasch M G, Muller T, Weiss C, Schwab K, Schubert H and Schwab M 2009c Heart rate variability analysis allows early asphyxia detection in ovine fetus *Reprod. Sci.* **16** 509–17

Frasch M G, Muller T, Wicher C, Weiss C, Lohle M, Schwab K, Schubert H, Nathanielsz P W, Witte O W and Schwab M 2007 Fetal body weight and the development of the control of the cardiovascular system in fetal sheep *J. Physiol.* **579** 893–907

Graham E M, Petersen S M, Christo D K and Fox H E 2006 Intrapartum electronic fetal heart rate monitoring and the prevention of perinatal brain injury *Obstet. Gynecol.* **108** 656–66

Graham E M, Ruis K A, Hartman A L, Northington F J and Fox H E 2008 A systematic review of the role of intrapartum hypoxia-ischemia in the causation of neonatal encephalopathy *Am. J. Obstet. Gynecol.* **199** 587–95

Green G C, Bradley B, Bravi A and Seely A J 2013 Continuous multiorgan variability analysis to track severity of organ failure in critically ill patients *J. Crit. Care.* **28** 879.e1–11

Grimes D A and Peipert J F 2010 Electronic fetal monitoring as a public health screening program: the arithmetic of failure *Obstet. Gynecol.* **116** 1397–400

Hornik K 2014 The R FAQ (available at: http://www.cran.r-project.org/doc/FAQ/R-FAQ.html)

Ivanov P C, Rosenblum M G, Peng C K, Mietus J, Havlin S, Stanley H E and Goldberger A L 1996 Scaling behaviour of heartbeat intervals obtained by wavelet-based time-series analysis *Nature* **383** 323–7

Kro G A, Yli B M, Rasmussen S, Norèn H, Amer-Wåhlin I, Saugstad O D, Stray-Pedersen B and Rosén K G 2010 A new tool for the validation of umbilical cord acid-base data *BJOG* **117** 1544–52

Kruger K, Kublickas M and Westgren M 1998 Lactate in scalp and cord blood from fetuses with ominous fetal heart rate patterns *Obstet. Gynecol.* **92** 918–22

Lucena F, Barros A K, Principe J C and Ohnishi N 2011 Statistical coding and decoding of heartbeat intervals *PLoS One* **6** e20227

Massimini M, Porta A, Mariotti M, Malliani A and Montano N 2000 Heart rate variability is encoded in the spontaneous discharge of thalamic somatosensory neurones in cat *J. Physiol.* **526** 387–96

Montano N, Porta A and Malliani A 2001 Evidence for central organization of cardiovascular rhythms *Ann. N Y Acad. Sci.* **940** 299–306

Moorman J R *et al* 2011 Mortality reduction by heart rate characteristic monitoring in very low birth weight neonates: a randomized trial *J. Pediatr.* **159** 900–6.e1

Nelson K B, Dambrosia J M, Ting T Y and Grether J K 1996 Uncertain value of electronic fetal monitoring in predicting cerebral palsy *N. Engl. J. Med.* **334** 613–9

Prout A P, Frasch M G, Veldhuizen R A, Hammond R, Ross M G and Richardson B S 2010 Systemic and cerebral inflammatory response to umbilical cord occlusions with worsening acidosis in the ovine fetus *Am. J. Obstet. Gynecol.* **202** 82.e1–9

Ross M G and Gala R 2002 Use of umbilical artery base excess: algorithm for the timing of hypoxic injury *Am. J. Obstet. Gynecol.* **187** 1–9

Saigal S and Doyle L W 2008 An overview of mortality and sequelae of preterm birth from infancy to adulthood *Lancet* **371** 261–9

Salmelin A, Wiklund I, Bottinga R, Brorsson B, Ekman-Ordeberg G, Grimfors E E, Hanson U, Blom M and Persson E 2013 Fetal monitoring with computerized ST analysis during labor: a systematic review and meta-analysis *Acta Obstet. Gynecol. Scand.* **92** 28–39

Schwarz G E 1978 Estimating the dimension of a model *Ann. Stat.* **6** 239–472

Shapiro G D, Fraser W D, Frasch M G and Séguin J R 2013 Psychosocial stress in pregnancy and preterm birth: associations and mechanisms *J. Perinat. Med.* **41** 1–15

Tibshirani R 1996 Regression skrinkage and selection via the lasso *J. R. Stat. Soc.* B **58** 267–88

Victory R, Penava D, Da Silva O, Natale R and Richardson B 2004 Umbilical cord pH and base excess values in relation to adverse outcome events for infants delivering at term *Am. J. Obstet. Gynecol.* **191** 2021–8

Warner H R and Cox A 1962 A mathematical model of heart rate control by sympathetic and vagus efferent information *J. Appl. Physiol.* **17** 349–55

3. DISCUSSION

3.1 L'arrêt adaptatif de l'activité EEG prédit l'acidémie critique chez le fœtus ovin proche du terme

3.1.1 L'EEG fœtal durant le travail peut permettre une détection précoce de l'acidémie

Nos trouvailles fournissent la preuve que le monitoring EEG fœtal durant le travail à haut risque chez l'homme peut permettre la détection précoce de l'acidémie à la naissance. L'EEG enregistré à partir du scalp fœtus ovin proche du terme montre des changements comparable à l'ECoG durant la normoxie (8) et pendant une hypoxie-acidémie aggravante. (9) Comparé au paradigme de l'OCO complète et fixe d'augmentation de fréquence que nous avons testé (7), la fréquence d'OCO n'a pas d'impact sur le patron de la réponse d'amplitude ECOG/EEG, mais a une influence sur les caractéristiques de la fréquence ECOG/EEG. La prochaine étape est de développer des algorithmes en ligne afin de détecter de telles réponses d'amplitudes et fréquences de l'EEG fœtal. En général, ceci confirme la notion que l'activité électrocorticographique acquise à partir des électrodes supra durales et l'activité électroencéphalographique acquise des électrodes de scalp devraient parallèlement refléter l'activité du champ potentiel de l'activité neuronale, quoique qu'avec une amplitude plus large que les signaux EEG correspondants. Les études cliniques avec des moniteurs de fonctions cérébrales chez les nouveaux nés avec suspicions d'encéphalopathie hypoxique-ischémique ont démontré la faisabilité de l'enregistrement de l'activité EEG à partir des électrodes du scalp et la valeur prédictive pour des séquelles neurologiques à long terme (49, 50). Cependant, cette capacité prédictive des enregistrements EEG, les signaux montrent que les séquelles existantes sont évolutives au niveau du cerveau à des degrés variables de mort cellulaire nécrotique et/ou apoptotique qu'elle soit primaire ou retardé (51) et leur impact sur l'activité de l'EEG, plutôt qu'une suppression adaptive de l'activité synaptique comme mécanisme protecteur. L'activité EEG comme mesure de la fonction cérébrale est aussi évaluée chez le fœtus humain durant les évènements relatif au travail après la rupture des membranes. Rosen et coll. sont les premiers à investiguer l'EEG chez le fœtus humain pendant les décennies 70 en plaçant deux électrodes EEG à ventouse transvaginalement sur le scalp fœtal à quelques distances séparées les unes des autres et ont été en mesure d'acquérir l'activité cérébrale durant les contractions utérines, épiduraux et administration des médicaments. (7, 52-57) Cependant, ces travaux ont été retardés en raison du manque d'avancement de la technologie computérisée pour l'analyse d'un grand

nombre de données et le besoin d'utiliser de multiples électrodes au niveau du scalp ce qui a rendu l'utilisation clinique impraticable. Récemment, Thaler et coll. ont utilisé l'analyse de la puissance spectrale en temps réel de l'EEG fœtal durant le travail pour faciliter le traitement et l'interprétation du signal. (58) Cependant, cette étude, démontrant clairement la présence de cycles d'état de sommeil chez le fœtus humain, était limité à 14 grossesses bien portantes avec issues normales, et encore ont utilisé de multiples électrodes du scalp afin d'obtenir l'EEG, ce qui encore n'est pas faisable pour une large utilisation clinique. En tant que tel, il y a un besoin constant de développer une sonde transvaginale originale capable d'acquérir les signaux EEG et RCF comme une première étape essentielle afin d'assurer la faisabilité clinique du monitoring afin d'évaluer la santé du fœtus durant le travail.

Nos résultats surmontent les limitations susmentionnées en fournissant 1) une sonde d'EEG qui peut être utilisée pratiquement et par chaque obstétricien formés en plaçant la sonde de cuir chevelu pour capter le RCF pendant le travail et 2) prouvant que l'utilisation de cette sonde EEG permettrait un dépistage précoce de d'une hypoxie acidémie aggravante permettant une intervention. Comme outil auxiliaire de la surveillance du RCF en intrapartum, le monitoring EEG fœtal devrait-elle attribuer un pouvoir de décision supplémentaire à l'obstétricien qui délivre s'il faut permettre au travail de continuer ou d'opter pour une césarienne, minimisant ainsi le nombre de bébés nés avec une acidémie sévère et un risque accru de lésions cérébrales d'une part et la diminution du nombre de césariennes inutiles d'un autre côté.

Les études cliniques prospectives sont nécessaires en urgence afin de valider cette nouvelle approche du monitoring électronique fœtal pendant le travail.

3.1.2 Les effets d'une hypoxie antérieure sur les réponses cardiovasculaires et à l'EEG suite aux occlusions du cordon ombilical

La principale trouvaille est que l'amplitude de l'ECoG chez les fœtus H/OCO était d' ~50% que des fœtus N/UCO pour la plupart des séries d'OCO. Ceci est accompagné d'une petite mais d'une importante réduction de la fréquence spectrale à l'ECoG (ECoG SEF) entre les occlusions pendant les séquences d'occlusions sévères quoique restant toujours fourchette de la bande thêta. Cette découverte est en ligne avec nos trouvailles antérieures ainsi que d'autres laboratoires. (6, 7) En contraste, l'amplitude à l'EEG était ~2 fois plus élevée chez le groupe

H/UCO que celui des N/UCO avant le début des expériences et durant les occlusions une fois que le patron synchronisé ECOG/EEG – FHR ait été observé. C'est probablement dû aux artéfacts de l'EEG chez le fœtus ovin. Nous anticipons que l'EEG du fœtus humain donnera un signal plus net tout en conservant le patron fondamental EEG-FHR que nous rapportons ici. Ceci est supporté par des études antérieures qui rapportent des états de sommeil bien dépeint perceptible à partir de l'EEG fœtal obtenu pendant le travail. (58)

Il y a eu également un effet prononcé d'une hypoxie précédente sur la réponse cardiovasculaire suite aux OCO. Le fœtus répond avec une augmentation de la Pression artérielle sanguine (PAS) pendant l'OCO, un comportement qui est modifié au fur et à mesure que le degré d'occlusions progresse et que l'acidémie augmente dans la mesure que la PAS n'augmente plus durant les occlusions.(7) Dans cette présente étude, nous avons observé que ce changement relatif de la PAS durant chaque occlusion, ΔPAS, était considérablement basse à travers chez le groupe H/OCO et similaire aux valeurs constatées durant le patron synchronisé ECOG/EEG-FHR chez les groupes N/OCO and H/OCO. D'ailleurs, pendant le patron synchronisé ECOG/EEG-FHR, les fœtus du groupe H/OCO a montré une profondeur de décélération du RCF d' ~60% plus bas que le groupe N/OCO (cf. ΔFHR in Table 1) due à une baisse du RCF moyen d' ~35% entre les OCO.

Ces trouvailles suggèrent que le patron synchronisé ECOG/EEG-RCF, pendant qu'il est corrélé dans le temps avec le début ΔPAS pathologique, n'est pas simplement secondaire compromis cardiovasculaire de l'autorégulation cérébrale, mais de préférence médié de manière neurale à un pH artérielle autour de 7.20. De plus, l'hypoxie chronique précédant des degrés d'OCO sévères n'ont pas d'impact sur le temps moyen d' ~53 minutes avant que le pH ne tombe au-dessous de 7.00 quand l'arrêt adaptatif cérébral est observé. Nous discutons d'éventuels mécanismes qui seraient liés aux changements systémiques du pH avec l'arrêt cérébral adaptatif du cerveau ailleurs. (59)

Remarquablement, nous avons pratiquement observé aucun effet d'hypoxie chronique sur les propriétés EEG suggérant que L'EEG va facilement traquer l'activité électrique cérébrale chez le fœtus indépendamment d'une hypoxie préexistante. Pendant le patron synchronisé ECOG/EEG-RCF, l'hypoxie chronique ampute la différence à L'EEG SEF pendant et entre chaque OCO, vu dans le groupe N/OCO. Ceci suggère que les efforts dans le développement de solides algorithmes automatisés pour la détection des patrons devraient viser à utiliser

l'amplitude des propriétés EEG plutôt que les propriétés de fréquence. L'hypoxie chronique probablement résulte de la suppression de l'ECoG dans le groupe des fœtus H/OCO, ce qui est la raison pour laquelle nous n'avons vu aucune différence entre les valeurs d'amplitude à l'ECOG et EEG et dans le groupe H/UCO comme nous l'avons fait dans le groupe N/UCO.

Les enfants avec retard de croissance et hypoxémie chronique due à la dysfonction placentaire sont à plus grand risque pour une acidémie alarmante à la naissance et de fait des effets neurologiques indésirables dus à hypoxémie aigue superposée pendant le travail. (3, 7, 11, 60) Qu'une hypoxie antérieure existe ou pas chez les fœtus RCIU, nos trouvailles montrent que le monitoring EEG-RCF peut permettre de détecter le schéma de synchronisation EEG-RCF comme un avertissement précoce d'une acidémie imminente.

3.1.3 L'arrêt cérébral adaptif est un mécanisme proactive qui n'est pas influencé par une hypoxie antérieure

Les considérations ci-dessus nous ont conduit à proposer que l'arrêt cérébral d'adaptation fœtal révèlent via le comportement synchronisé ECOG/EEG-FHR est un mécanisme proactif et probablement neuroprotecteur. Premièrement, il existe une cohérence remarquable à un pH de ~7.20, lorsque le patron apparaît dans le groupe N/OCO et H/OCO. Cela suggère un mécanisme actif déclenchant un arrêt cérébral d'adaptation. La littérature existante suggère que le récepteur adénosine (A1) assure la médiation du processus métabolique d'arrêt cérébral d'adaptation chez le fœtus.(61-63) En outre, en utilisant le même modèle animal avec mesures simultanées du débit sanguin cérébral et taux métabolique, nous avons démontré que lorsque la livraison de l'oxygène au cerveau est sévèrement compromise comme durant les OCO complètes l'ECOG aplatit reflétant une baisse d'activité synaptique comme un mécanisme neuroprotecteur. (60) Deuxièmement, les effets de l'hypoxie sont observés le plus souvent dans les réponses cardiovasculaires et les amplitudes de l'ECoG (diminution chez les H/OCO comparé au N/OCO), mais au niveau du pH ou du temps moyen où nous observons le schéma synchronisé ECOG/EEG-RCF. Cette trouvaille est également cohérente avec la littérature sur ce modèle animal. (6, 64, 65)

3.1.4 Significations et orientations futures

L'utilité de joindre le monitoring EEG-RCF est basée sur l'émergence logique des changements synchronisé EEG-RCF déclenchés par les OCO avant d'atteindre un degré sévère d'acidémie fœtale au cours de laquelle une atteinte cérébrale puisse survenir. Ce changements est dû à un mécanisme d'arrêt cérébral adaptatif enclenché à un pH de ~7.20 et ne dépend pas d'un comportement cardiovasculaire antérieure résultant d'une hypoxie chronique. Ceci fait que probablement ce mécanisme sera observé chez une large population de fœtus avec ou sans hypoxie précédant le début du travail. **Le monitoring de l'EEG fœtal pendant le travail a le potentiel de servir d'ajout technologique accessoire au monitoring électronique fœtal (MEF). Incorporé au MEF, l'EEG peut devenir un outil précieux, peu couteux, d'implantation et d'interprétation facile, afin de prédire avec précision une acidémie fœtale débutante chez les fœtus.**

3.2 Le taux d'échantillonnage de la variabilité cardiaque influence la capacité de détecter l'acidémie chez les fœtus ovins proches du terme

Dans cette étude, le RMSSD augmente tôt avec une hypoxie-acidémie aggravante chez chaque fœtus quand échantillonné à 1000 Hz. Ceci est en ligne avec les observations antérieures chez le fœtus ovin proche du terme subissant les OCO répétées et donnant lieu à une augmentation graduelle d'une hypoxie-acidémie aggravante. (16) Cependant, quand l'ECG fœtal a été échantillonné à 4 Hz de préférence simulant un taux d'échantillonnage bas pour la VRCf utilisée au sein des moniteurs électroniques de RCF, le RMSSD n'a pas augmenté de manière importante chez 5 des fœtus ovins et augmente uniquement à la fin de l'expérience avec une hypoxie-acidémie sévère chez les 4 autres animaux. La raison méthodologique de cette trouvaille est une surestimation de la VRCf en raison de son sous-échantillonnage. (66) (67) Comme mentionné par Merri *et coll.*, cette surestimation peut être davantage affectée par le degré de variabilité biologique lui-même introduisant un facteur de confusion au sein des mesures de VRCf dérivées de données de RCF très bas échantillonnés.

3.2.1 L'impact du taux d'échantillonnage sur l'estimation correcte des propriétés de la VRCf

Il a plusieurs raisons pour lesquelles le monitoring RCF manqué de détecter une hypoxie-acidémie tel présentement utilisé en clinique. Premièrement, l'information, provenant de l'analyse visuelle du patron du RCF et des contractions utérines, est limitée. Deuxièmement, la technologie actuelle pour la détection des évènements bioélectriques du cœur fœtal est limitée par la pauvreté du vrai signal bioélectrique. Les sondes Doppler transabdominale fonctionnent à partir de la moyenne de signaux biophysiques, et les électrodes du scalp, sont soit filtrés ou échantillonnés à basse fréquence, détecte un signal QRS robuste mais avec le moins de bruit possible. (27) Ceci résulte en une perte d'informations encastrées dans la VRCf. (13, 68) L'échelle de temps d'évènements subtiles de la VRCf nécessaire la résolution temporelle de détection des pics R au sein du complexe QRS dans moins de 1 milliseconde. (15, 28, 29) Notre approche et nos trouvailles chez le modèle ovin ont fait écho et sont supportées par des publications récentes d'études prospectives sur la VRCf chez l'homme. (67) L'acquisition commerciale d'un logiciel de RCF d'un moniteur conventionnel de cardiotocogramme utilisé dans cette étude dans laquelle le RCF échantillonné dérive d'un signal Doppler chaque 2.5 s. Les chercheurs ont modifié cet algorithme pour lire le RCF chaque 0.5 s (ce qui correspond à 2 Hz, deux fois plus bas que le taux d'échantillonnage utilisé dans la présente étude), donc augmenté de quelque peu la précision de l'estimation de la VRCf. En dépit de ce taux d'échantillonnage très bas de la VRCf, les mesures linéaires et non linéaires de la VRCf détermine à partir de ces données ont permis aux auteurs de détecter les différences entre la VRCf des fœtus de retard de croissance intra-utérin (RCIU) et les fœtus en bonne santé. Notamment, les auteurs ont rapporté qu'il n'a eu aucune différence au niveau de la puissance spectrale de haute fréquence de la VRCf entre les deux groupes. Ceci est cohérent avec la trouvaille principale de cette étude que le taux d'échantillonnage bas surestime probablement la VRC, ainsi cachant les vrais changements de la VRC dans un état pathophysiologiques

3.2.2 Signification clinique

Pour la détection précoce de l'acidémie fœtale pendant le travail tel que montré ici, le RMSSD comme mesure de la VRCf, des moyennes plus sensibles d'acquérir le RCF sont recommandées que celles actuellement déployés dans le monitoring électronique fœtal. Les candidats pour des moyennes alternatives dans l'évaluation fœtal dans la détection du commencement d'une hypoxie-acidémie inclus l'ECG transabdominale, déjà en utilisation au chevet du patient dans certaines juridictions, ou des approches expérimentales immisçant l'EEG fœtal pendant le travail.(7, 69, 70) L'ECG du scalp fœtal peut être aussi échantillonné à 1000 Hz, permettant ainsi une vrai analyses de la VRCf tel que présentée ici.

3.2.3 Les forces et faiblesses de l'étude

Les limitations de cette étude réside dans le fait que l'échantillon est de petite taille et que le focus est concentré sur une mesure particulière reflétant les modulations vagales de la VRCf, le RMSSD. De plus large études prospectives fondamentales chez le modèle ovin fœtal et clinique chez l'homme de monitoring du RCF pendant le travail sont nécessaires pour fournir une haute résolution des données R-R avec des paramètres cliniques corrélées tel que le pH et l'EB à la naissance. De telles données peuvent être alors étudiées avec un plus vaste groupe de mesures de VRCf pour valider leur utilité dans la surveillance du RCF en intrapartum pour la détection précoce de l'acidémie fœtal. Les premières étapes dans cette direction ont été effectuées avec le respect de la taille de d'échantillon, mais pas encore avec le respect de la résolution temporelle R-R, *i.e.*, le taux d'échantillonnage. (71)

3.2.4 Perspectives

Un monitoring continue de la VRCf battement par battement est capable de détecter l'activation vagale due à une acidémie fœtale peut être un outil profitable pour la détection précoce de l'hypoxie-acidémie à l'approche du terme.

3.3 Corréler l'analyse multidimensionnelle de la variabilité du rythme cardiaque avec l'équilibre acide-base à la naissance

3.3.1 Signification clinique

Cette étude présente de nouvelles connaissances sur le monitoring de continu du rythme cardiaque fœtal durant le travail utilisant l'ECGf non invasive à une fréquence d'échantillonnage qui dépassent de loin celles actuellement utilisées pour la surveillance cardiotocographique standard. Nous avons développé un modèle pour prédire le pH et l'EB à la naissance basée sur la VRCf dans l'heure précédant le deuxième stade travail. Le modèle à l'aide de données provenant de cette dernière heure représente bien une large gamme de pH physiologique et pathologique et des valeurs de l'EB. Nos découvertes s'appuient sur les précédents résultats obtenus chez le modèle ovin du travail humain où l'acidémie fœtale aggravante peut être prédite au début (1-2 heures avant la chute de pH à ≤ 7,00) à l'aide de vraies mesures de variabilité battement à battement cardiaque comme la moyenne quadratique des différences successives ou entropie de l'échantillon.(16, 27) (30) Dans la présente étude, nous avons élargi la portée de l'analyse de la VRCf pour inclure le plus vaste outil d'analyse de VRC actuellement disponible et cliniquement validé, la plateforme CIMVA. Nos résultats indiquent que le statut acido-basique à la naissance est prévisible avant le début du travail actif, c'est-à-dire, avant de pousser.

3.3.2 La VRCf comme code neural véhiculant l'information de l'axe cerveau-cœur détectant acidémie et inflammation

La base physiologique appliquant l'analyse multidimensionnelle de la VRCf avant le travail pour prédire le statut acide-base fœtal à la naissance est la compréhension grandissante que cette variabilité du rythme cardiaque est le résultat d'influences neurales complexes, subtilement codé en fluctuations de milliseconde.(15, 28, 29) La résolution temporelle de la VRCf nécessite par conséquent un échantillonnage plus élevé des signaux de fréquence cardiaque à celle actuellement utilisée en clinique obstétrique. Nous avons pu acquérir ces données hautement échantillonnées à l'aide d'ECGf transabdominale, une technologie bien supérieure, à cet égard,

au monitoring électronique fœtal conventionnel. Il y a de plus en plus d'évidences que la VRC véhicule un code neural avec des propriétés fortement non linéaire du signal (72) qui reflètent les influences superposées des rythmes du tronc cérébral et supra bulbaire, particulièrement thalamocorticale.(73-75) Vu le manque de connaissances quant à laquelle les propriétés de la VRC sont en meilleure corrélation avec la neurophysiologie, notre objectif était d'analyser la réponse à un défi comme le travail, en déployant une approche multidimensionnelle qui incorpore cinq domaines mis en place pour l'analyse de la variabilité (tableau 1).(76)

Notre modèle de prédiction contenait seulement 5 fHRV mesures communes au pH et à l'EB. Plusieurs mécanismes potentiellement complémentaires peuvent sous-tendre cette conclusion. Tout d'abord, comme les propriétés de VRCf reflètent la modulation de stimulus-réponse du cerveau de la fréquence cardiaque, on pense que le faible nombre de mesures communes peut-être provenir de différentes réponses neurostimulatoires aux changements du pH et de l'EB, respectivement. Cela donne à penser que les mesures de VRCf sélectionnés pour chaque modèle de prédiction peuvent refléter l'activation différentielle des patrons au niveau du système nerveux. Dans le modèle ovin du travail humain, nous avons montré que l'augmentation du niveau d'acidémie fœtale a entraîné une réponse inflammatoire fœtale élevée, en l'absence de tous stimuli pathogènes exogènes.(10) Nous croyons que l'EB à la naissance reflète l'activité neurale liée aux chémorécepteurs et la stimulation inflammatoire, alors que le pH à la naissance rend compte des réponses neuronales cumulatives médiée par les chémorécepteurs, d'augmentations progressives de l'acidémie métabolique. Ce dernier se produit pendant le travail et en phase finale d'une poussée d'hypercapnie dû à une diminution de la perfusion de la capacité placentaire et la clairance pour le CO_2.(11) En second lieu, nos résultats concordent avec la littérature qui rapporte qu'EB lors du travail corrèle plus étroitement avec l'acidémie métabolique (le lactate étant le principal contributeur de l'acide fixe) qu'aux changements de pH.(11, 77-79) Avec l'avancement du travail et l'acidémie, le pH augmente de façon non linéaire tandis que BE augmente linéairement comme la production anaérobiques de lactate augmente dans les tissus fœtaux.(77, 78, 80) En troisième lieu, les mesures de EB pour le sang du cordon ombilical sont plus sujettes à l'erreur que les mesures de pH, en raison des fluctuations de la pCO_2.(77)

En substance, le pH évalue l'acidémie métabolique et respiratoire et est donc un bon outil de surveillance. L'EB corrèle plus étroitement avec le lactate. De futures études de cohortes pourraient s'étendre à la recherche des facteurs prédictifs du taux de lactate à la naissance.
La notion de prédire le résultat du travail en évaluant le fonctionnement du cerveau fœtal n'est pas nouveau. L'analyse directe des patrons d'ECG fœtaux utilisant la technologie d'électrode du cuir chevelu repose sur l'hypothèse que le métabolisme myocardique fœtal peut être un substitut fiable d'une réactivité et d'un métabolisme cérébral faibles.(81) Cette hypothèse peut expliquer les données cliniques controversées jusqu'ici signalées par des essais d'analyse informatisée du segment ST.(82) Similairement, la méthode et les résultats présentés ici ont besoin de validation dans des études plus larges.

3.3.3 Les forces et faiblesses de l'étude

Les points forts de cette étude sont de deux ordres. Tout d'abord, c'est une étude de validation adaptant et prorogeant une plateforme de type CIMVA pour l'obstétrique. Les Résultats actuels suggèrent que la surveillance de VRCf via une plate-forme CIMVA est un instrument potentiellement précieux pour améliorer la surveillance fœtale en intrapartum.
Deuxièmement, cette étude peut être instructive comme un prototype pour le type d'analyse qui peut être appliquée aux autres mondes des soins cliniques. A l'instar de la bio-informatique qui favorise une compréhension des modèles d'expression de gènes, nous avons développé et déployé une nouvelle approche qui utilise des signaux bio-informatiques complexes pour prédire l'acidémie fœtale à la naissance. Cette approche confère des avantages par rapport aux méthodes existantes : il prend en compte les considérations physiologiques et est validé au sein d'une cohorte pilote à l'aide d'une scission de la validation croisée de 80/20. La méthodologie développée ici est largement généralisable au sein et au-delà de l'obstétrique et en diagnostic de santé fœtale. Il peut être appliqué à toute prévision d'issues cliniques liées à la stimulation neurocardiovasculaire ou neuroimmunologiques qui implique la stimulation afférente et efférente des branches sympathiques et parasympathiques du système nerveux autonome et affecte les propriétés de la VRC. Nous prévoyons qu'elle peut être déployée dans une variété de défis de la recherche clinique tels que prédire le degré d'inflammation (pré, péri-et après la naissance), retard de croissance intra-utérin, ou un commencement précoce de pré-éclampsie ou

de septicémie, parce que toutes ces conditions sont associées avec des réponses du système nerveux autonome via la voie cholinergique anti-inflammatoire ou l'activation de l'axe hypothalamo-hypophyso-surrénalien.(83)

Néanmoins, il y a plusieurs limites. La taille de notre échantillon était relativement faible. Par conséquent, il y avait seulement deux cas d'acidémie fœtale dans la cohorte (pH < 7.00 ou BE <-12 mmol/L; une avec pH et BE remplissant les critères et l'autre avec BE uniquement), ce qui est insuffisant pour tester l'acidémie comme un résultat binaire (présents ou absents). De plus grandes cohortes seront nécessaires pour valider la prédiction d'acidémie fœtale par ces modèles. Nous gageons que plus grandes cohortes renforceront la sélection des mesures de VRCf et affiner la prévisibilité du pH et de l'EB. Ceci est basé sur l'observation que notre modèle a obtenu de faibles erreurs de prévision du pH et de l'EB. Le concept de cette modélisation est prometteur et le modèle de prévision actuel peut encore être amélioré par une formation sur plusieurs séries de données.

3.3.4 Conclusions et directions futures

Le développement des nouvelles technologies, telles que le combinaison de l'ECG transabdominale fœtal et de la bio-informatique (par exemple, la plate-forme CIMVA), donne des motifs pour revisiter l'utilité du suivi de fréquence cardiaque fœtale en intrapartum. **Nos résultats validés dans une large gamme des valeurs physiologiques et physiopathologiques du pH et de l'EB, suggèrent qu'il est possible de prédire le statut acido-basique à la naissance par l'analyse des variables de VRCf avant le début de la deuxième étape du travail**. De plus grandes cohortes cliniques sont encore nécessaires pour valider ces résultats, affiner les modèles de prédiction et d'évaluer les performances cliniques du modèle comme un nouvel outil pour prédire l'état acido-basique à la naissance et donc sa capacité à orienter le début de la prise en charge obstétricale du travail et de la prédiction de bien-être néonatal.

3.4 Une signature de la réponse inflammatoire systémique fœtale dans le patron temporel des mesures de variabilité de la fréquence cardiaque : une étude prospective de septicémie induite par le lipopolysaccharide chez le modèle ovin

Nous démontrons qu'en **déployant des analyses multidimensionnelles de la VRC des sous-ensembles distinctifs des mesures de VRCf qui corrèle avec l'état d'inflammation fœtale peuvent être identifiées. Cela ouvre des voies à l'étude de la réponse inflammatoire fœtale comme en témoigne une fonction du comportement neuroimmunologiques dans les patrons de VRCf et éventuellement à la conception de moniteurs de chevet capables de détection précoce de l'inflammation subclinique chez le fœtus**.

La morphométrie de notre cohorte expérimentale, les gaz du sang artériel, le statut acide-base et les caractéristiques cardiovasculaires étaient dans les limites physiologiques et représentatives de fœtus ovin en fin de gestation comme modèle du développement du fœtus humain près du terme. (13) (84) L'effet de la faible dose de LPS que nous avons administré sur les réponses des gaz du sang artériel, du statut acide-base et cardiovasculaires est compatible avec une légère septicémie (légère acidémie métabolique compensée et hypoxie) témoigne d'une augmentation transitoire de l'IL-6 à 3 heures sans choc septique manifeste avec décompensation cardiovasculaire. Remarquablement, la montée de la cytokine était accompagnée d'une légère baisse de pression sanguine artérielle moyenne (PASM) et une augmentation de RCF. C'est ce qui explique pourquoi le RCF moyen a été sélectionné comme l'une des mesures de la VRCf pour dresser un profilage de l'inflammation. L'augmentation sélective de l'IL-6, mais pas de TNF-α est conforme à la littérature à ce stade de développement. (85) (86) Nous rapportons ici que malgré l'absence d'un moment zéro dans le changement des concentrations du TNF-α au fil du temps, le LPS a causé une diminution globale de la concentration de TNF-α.

3.4.1 Surveillance de la voie cholinergique anti-inflammatoires avec la VRC

Fairchild et coll. ont abordées dans leur élégant article une question importante de savoir comment une septicémie induite par l'agent pathogène et la réponse inflammatoire chez la souris adulte ont un impact sur les caractéristiques de fréquence cardiaque (FC) de premier ordre lesquelles peuvent être dérivés de la variabilité du Rythme Cardiaque (VRC) (87). Ces caractéristiques du RC peuvent être surveillées en permanence et de façon non invasive fournissant des aperçus de l'activité du système nerveux autonome (SNA) , du nerf vague en particulier, et son contrôle des réponses immunitaires innées à l'infection via la voie cholinergique anti-inflammatoire (VCA) (88). Les auteurs ont émis l'hypothèse que la VRC

devrait augmenter à la suite de l'activation de la VAC en réponse à l'infection. Leurs conclusions apparemment réfutent l'hypothèse initiale et soutiennent le phénomène clinique connu de « VRC supprimé », plutôt que d'une VRC élevée. La VAC a été identifié chez les animaux adultes et les humains (45, 46, 89). Plusieurs études épidémiologiques ont montré qu'une VRC basse, comme en témoigne en moyenne quadratique des différences successives des intervalles R-R de l'ECG (RMSSD) ou de puissance de bande spectrale de haute fréquence (HF), peut servir de marqueur de modulation vagale de l'activité inflammatoire chez l'adulte (90, 91). Les études clinico-pathologiques indiquent que la perte d'influence inhibitrice de la VAC libère l'immunité innée, produisant des niveaux plus élevés de médiateurs pro-inflammatoires qui exacerbent les lésions tissulaires, et diminue l'échelle de temps à court terme de la VRC (90-99). Fairchild et coll. se sont concentrés uniquement sur l'échelle de temps à long terme de la VRC, alors que l'hypothèse de l'auteur et le circuit de la VAC impliquent qu'infection et une septicémie moduleront la signalisation vagale. Autrement dit, l'échelle de temps de la VRC à court terme augmenteraient, mais pas nécessairement l'échelle temporelle de la VRC à long terme. Des exemples classiques de la VRC à court terme sont le RMSSD et la puissance de bande spectrale de HF (19). La relation entre ces mesures VRC à la VAC est maintenant bien documentée par des études cliniques citées ci-dessus, au moins chez l'organisme adulte.

Furukawa et coll. ont démontré que la VAC est active chez les rats néonataux et diminue les dommages hypoxiques-ischémiques du cerveau (100, 101). Chez le fœtus ovin, nous avons montré que le blocage de l'atropine n'a aucun effet sur la SDNN (16), tandis que d'autres ont démontré une diminution de la SDNN chez la souris adulte (102). Les deux études rapportent une tachycardie importante en conséquence. Ces différences suggèrent qu'il puisse exister des variations subtiles, mais pertinentes selon l'espèce dans les échelles de temps de la VRC à laquelle l'activité vagale fonctionne. En outre, le développement su SNA dépend des trajectoires individuelles de croissance in utero (13) et est aussi dépendante de l'espèce en ce qui concerne les modes d'activation sympathique et vagale (103). La notion même d'activation sympathique versus parasympathique a été contestée en jetant les bases du concept de co-activation sympathico-vagale comme le montrent différentes études, espèces et stades de développement. (103) (104) Cela se traduit par l'obligation de présumer et demander des signatures plus complexes du comportement intrinsèque et contesté de la SNA reflété dans la VRC que des états simples de dominance sympathique ou vagale.

Ainsi, des études plus intégrées dans des modèles de septicémie néonatales sont nécessaires pour élucider la conduite d'observation clinique des auteurs de bradycardie et de dépression de la VRC sur une échelle à long terme au cours d'une septicémie et comment ce phénomène est lié à l'activité de la VAC. Nous suggérons que ces études ne devraient pas se concentrer sur la dépression de VRC en soi, mais plutôt pour des modèles de VRC représentées par ses caractéristiques multidimensionnelles, par exemple comme cela se fait par le système CIMVA que nous avons déployé dans la présente étude. Une telle approche nous a permis d'éviter de se limiter a priori à des mesures de la VRCf particulier, mais, plutôt, de chercher les mesures de la VRC reflétant des signatures incontestées, des états de base et d'inflammation.

3.4.2. Le cerveau est-il sensible dans la détection de l'inflammation fœtale encodée dans la VRCf ?

Notre compréhension de la dynamique de la VRCf chez les fœtus humains et ovins pendant des conditions physiologiques (par exemple, cycle du sommeil) et physiopathologiques (p. ex., asphyxie, septicémie) a évolué au cours des deux dernières décennies. (105) (41) (106) (44) La fin de gestation des fœtus humains expose une dynamique cardiaque non linéaire et un tonus vagal plus élevé qui est associé à une régulation plus efficace de l'homéostasie. (107, 108) La RCF et la VRCf sont régulés par une interaction complexe des systèmes nerveux sympathiques et parasympathiques comptant pour le RCF de base, mais aussi la VRCf à court terme et à long terme montrant des propriétés linéaires et non linéaires. (15) Ces propriétés de la VRCf sont affectées différemment par la réponse inflammatoire fœtale et néonatale induite par la LPS (109) (41) (42) (110) Une VRC fœtale et néonatale et des décélérations cardiaques transitoires et répétitives coïncident avec ou les signes cliniques prémonitoires de la septicémie. (111) (112) (44) Cela peut être dû à un tonus vagal altéré avec des impulsions vagales intermittentes dans le cadre d'une réponse inflammatoire systémique de fœtus au cours d'une septicémie. (44) ans un modèle expérimental d'infection chez l'adulte, l'activation sympathique par une perfusion d'adrénaline avant l'administration d'endotoxine réduit la VRC haute fréquence, suggérant une hypo réactivité vagale. (90) Une septicémie sévère pourrait induire un état de diminution générale d'impulsions ou de réactivité vagale, menant à quelques petites décélérations normales du RCF. En revanche, l'activation de la VAC en septicémie via signalisation vagale efférente

diminuerait la RCF et augmenterait la VRCf. (44) Basé sur l'évidence clinique périnatal chez l'homme et expérimentale chez l'animal , nous proposons de développer une surveillance longitudinale et complète de la VRCf chez un modèle de l'inflammation induite par LPS qui nous permettrait de construire des algorithmes afin d'améliorer le diagnostic précoce de l'infection. Une telle surveillance saisirait les propriétés linéaire et non linéaire de la VRCf, une stratégie qui s'est révélée efficace chez des adultes septiques et les patients néonatals. (43, 113, 114)

Nos études chez le fœtus ovin proche du terme suggèrent plus loin qu'une évaluation continue de la VRCf entre et durant les décélérations du RCF à des niveaux de précision supérieurs plutôt que ceux actuellement déployés en clinique avec des non-stress tests de CTG peuvent fournir d'autres aperçus de la dynamique des réponses du système nerveux autonome à l'acidémie à cause des compressions de cordon ombilical. Les mesures dérivées de la VRCf montrent le potentiel pour servir d'indicateurs d'acidémie fœtale à la naissante aussi tôt que 60 min avant la chute du pH à moins de 7,00.(16, 103) (115) (27)

3.4.3 Signification et perspectives

Nous avons identifié un sous-ensemble des mesures VRC qui semblent mieux caractériser l'état inflammatoire soit individuellement (plus forte corrélation avec le profil inflammatoire temporel prévu) ou lorsqu'il est utilisé en tant que groupe (analyse statistique de carte de chaleur). Ce sous-ensemble de mesures de VRC appartient aux différents domaines du VRC qui suggère que cette représentation multidimensionnelle des VRC reflète des codes sous-jacents véhiculant l'information sur les interactions neuroimmunologiques et éventuellement cardiaque intrinsèque, modulée par l'état du système. Donc, les futurs travaux devront mettre l'accent sur le tracé plus détaillée des signatures intrinsèque vs celles modulées par le SNA dans les contextes physiologiques et physiopathologiques. Le contexte physiologique inclura la liaison des différents domaines analytiques du signal de la VRC tels que la variabilité fractale et la complexité pour les processus sous-jacents caractéristiques de tout organisme vivant comme la production d'entropie et de métabolisme. (116) (117)

Mettre en valeur le contexte physiopathologique fournira le cadre afin d'accroître la compréhension fondamentale et clinique des signatures présentées ici et conduire au développement d'algorithmes de chevet pour la détection de l'inflammation foetale.

3.5 REMERCIEMENTS

Financée par les IRSC, FRQS, MITACS/NeuroDevNet, la Molly Towell Perinatal Research Foundation (pour MGF et AJES), Centre Conseil de développement des femmes de la London Health Sciences (MGF, BSR, MGR) et au QTNPR financée les IRSC (pour LDD). Les auteurs remercient Carmen Movila pour son assistance technique avec le manuscrit ainsi que Maria Sinacori, Brad Matushewski, Ashley Keen, Jennifer Thompson, Karolina Piorkowska et Dora Siontas pour l'assistance technique. Nous remercions également la contribution de la recherche présentée grâce à un atelier organisé par la Mathematical Biosciences Institute (MBI) à l'Ohio State University, Columbus, OH et le Fields Institute à l'Université de Toronto.

3.6 PUBLICATIONS DE CETTE THESE

Martin G. FRASCH**, L. Daniel DUROSIER**, Alex XU, Mingju CAO, Brad MATUSHEWSKI, Lynn KEENLISIDE, Yoram LOUZOUN, Michael G. ROSS, Bryan S. RICHARDSON. Adaptive shut-down of EEG activity predicts early onset of critical acidemia in the near-term ovine fetus. (Soumis en Mars 2014.) *En revision. J of Neuroscience.*

Durosier LD, Green G, Batkin I, Seely AJE, Ross MG, Richardson BS, et al. Sampling rate of heart rate variability impacts the ability to detect acidemia in ovine fetuses near-term. 2014. *Front Pediatr - Neonatalogy*. May 5;2:38. doi: 10.3389/fped.2014.00038.

Frasch MG. Xu Y, Stampalija T, **Durosier L.D**, Herry C, Wang X, Casati D, Seely AJ, Alfirevic Z, Gao X, Ferrazzi E. Multidimensional heart rate variability analysis prototype in the obstetric setting accurately predicts pH at birth for critical decision-making. 2014. *Physiological Measurement*. 35 L1 doi:10.1088/0967-3334/35/12/L1

LD Durosier, C. Herry, M. Cao, P Burns, A. Desrochers, G. Fecteau, A.J.E. Seely, M.G. Frasch. Does heart rate variability provide a signature of fetal systemic inflammatory response in a fetal sheep model of lipopolysaccharide-induced sepsis? Under review. (Submitted September 2014) *Pediatric Critical Care Medicine.*

4. References

1. Liston R, Crane J, Hamilton E, Hughes O, Kuling S, MacKinnon C, et al. Fetal health surveillance in labour. J Obstet Gynaecol Can. 2002;24(3):250-76; quiz 77-80.
2. Liston R, Crane J, Hughes O, Kuling S, MacKinnon C, Milne K, et al. Fetal health surveillance in labour. J Obstet Gynaecol Can. 2002;24(4):342-55.
3. Liston R, Sawchuck D, Young D. Fetal health surveillance: antepartum and intrapartum consensus guideline. J Obstet Gynaecol Can. 2007;29(9 Suppl 4):S3-56.
4. Gardner DS, Fletcher AJ, Bloomfield MR, Fowden AL, Giussani DA. Effects of prevailing hypoxaemia, acidaemia or hypoglycaemia upon the cardiovascular, endocrine and metabolic responses to acute hypoxaemia in the ovine fetus. J Physiol. 2002;540(Pt 1):351-66.
5. Fletcher AJ, Gardner DS, Edwards CM, Fowden AL, Giussani DA. Development of the ovine fetal cardiovascular defense to hypoxemia towards full term. American journal of physiology Heart and circulatory physiology. 2006;291(6):H3023-34.
6. Wassink G, Bennet L, Davidson JO, Westgate JA, Gunn AJ. Pre-existing hypoxia is associated with greater EEG suppression and early onset of evolving seizure activity during brief repeated asphyxia in near-term fetal sheep. PLoS ONE. 2013;8(8):e73895.
7. Frasch MG, Keen AE, Gagnon R, Ross MG, Richardson BS. Monitoring fetal electrocortical activity during labour for predicting worsening acidemia: a prospective study in the ovine fetus near term. PloS one. 2011;6(7):e22100.
8. Frasch M, Keen A, Matushewski B, Richardson B. Comparability of electroenkephalogram (EEG) versus electrocorticogram (ECOG) in the ovine fetus near term. Reprod Sci. 2010;17(3 (Suppl)):51A.
9. Frasch M, Durosier L, Duchatellier C, Richardson B. Fetal sheep electrocorticogram and electroencephalogram changes accompanying variable fetal heart rate decelerations warn early of acidemia. Reprod Sci. 2012;19(3 (Suppl)):F-090.
10. Prout AP, Frasch MG, Veldhuizen RA, Hammond R, Ross MG, Richardson BS. Systemic and cerebral inflammatory response to umbilical cord occlusions with worsening acidosis in the ovine fetus. Am J Obstet Gynecol. 2010;202(1):82 e1-9.

11. Frasch MG, Mansano RZ, Gagnon R, Richardson BS, Ross MG. Measures of acidosis with repetitive umbilical cord occlusions leading to fetal asphyxia in the near-term ovine fetus. American Journal of Obstetrics and Gynecology. 2009;200(27):200.e1-7.

12. Rees S, Inder T. Fetal and neonatal origins of altered brain development. Early human development. 2005;81(9):753-61.

13. Frasch MG, Muller T, Wicher C, Weiss C, Lohle M, Schwab K, et al. Fetal body weight and the development of the control of the cardiovascular system in fetal sheep. J Physiol. 2007;579(Pt 3):893-907.

14. Van Leeuwen P, Lange S, Bettermann H, Gronemeyer D, Hatzmann W. Fetal heart rate variability and complexity in the course of pregnancy. Early Hum Dev. 1999;54(3):259-69.

15. Frasch MG, Muller T, Hoyer D, Weiss C, Schubert H, Schwab M. Nonlinear properties of vagal and sympathetic modulations of heart rate variability in ovine fetus near term. American journal of physiology Regulatory, integrative and comparative physiology. 2009;296(3):R702-7.

16. Frasch MG, Muller T, Weiss C, Schwab K, Schubert H, Schwab M. Heart rate variability analysis allows early asphyxia detection in ovine fetus. Reprod Sci. 2009;16(5):509-17.

17. Siira SM, Ojala TH, Vahlberg TJ, Rosen KG, Ekholm EM. Do spectral bands of fetal heart rate variability associate with concomitant fetal scalp pH? Early human development. 2013;89(9):739-42.

18. Kwon JY, Park IY, Shin JC, Song J, Tafreshi R, Lim J. Specific change in spectral power of fetal heart rate variability related to fetal acidemia during labor: comparison between preterm and term fetuses. Early human development. 2012;88(4):203-7.

19. Heart rate variability: standards of measurement, physiological interpretation and clinical use. Task Force of the European Society of Cardiology and the North American Society of Pacing and Electrophysiology. Circulation. 1996;93(5):1043-65.

20. Frasch MG. Monitoring of fetal heart rate variability. Montebello Round Table Complexity and Variability at the Bedside; 2011; Montebello, Québec, Canada: J of Critical Care; 2010. p. e24.

21. Saigal S, Doyle LW. An overview of mortality and sequelae of preterm birth from infancy to adulthood. Lancet. 2008;371(9608):261-9.

22. Graham EM, Ruis KA, Hartman AL, Northington FJ, Fox HE. A systematic review of the role of intrapartum hypoxia-ischemia in the causation of neonatal encephalopathy. American journal of obstetrics and gynecology. 2008;199(6):587-95.

23. Chen HY, Chauhan SP, Ananth CV, Vintzileos AM, Abuhamad AZ. Electronic fetal heart rate monitoring and its relationship to neonatal and infant mortality in the United States. American journal of obstetrics and gynecology. 2011;204(6):491 e1-10.

24. Grimes DA, Peipert JF. Electronic fetal monitoring as a public health screening program: the arithmetic of failure. Obstet Gynecol. 2010;116(6):1397-400.

25. Nelson KB, Dambrosia JM, Ting TY, Grether JK. Uncertain Value of Electronic Fetal Monitoring in Predicting Cerebral Palsy. N Engl J Med. 1996;334(10):613-9.

26. Graham EM, Petersen SM, Christo DK, Fox HE. Intrapartum electronic fetal heart rate monitoring and the prevention of perinatal brain injury. Obstet Gynecol. 2006;108(3 Pt 1):656-66.

27. Durosier L, Cao M, Batkin I, Matushewski BJ, Keenliside L, Herry C, et al. Continuous multivariate electronic fetal monitoring during labor detects early onset of acidemia: Prospective study in fetal sheep model. 11th Annual International Conference on Complexity in Acute Ilness (ICCAI): Journal of Critical Care; 2013. p. e5-e6.

28. Warner HR, Cox A. A mathematical model of heart rate control by sympathetic and vagus efferent information. J Appl Physiol. 1962;17:349-55.

29. Akselrod S, Gordon D, Ubel FA, Shannon DC, Berger AC, Cohen RJ. Power spectrum analysis of heart rate fluctuation: a quantitative probe of beat-to-beat cardiovascular control. Science. 1981;213(4504):220-2.

30. Durosier LD, Green G, Batkin I, Seely AJE, Ross MG, Richardson BS, et al. Sampling rate of heart rate variability impacts the ability to detect acidemia in ovine fetuses near-term. Front Pediatr - Neonatalogy. May 5;2:38. doi: 10.3389/fped.2014.00038.

31. Green GC, Bradley B, Bravi A, Seely AJ. Continuous multiorgan variability analysis to track severity of organ failure in critically ill patients. Journal of critical care. 2013;28(5):879 e1- e11.

32. Bravi A, Green G, Longtin A, Seely AJ. Monitoring and identification of sepsis development through a composite measure of heart rate variability. PloS one. 2012;7(9):e45666.

33. Moorman JR, Carlo WA, Kattwinkel J, Schelonka RL, Porcelli PJ, Navarrete CT, et al. Mortality reduction by heart rate characteristic monitoring in very low birth weight neonates: a randomized trial. The Journal of pediatrics. 2011;159(6):900-6 e1.

34. Lahra MM, Jeffery HE. A fetal response to chorioamnionitis is associated with early survival after preterm birth. American Journal of Obstetrics and Gynecology. 2004;190(1):147-51.

35. Gotsch F, Romero R, Kusanovic JP, Mazaki-Tovi S, Pineles BL, Erez O, et al. The fetal inflammatory response syndrome. Clinical obstetrics and gynecology. 2007;50(3):652-83.

36. Grether JK, Nelson KB. Maternal infection and cerebral palsy in infants of normal birth weight. JAMA : the journal of the American Medical Association. 1997;278(3):207-11.

37. Garnier Y, Kadyrov M, Gantert M, Einig A, Rath W, Huppertz B. Proliferative responses in the placenta after endotoxin exposure in preterm fetal sheep. European journal of obstetrics, gynecology, and reproductive biology. 2008;138(2):152-7.

38. Garite TJ. Management of premature rupture of membranes. Clinics in perinatology. 2001;28(4):837-47.

39. Fahey JO. Clinical management of intra-amniotic infection and chorioamnionitis: a review of the literature. Journal of midwifery & women's health. 2008;53(3):227-35.

40. Frasch MG. Developmental effects of vagal activity of autonomic nervous system on the cardiovascular system: Are twins special? Reproductive Sciences. 2008;15(9):863-4.

41. Lake DE, Griffin MP, Moorman JR. New mathematical thinking about fetal heart rate characteristics. Pediatr Res. 2003;53(6):889-90.

42. Kovatchev BP, Farhy LS, Cao H, Griffin MP, Lake DE, Moorman JR. Sample asymmetry analysis of heart rate characteristics with application to neonatal sepsis and systemic inflammatory response syndrome. Pediatr Res. 2003;54(6):892-8.

43. Griffin MP, Lake DE, Bissonette EA, E HF, Jr., O'Shea TM, Moorman JR. Heart rate characteristics: novel physiomarkers to predict neonatal infection and death. Pediatrics. 2005;116(5):1070-4.

44. Fairchild KD, O'Shea TM. Heart Rate Characteristics: Physiomarkers for Detection of Late-Onset Neonatal Sepsis. Clinics in perinatology. 2010;37(3):581-98.

45. Tracey KJ. Physiology and immunology of the cholinergic antiinflammatory pathway. The Journal of clinical investigation. 2007;117(2):289-96.

46. Tracey KJ. Reflex control of immunity. Nature reviewsImmunology. 2009;9(6):418-28.
47. Wang H, Liao H, Ochani M, Justiniani M, Lin X, Yang L, et al. Cholinergic agonists inhibit HMGB1 release and improve survival in experimental sepsis. Nature medicine. 2004;10(11):1216-21.
48. Yeboah MM, Xue X, Javdan M, Susin M, Metz CN. Nicotinic acetylcholine receptor expression and regulation in the rat kidney after ischemia-reperfusion injury. American journal of physiology Renal physiology. 2008;295(3):F654-61.
49. Thordstein M, Flisberg A, Lofgren N, Bagenholm R, Lindecrantz K, Wallin BG, et al. Spectral analysis of burst periods in EEG from healthy and post-asphyctic full-term neonates. Clinical neurophysiology : official journal of the International Federation of Clinical Neurophysiology. 2004;115(11):2461-6.
50. de Vries LS, Hellstrom-Westas L. Role of cerebral function monitoring in the newborn. Archives of disease in childhoodFetal and neonatal edition. 2005;90(3):F201-7.
51. Williams CE, Gunn A, Gluckman PD. Time course of intracellular edema and epileptiform activity following prenatal cerebral ischemia in sheep. Stroke; a journal of cerebral circulation. 1991;22(4):516-21.
52. Prout AP, Frasch MG, Veldhuizen R, Hammond R, Matushewski B, Richardson BS. The impact of intermittent umbilical cord occlusions on the inflammatory response in pre-term fetal sheep. PLoS One. 2012;7(6):e39043.
53. Ross MG, Amaya K, Richardson B, Frasch MG. Association of atypical decelerations with acidemia. Obstet Gynecol. 2013;121(5):1107-8.
54. Ross MG, Jessie M, Amaya K, Matushewski B, Durosier LD, Frasch MG, et al. Correlation of arterial fetal base deficit and lactate changes with severity of variable heart rate decelerations in the near-term ovine fetus. Am J Obstet Gynecol. 2013;208(4):285 e1-6.
55. Borgstedt AD, Rosen MG, Chik L, Sokol RJ, Bachelder L, Leo P. Fetal electroencephalography. Relationship to neonatal and one-year developmental neurological examinations in high-risk infants. American Journal of Diseases of Children (1960). 1975;129(1):35-8.
56. Chik L, Sokol RJ, Rosen MG, Borgstedt AD. Computer interpreted fetal electroencephalogram. I. Relative frequency of patterns. American Journal of Obstetrics and Gynecology. 1976;125(4):537-40.

57. Sokol RJ, Rosen MG, Chik L. Fetal electroencephalographic monitoring related to infant outcome. American Journal of Obstetrics and Gynecology. 1977;127(3):329-30.

58. Thaler I, Boldes R, Timor-Tritsch I. Real-time spectral analysis of the fetal EEG: a new approach to monitoring sleep states and fetal condition during labor. Pediatr Res. 2000;48(3):340-5.

59. Xu A, Durosier L, Ross MG, Hammond R, Richardson BS, Frasch MG. Adaptive brain shut-down counteracts neuroinflammation in the near-term ovine fetus. Front Neurol - Neuropediatrics. 2014 Jun 30;5:110. doi: 10.3389/fneur.2014.00110.

60. Kaneko M, White S, Homan J, Richardson B. Cerebral blood flow and metabolism in relation to electrocortical activity with severe umbilical cord occlusion in the near-term ovine fetus. Am J Obstet Gynecol. 2003;188(4):961-72.

61. Blood AB, Hunter CJ, Power GG. Adenosine mediates decreased cerebral metabolic rate and increased cerebral blood flow during acute moderate hypoxia in the near-term fetal sheep. J Physiol. 2003;553(Pt 3):935-45.

62. Hunter CJ, Bennet L, Power GG, Roelfsema V, Blood AB, Quaedackers JS, et al. Key neuroprotective role for endogenous adenosine A1 receptor activation during asphyxia in the fetal sheep. Stroke. 2003;34(9):2240-5.

63. Pearce W. Hypoxic regulation of the fetal cerebral circulation. J Appl Physiol (1985). 2006;100(2):731-8.

64. Keunen H, Hasaart TH. Fetal arterial pressure and heart rate changes in surviving and non-surviving immature fetal sheep following brief repeated total umbilical cord occlusions. Eur J Obstet Gynecol Reprod Biol. 1999;87(2):151-7.

65. Pulgar VM, Zhang J, Massmann GA, Figueroa JP. Mild chronic hypoxia modifies the fetal sheep neural and cardiovascular responses to repeated umbilical cord occlusion. Brain Res. 2007;1176:18-26.

66. Merri M, Farden DC, Mottley JG, Titlebaum EL. Sampling frequency of the electrocardiogram for spectral analysis of the heart rate variability. IEEE transactions on bio-medical engineering. 1990;37(1):99-106.

67. Signorini MG, Fanelli A, Magenes G. Monitoring fetal heart rate during pregnancy: contributions from advanced signal processing and wearable technology. Computational and mathematical methods in medicine. 2014;2014:707581.

68. Frasch MG, Muller T, Hoyer D, Weiss C, Schubert H, Schwab M. Nonlinear properties of vagal and sympathetic modulations of heart rate variability in ovine fetus near term. American journal of physiologyRegulatory, integrative and comparative physiology. 2009;296(3):R702-7.

69. Patrick J, Campbell K, Carmichael L, Natale R, Richardson B. Daily relationships between fetal and maternal heart rates at 38 to 40 weeks of pregnancy. Can Med Assoc J. 1981;124(9):1177-8.

70. Graatsma EM, Jacod BC, van Egmond LA, Mulder EJ, Visser GH. Fetal electrocardiography: feasibility of long-term fetal heart rate recordings. Bjog. 2009;116(2):334-7; discussion 7-8.

71. Chudacek V, Spilka J, Bursa M, Janku P, Hruban L, Huptych M, et al. Open access intrapartum CTG database. BMC pregnancy and childbirth. 2014;14:16.

72. Ivanov PC, Rosenblum MG, Peng CK, Mietus J, Havlin S, Stanley HE, et al. Scaling behaviour of heartbeat intervals obtained by wavelet-based time-series analysis. Nature. 1996;383(6598):323-7.

73. Lucena F, Barros AK, Principe JC, Ohnishi N. Statistical coding and decoding of heartbeat intervals. PloS one. 2011;6(6):e20227.

74. Massimini M, Porta A, Mariotti M, Malliani A, Montano N. Heart rate variability is encoded in the spontaneous discharge of thalamic somatosensory neurones in cat. J Physiol. 2000;526 Pt 2:387-96.

75. Montano N, Porta A, Malliani A. Evidence for central organization of cardiovascular rhythms. Annals of the New York Academy of Sciences. 2001;940:299-306.

76. Bravi A, Longtin A, Seely AJ. Review and classification of variability analysis techniques with clinical applications. Biomed Eng Online. 2011;10:90.

77. Kro GA, Yli BM, Rasmussen S, Norèn H, Amer-Wåhlin I, Saugstad OD, et al. A new tool for the validation of umbilical cord acid-base data. BJOG. 2010;117(12):1544-52.

78. Kruger K, Kublickas M, Westgren M. Lactate in scalp and cord blood from fetuses with ominous fetal heart rate patterns. Obstet Gynecol. 1998;92(6):918-22.

79. Victory R, Penava D, Da Silva O, Natale R, Richardson B. Umbilical cord pH and base excess values in relation to adverse outcome events for infants delivering at term. Am J Obstet Gynecol. 2004;191(6):2021-8.

80. Ross MG, Gala R. Use of umbilical artery base excess: algorithm for the timing of hypoxic injury. American Journal of Obstetrics and Gynecology. 2002;187(1):1-9.
81. Amer-Wahlin I, Marsal K. ST analysis of fetal electrocardiography in labor. Semin Fetal Neonatal Med. 2011;16(1):29-35.
82. Salmelin A, Wiklund I, Bottinga R, Brorsson B, Ekman-Ordeberg G, Grimfors EE, et al. Fetal monitoring with computerized ST analysis during labor: a systematic review and meta-analysis. Acta Obstet Gynecol Scand. 2013;92(1):28-39.
83. Shapiro GD, Fraser WD, Frasch MG, Séguin JR. Psychosocial stress in pregnancy and preterm birth: associations and mechanisms. J Perinat Med. 2013:1-15.
84. Rurak D, Bessette NW. Changes in fetal lamb arterial blood gas and acid-base status with advancing gestation. Am J Physiol Regul Integr Comp Physiol. 2013;304(10):R908-16.
85. Duncombe G, Veldhuizen RA, Gratton RJ, Han VK, Richardson BS. IL-6 and TNFalpha across the umbilical circulation in term pregnancies: relationship with labour events. Early human development. 2010;86(2):113-7.
86. Chan CJ, Summers KL, Chan NG, Hardy DB, Richardson BS. Cytokines in umbilical cord blood and the impact of labor events in low-risk term pregnancies. Early human development. 2013;89(12):1005-10.
87. Fairchild KD, Srinivasan V, Moorman JR, Gaykema RP, Goehler LE. Pathogen-induced heart rate changes associated with cholinergic nervous system activation. American journal of physiologyRegulatory, integrative and comparative physiology. 2011;300(2):R330-9.
88. Olofsson PS, Rosas-Ballina M, Levine YA, Tracey KJ. Rethinking inflammation: neural circuits in the regulation of immunity. Immunol Rev. 2012;248(1):188-204.
89. Tracey KJ. The inflammatory reflex. Nature. 2002;420(6917):853-9.
90. Haensel A, Mills PJ, Nelesen RA, Ziegler MG, Dimsdale JE. The relationship between heart rate variability and inflammatory markers in cardiovascular diseases. Psychoneuroendocrinology. 2008;33(10):1305-12.
91. von Kanel R, Nelesen RA, Mills PJ, Ziegler MG, Dimsdale JE. Relationship between heart rate variability, interleukin-6, and soluble tissue factor in healthy subjects. Brain, behavior, and immunity. 2008;22(4):461-8.

92. Sloan RP, McCreath H, Tracey KJ, Sidney S, Liu K, Seeman T. RR interval variability is inversely related to inflammatory markers: the CARDIA study. Molecular medicine (Cambridge, Mass). 2007;13(3-4):178-84.

93. Thayer JF, Fischer JE. Heart rate variability, overnight urinary norepinephrine and C-reactive protein: evidence for the cholinergic anti-inflammatory pathway in healthy human adults. Journal of internal medicine. 2009;265(4):439-47.

94. Thayer JF, Sternberg E. Beyond heart rate variability: vagal regulation of allostatic systems. Annals of the New York Academy of Sciences. 2006;1088:361-72.

95. Tateishi Y, Oda S, Nakamura M, Watanabe K, Kuwaki T, Moriguchi T, et al. Depressed heart rate variability is associated with high IL-6 blood level and decline in the blood pressure in septic patients. Shock (Augusta, Ga). 2007;28(5):549-53.

96. Holman AJ, Ng E. Heart rate variability predicts anti-tumor necrosis factor therapy response for inflammatory arthritis. Autonomic Neuroscience : Basic & Clinical. 2008;143(1-2):58-67.

97. Marsland AL, Gianaros PJ, Prather AA, Jennings JR, Neumann SA, Manuck SB. Stimulated Production of Proinflammatory Cytokines Covaries Inversely With Heart Rate Variability. Psychosomatic medicine. 2007;69(8):709-16.

98. Lindgren S, Stewenius J, Sjolund K, Lilja B, Sundkvist G. Autonomic vagal nerve dysfunction in patients with ulcerative colitis. Scandinavian journal of gastroenterology. 1993;28(7):638-42.

99. Lanza GA, Sgueglia GA, Cianflone D, Rebuzzi AG, Angeloni G, Sestito A, et al. Relation of heart rate variability to serum levels of C-reactive protein in patients with unstable angina pectoris. The American Journal of Cardiology. 2006;97(12):1702-6.

100. Furukawa S, Sameshima H, Yang L, Ikenoue T. Acetylcholine receptor agonist reduces brain damage induced by hypoxia-ischemia in newborn rats. Reproductive sciences (Thousand Oaks, Calif). 2011;18(2):172-9.

101. Furukawa S, Sameshima H, Yang L, Ikenoue T. Activation of acetylcholine receptors and microglia in hypoxic-ischemic brain damage in newborn rats. Brain Dev. 2012.

102. Laude D, Baudrie V, Elghozi JL. Effects of atropine on the time and frequency domain estimates of blood pressure and heart rate variability in mice. Clin Exp Pharmacol Physiol. 2008;35(4):454-7.

103. Frasch MG, Frank B, Last M, Muller T. Time scales of autonomic information flow in near-term fetal sheep. Frontiers in physiology. 2012;3:378.
104. Beuchee A, Hernandez AI, Duvareille C, Daniel D, Samson N, Pladys P, et al. Influence of hypoxia and hypercapnia on sleep state-dependent heart rate variability behavior in newborn lambs. Sleep. 2012;35(11):1541-9.
105. Karin J, Hirsch M, Akselrod S. An estimate of fetal autonomic state by spectral analysis of fetal heart rate fluctuations. Pediatr Res. 1993;34(2):134-8.
106. Frank B, Frasch MG, Schneider U, Roedel M, Schwab M, Hoyer D. Complexity of heart rate fluctuations in near-term fetal sheep during sleep. Biomed Tech (Berl). 2006;51(4):233-6.
107. Groome LJ, Loizou PC, Holland SB, Smith LA, Hoff C. High vagal tone is associated with more efficient regulation of homeostasis in low-risk human fetuses. Dev Psychobiol. 1999;35(1):25-34.
108. Groome LJ, Mooney DM, Holland SB, Smith LA, Atterbury JL, Loizou PC. Human fetuses have nonlinear cardiac dynamics. J Appl Physiol. 1999;87(2):530-7.
109. Lake DE, Richman JS, Griffin MP, Moorman JR. Sample entropy analysis of neonatal heart rate variability. Am J Physiol Regul Integr Comp Physiol. 2002;283(3):R789-97.
110. Stone ML, Tatum PM, Weitkamp JH, Mukherjee AB, Attridge J, McGahren ED, et al. Abnormal heart rate characteristics before clinical diagnosis of necrotizing enterocolitis. Journal of perinatology : official journal of the California Perinatal Association. 2013;33(11):847-50.
111. Rudolph AJ, Vallbona C, Desmond MM. Cardiodynamic studies in the newborn. 3. Heart rate patterns in infants with idiopathic respiratory distress syndrome. Pediatrics. 1965;36(4):551-9.
112. Cabal LA, Siassi B, Zanini B, Hodgman JE, Hon EE. Factors affecting heart rate variability in preterm infants. Pediatrics. 1980;65(1):50-6.
113. Seely AJ, Macklem PT. Complex systems and the technology of variability analysis. Critical care (London, England). 2004;8(6):R367-84.
114. Ahmad S, Ramsay T, Huebsch L, Flanagan S, McDiarmid S, Batkin I, et al. Continuous Multi-Parameter Heart Rate Variability Analysis Heralds Onset of Sepsis in Adults. PLoS One. 2009;4(8):e6642.

115. Frasch MG. Fetal heart rate variability monitoring. Montebello Round Table. Complexity and Variability at the Bedside. September 28 - October 1. Montebello, QC, Canada. Journal of critical care. 2011;26(3):325-7.
116. Macklem PT. Emergent phenomena and the secrets of life. Journal of applied physiology. 2008;104(6):1844-6.
117. Seely AJ, Macklem P. Fractal variability: an emergent property of complex dissipative systems. Chaos. 2012;22(1):013108.